ENHANCEMENT OF MASS TRANSFER USING ROTATING CYLINDER PROMOTERS

A Thesis

Submitted to the College of Engineering of Al-Nahrain University
in Partial Fulfillment of the Requirements for the
Degree of Master of Science in
Chemical Engineering

by

BURAQ SHIHAB AHMED

(B.Sc. in Chemical Engineering 2008)

Dhu al-Hijjah   **1434**

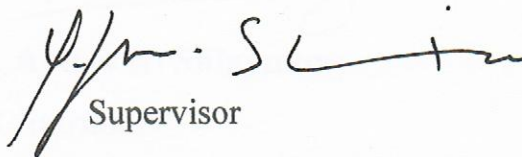**October**   **2013**

Supervisor Certification

I certify that this thesis was prepared under my supervision at College of Engineering / Alnahrain University in partial fulfillment of the requirements for the degree of **Master of Science in Chemical Engineering**.

Supervisor

Prof. Emeritus Dr. Qasim J. M. Slaiman

2013 /   /

PhD in Corrosion and Transport Phenomena

In view of the available recommendation, I forward this thesis for debate by the examining committee.

Asst.   eer A. Al Habobi

Chairman, department of chemical engineering

2013/   /

Committee Certificate

We the Examining Committee, after reading this thesis and examining the student **"Buraq Shihab Ahmed "** in its content, find it is adequate as a thesis for the degree of **Master of Science in Chemical Engineering**.
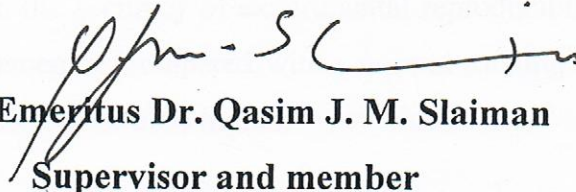
Prof. Dr. Abbas H. Sulaymon

Chairman

Dr. Sarmad Talib Najim

Member

Asst. Prof. Dr. Naseer A. Al Habobi

Member

Prof. Emeritus Dr. Qasim J. M. Slaiman

Supervisor and member

Approved by the College of Engineering / Alnahrain University.

Prof. Dr. Jassim Abbood Abbas Aldabbagh

Acting Dean, Collage of Engineering / Alnahrain University

2013/ 4 / 26

Abstract

The aim of present work is to determine experimentally the degree of mass transfer enhancement of dissolved oxygen using turbulent promoters of longitudinal leg extensions constructed on Rotating Cylinder Electrode (RCE) made of brass. The limiting current density (LCD) was evaluated under turbulent flow conditions at three different temperatures 35, 45, and 55   C. The experimental runs were carried out in 0.1 N NaCl salt solution of pH = 6 using a rotational velocity range from 200 – 1000 rpm. The effects of hydrogen evolution on LCD at pH 5, 6, and 7 were also investigated.

Two types of rotating cylinder made of brass, were examined : an enhanced cylinder one, with four leg rectangular extensions 10 mm long, 10 mm wide, and 1mm thick, and an enhanced cylinder two with four extensions 30 mm long, 10 mm wide, and 1mm thick.

The results showed that the relation between LCD, i_l, and pH is almost horizontal, showing that the effect of hydrogen evolution in this pH range on i_l values is negligible when compared with velocity and temperature. A better performance was obtained using enhanced cylinder two. The difference between enhanced cylinder one and two is within the accuracy of experimental reproducibility of results. The mass transfer enhancement as compared with a normal rotating cylinder electrode, devoid of promoters, is 53% or 58% higher.

The enhancement percentage decreased as rotational velocity increased further, since, seemingly, optimum turbulence has been reached practically by means of rotation in presence of turbulence promoters. Also, enhancement percentage decreased with increasing temperature. As temperature increased mass transfer coefficient increased on both normal and enhanced cylinder electrodes in spite of the fact that solubility of dissolved oxygen decreased. Thus the effect of extensions acting as turbulent promoters was diminished leading to mass transfer coefficient values to be approximately close to each other and enhancement percentage being

reduced. The effect of extensions length on the enhancement was found little, i.e., limited under present conditions. Also, mass transfer due to temperature rise surpassed the effect of reduced oxygen solubility.

List of Contents

Chapter One : Introduction

Chapter Two: Theory and Literature review

Nomenclature

Symbol	Meaning	Units
A	short mesh aperture	m
a	Constant in Eq (2-13)	
C_A	Concentration of component A	mol/m^3
C_b	Bulk concentration	ppm (mg/L)
C_i	Interfacial concentration	ppm (mg/L)
D	Diffusivity	cm^2/s
d	Diameter of specimens	cm
E_a, E	Electrode potential	V
F	Faraday No. (96500)	Columb/equivale
H	distance between wires	nt
I	Total Current	m
i	Total current density	A
i_L	Limiting current density	A/cm^2
k	Mass transfer coefficient	cm/s
N_A	Rate of mass transfer	$mol/cm^2.s$
n	constant for a particular system in Eq (2-11)	
n_e	No. of electrons transferred(valance)	
R	Gas constant (8.314)	J /mol. K
Re	Reynolds number ρ Ud/ μ	
T	Temperature	^0C

$\bar{r}$	mean radius	cm
r_1, r_2	internal and external radius of specie	cm
Sc	Schmidt number ν/D	
Sh	Sherwood number $k\text{d}/D$	
Ta	Taylor number $4\Omega^2 r^4/\nu^2$	
U	Velocity	m/s
$\bar{V}$	oxygen discharge rate	$cm^3 cm^{-2} s^{-1}$

Greek symbols

Symbol	Meaning	Units
δ_h	Hydrodynamic boundary layer	Ohm.cm
ε_ψ	Eddy momentum diffusivity	m^2/s
ψ	Electrostatic potential	
ε_D	Eddy diffusivity for mass transfer	cm^2/s
ν	Kinematics viscosity	cm^2/s
Ω	angular velocity	radius/s
ω	rotational velocity	rpm
ρ	density	g/cm^3
μ	Viscosity	g/cm.s

Abbreviations

Abbreviation	Meaning
RCE	Rotating cylinder electrode
LCDT	Limiting current density technique
LCD	Limiting current density
pp	Polypropene
RVCRCE	Reticulated Vitreous Carbon Rotating Cylinder Electrode
EP	Enhancement Percentage

List of Tables

List of Figures

Chapter one

INTRODUCTION

1.1 Introduction

Many electrochemical processes suffer in varying degrees from mass transfer limitations. These limitations may require operation at considerably less than economic optimum current densities. Also, the rotating cylinder electrode, whose good mass-transfer conditions are achieved by the movement of the electrode, has been recognized as a helpful tool in applied electrochemical fields. Mass transfer to a surface of rotating cylinder electrode may be considerably enhanced by:

(i)   Roughening the rotating cylinder surface [1,2].

(ii)   Using a wiper blade [3,4].

(iii)   Evolving gas simultaneous with the main reaction on the surface of the rotating cylinder [5].

(iv)   Superimposing axial flow on the flow induced by cylinder rotation in a continuous flow reactor [6,7].

(v)   Expanding the rotating cylinder active area by using reticulated vitreous carbon rotating cylinder [8] and rotating cylinder of screen and expanded metal [9,10].

The mass transfer coefficients are usually determined experimentally by the limiting current technique. The advantages of limiting current method stem from the fact that currents and potentials, i.e., fluxes and driving forces can be measured and controlled with high precision and resolution [11]. Therefore, the limiting current is defined as the maximum current that can be generated by a given electrochemical reaction, at a given reactant concentration, under well-established hydrodynamic steady state conditions [12].

The limiting current density i_L is obtained from polarization curves for a rotating cylinder electrode under static and dynamic conditions. The limiting current plateau is not generally well defined, thus the method given by Gabe and Makanjoula [13]

will be adopted in the present work to estimate the limiting current density values using equation (1.1) as illustrated in Figure1-1.

$$i_L = \frac{i_1 + i_2}{2} \qquad\qquad (1.1)$$

Where i_1 and i_2 are the currents associated with E_1 and E_2 respectively.
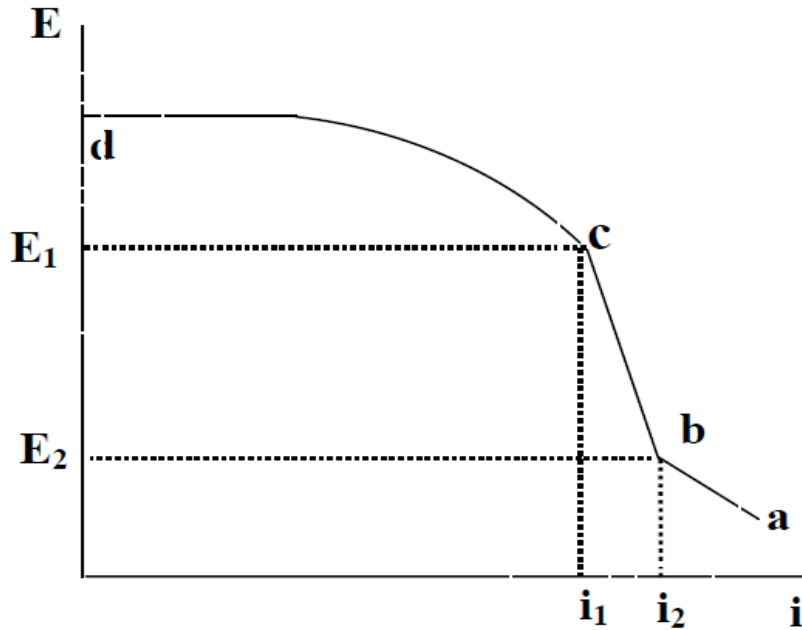
Figure 1-1 Typical polarization curve of dissolved O_2 in aqueous salt solution[13].

In electrochemical engineering, one of the main ways to increase mass transfer of various processes is the relative movement of the electrode-electrolyte. Besides allowing the use of higher current densities and thereby increasing the production rate and improving the flow regime, it can also help for the removal of the air or of the generated hydrogen gas, or to provide a steady pH and temperature in the cathode area.

The main processes applied for the improvement of electrode-electrolyte relative movement are: the use of turbulence promoters, particle fluidized bed, electrolyte

recirculation, mechanical stirring of the electrolyte, electrode spinning. Induction of turbulence near electrode surface enhances mass transport [14]. The mechanism leading to an increased mass transfer varies depending on the type and orientation of the metal electrode and on the electrolyte flow direction. Mass transfer is improved when the geometry of the electrode does not inhibit the release of bubbles that are generated by the electrochemical process and also introduces additional turbulence to the system.

1.3 The Scope of Present Work

The aim of present work is enhancement of mass transfer of dissolved oxygen using turbulent promoters in 0.1N NaCl solution of pH = 6 at various temperatures under rotational flow conditions. A rotating cylinder electrode is adopted with longitudinal leg extensions to create additional turbulence leading to enhancement of mass transfer characteristics as compared with normal rotating cylinder devoid of promoters.

Chapter two

Theory and literature survey

2.1. Introduction

The electrochemical techniques are widely used in many variable fields because they are accurate and easy to adopt, for example, the increasing requirements of legal limitations for environmental protection demand the development of reliable and cost-effective processes for the treatment of effluents with small concentration of dangerous species [15]. The electrochemical treatment of effluents can be efficiently performed with the use of the rotating cylinder electrode.

The rotating cylinder electrochemical reactor (RCE) is one of the most common geometries for different types of studies, such as metal ion recovery, alloy formation, electro-synthesis, corrosion, effluent treatment, and Hull cell studies [15].

The main features of the RCE which give it unique experimental characteristics are

(a) It generates turbulent convection at Re > 100, thereby providing simulation conditions of this type of convection at relatively low rotation rates.

(b) The potential and current densities are substantially uniform thereby promoting uniform reaction rates over the cathode surface.

(c) Mass transport is high and can be further enhanced through development or use of roughened surfaces or enhancement promoters.

(d) The mass transfer equations are well-established.

(e) Superimposed axial flow does not usually alter the mass transfer control.

(f) The most convenient design utilizes a rotating inner cylindrical electrode with a concentric outer counter electrode but the converse is possible. The active (working) electrode may be either cathode or anode [16].

The RCE has now established itself as a major tool for studying electrochemical mass transport especially under turbulent conditions. During the 15 years, over 100 applications have been recorded in a number of fields and the versatility of the RCE has been fully demonstrated [16].

2.2 **Rotating cylinder electrode**

The rotating cylinder will cause spinning or swirling of the fluid because of the surface drag whose extent will depend on the exact geometry. A favored experimental arrangement is one involving the presence of a concentric stationary outer cylinder around the inner rotating cylinder [17].

Silverman [18] showed that one practical geometry is the rotating cylinder electrode (RCE), which is useful for studying and predicting corrosion under dynamic conditions (turbulent flow). An equation was presented that allows rotation rates to be chosen so that mass transfer coefficient for the rotating cylinder electrode will be those for the modeled geometry of pipes, annuli or wall jets. These equations allow mass transfer controlled corrosion rates to be predicated exactly for geometries discussed using only one of the geometries for experimentation.

Newman [19], stated that three flow regimes need to be defined, firstly, at low rotational speeds flow is tangential and laminar, secondly, laminar but vortices develop giving superimposed radial and axial motion, and thirdly, above a critical Re true turbulence develops .

Where there is a change in flow, thickness of the hydrodynamic boundary layer (δ_h) changes with the linear flow velocity, V, as follows [20].

For laminar flow $\delta_h \propto 1/V^{0.5}$ (2-1)

For turbulent flow $\delta_h \propto 1/V^{0.9}$ (2-2)

At a very low rotation speeds, simple flow of the fluid produces concentric circles as shown in fig. 2-1.

Because of the fluid velocity , at a very low speed , is perpendicular to the direction of mass transfer , it is not of much practical interest as the flow simply carries the material in circles and does not lead to any enhancement of the rate of mass transfer [21].
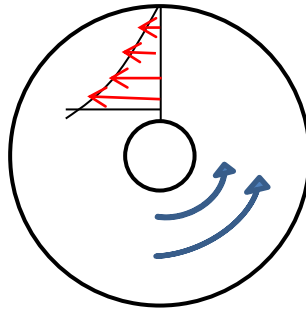
Figure 2-1 Velocity distribution for concentric stream lines between rotating cylinders [21].

This simple flow pattern becomes unstable, at higher rotation speeds, particularly when the inner electrode rotates. The flow then has a cellular motion superimposed upon the flow around the inner cylinder. These so-called Taylor vortices are shown in fig. 2-2. Now there is a component of the velocity in the direction from one cylinder to the other and rate of mass transfer can be enhanced [21].

At higher rotational velocities, the flow becomes turbulent and is characterized by rapid and random fluctuation of velocity and pressure.
These include a fluctuating velocity component in the direction from one cylinder to the other. Therefore; the rate of mass transfer can be enhanced considerably in a uniform manner over the surface of the cylinder. At a solid surface, the fluid velocity is equal to that of the solid. Since the fluid cannot flow through the surface and since frictional effects do not allow a discontinuity in the tangential velocity, thus the velocity fluctuations die away as a solid surface is approached [21].
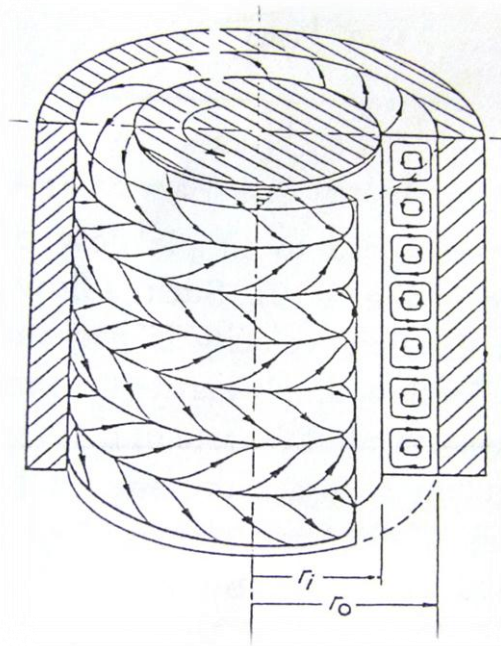
Figure 2-2 Sketch of Taylor vortices [21].

• **Mass transfer to a Rotating Cylinder**

The prediction and measurement of mass transport using RCEs continue to attract interest for several reasons [15]:

(i) In metal and polymer electro-deposition applications, the maximum rate of plating depends on the limiting current density at the electrode surface.

(ii) In environmental applications, the mass transport performance of RCE will govern the rate of removal of a toxic solution species such as heavy metal ions.

(iii) For batch electro-synthesis, the achievement of a high reactant conversion in a reasonable electrolysis time requires a high rate of mass transport.

(iv) In the laboratory, controlled-potential coulometric studies using exhaustive electrolysis techniques again require high mass transport (and/or electrode area) to maintain a short analysis time.

(v) Mass transport to or from an inner RCE can be altered/controlled by a diverse number of factors including predetermined surface roughness or developing roughness (as in the case of deposition of roughened deposits or anodic formation of corrosion pits) [22]

Study of mass transfer at working electrodes is of fundamental importance in analysis of electrode phenomena and in consideration of concentration polarization, limiting currents, and rates of electrode reactions [23].

An electrode reaction proceeding at a finite rate involves movement of reacting materials between the electrode and the solution surrounding it. The ions are transferred from solution to an electrode by three principal mechanisms: (a) migration, (b) diffusion, and (c) convection [24].

(a) Migration

This occurs when charged particles placed in an electric field. Thus a negatively charged ion is attracted towards a positive electrode and vice versa. This movement is due to a gradient in the electrical potential [25].

(b) Diffusion

This occurs whenever a species moves from a region of high concentration to one of low concentration, thus it is movement due to concentration gradient [25].

(c) Convection

It occurs from a movement of the fluid by forced means (stirring, for example), or from density gradient within fluid. Generally fluid flow occurs because of natural or forced convection.

Assuming that the transfer is steady and unidirectional in the Y direction perpendicular to the surface of the electrode [8], the rate of transfer of a reacting species is expressed as

$$N_A = (D + \varepsilon_\psi)C_A \left(\frac{n_e}{RT}\right)\left(\frac{\partial \psi}{\partial Y}\right) - (D + \varepsilon_D)\left(\frac{\partial C_A}{\partial Y}\right) + VC_A \qquad (2\text{-}3)$$

And the current density at the electrode is expressed as

$$N_A = \frac{i}{Fn_e} \qquad (2\text{-}4)$$

The three terms on the right of equation (2-3) represent the contribution of migration, diffusion, and convection, respectively.

The last term for convection vanishes in the redox processes because there is no net bulk flow in the Y direction, but it does not vanish in the process of metal depositing on the electrode because there is a net bulk flow. However, its effect

is very small at ordinary conditions and usually negligible. For example, Wilke et al [9] show that the error from neglecting this effect was never larger than 0.3% for the maximum flux of deposit in their experiment. Therefore, the last term of equation (2-3) may be assumed zero [26].

Next, a simplification can be achieved concerning the migration term by adding a large excess of an unreactive electrolyte (supporting electrolyte) to the solution. If such electrolytes, which do not react at electrode, exist in the solution in relatively high concentrations and have high conductivity compared with the reacting species of ions, there should be no sharp potential gradient near the electrode, i.e., $\frac{\partial \psi}{\partial Y}$ may be assumed to be zero. Thus the migration term in Eq. (2-3) can be neglected and only the diffusion term remains to give

$$N_A = -(D + \varepsilon_D)\frac{\partial C_A}{\partial Y} \tag{2-5}$$

In general case, the integration of Eq. (2-5) gives the following expression for the rate of mass transfer [26].

$$N_A = k(C_b - C_i) \tag{2-6}$$

Substituting Eq.(2-4) into Eq.(2-6) gives

$$\frac{i}{F \ n_e} = k(C_b - C_i) \tag{2-7}$$

Or

$$k = \frac{i}{n_e F(C_b - C_i)} \tag{2-8}$$

From Eq. (2-8), the mass transfer coefficient, k, could be calculated for any current density (i), if in addition to the bulk concentration, (C_b), the interfacial concentration ,(C_i), were known. An accurate experimental determination of (C_i) is extremely difficult, hence mass transfer coefficient, k, is most conveniently obtained from limiting current (i_L), i.e., $C_i=0$ and Eq. (2-7) and Eq.(2-8) becomes

$$\frac{i_L}{n_e F} = k \ C_b \tag{2-9}$$

And

$$k = \frac{i_L}{n_e F C_b} \tag{2-10}$$

Though the diffusion-controlling electrochemical reaction is a very strong weapon to attack transport phenomena in liquids, it should be noted that there are several limits in using this method. First, it is limited to liquids; accordingly, the data of mass transfer are limited for high Sc. Second, only certain kinds of liquid mixtures can be used, i.e. , those in which a diffusion-controlling electrolytic reaction occurs .Furthermore, this method cannot be used for a velocity larger than a critical flow rate at which the reaction resistance at the cathode becomes relatively significant compared with decreasing resistance of diffusion.

For practical purposes, it is better to choose the condition in which the limiting current is reached before the potential becomes larger than the hydrogen overvoltage, otherwise, the discharge current of hydrogen ions is added and the limiting current cannot be clearly identified.

2.3 Limiting Current Density Technique

The concept of limiting current density was first recognized in 1904 by Nernst and Brunner. Later it was established through the work of Eucken ,Agar , Levich, and Wagner [11]. Consequently, the limiting current density technique has matured, gaining wide applications not only for studies of specific electrochemical systems but mainly as a tool for obtaining transport correlations under forced and free convection [11], for mass transport analogies[27], and for hydrodynamic studies [28]. The later include friction factor determinations [29], shear stress measurements [30], turbulent flow studies [31], and fluid velocity measurements [32].

Generally mass transfer coefficients are usually determined experimentally by the dissolving wall method, the limiting current technique, and the analogy with heat transfer. In the dissolving wall method a specimen is made of or coated with material that is soluble in the test environment. Results obtained by dissolving surfaces are of uncertain reliability because, as pointed out by Sherwood and Linton, small fissures and surface roughness can develop while the dissolution is progressing. Consequently, in recent years the electrochemical technique (LCDT) has been in greater favor [33].

In practical mass transfer measurements, using the limiting current method, provide convenient and accurate means for the determination of local and average transport rates. The advantages of limiting current method stem from the fact that currents and potentials, i.e., fluxes and driving forces can be measured and controlled with high precision and resolution [11].

2.4 Limiting Current Density (LCD)

The limiting current is an important parameter for the characterization of mass transport rates in electrochemical systems [34]. When an electrochemical system operates under limiting current conditions, the reaction proceeds at the maximum rate and hydrodynamic properties can be characterized, facilitating comparison with other electrochemical systems [12].

Therefore; the limiting current is defined as the maximum current that can be generated by a given electrochemical reaction, at a given reactant concentration, under well-established hydrodynamic steady state conditions.

For rotating cylinder system, as shown in fig. 2-3 the limiting current density (i_L) can be determined experimentally as follows:
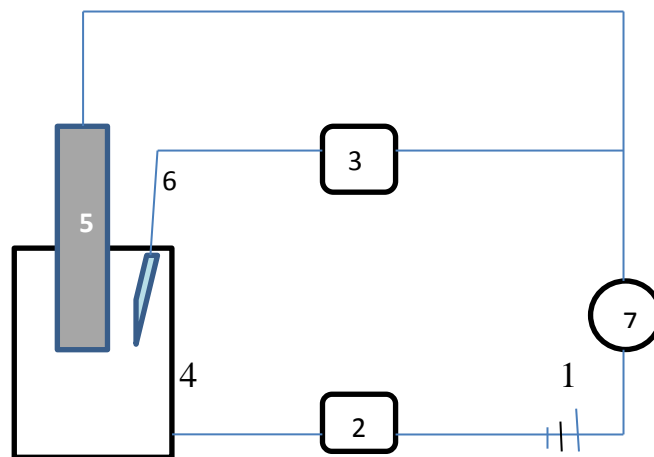
Figure 2-3 Electrical circuit unit for RCE;1-power supply,2-Ammeter,3-Voltmeter ,4-Stationary electrode (Anode),5-Rotating electrode (Cathode), 6-Riference Electrode,7-Rheostat.

A potential applied between the cathode and anode, is adjusted with a rheostat, and the current in the circuit is measured. After the flow conditions are

set, current is passed through the cell and increased in small increments at intervals of some time until the limiting current is reached and usually increased further to the hydrogen evolution point [26].

Approximately one or two minute is recommended as the time interval at each rheostat setting because this is long enough to make the potential and the current reach a steady state. So the polarization curve can be drawn, as shown in Fig (2-4) [26].
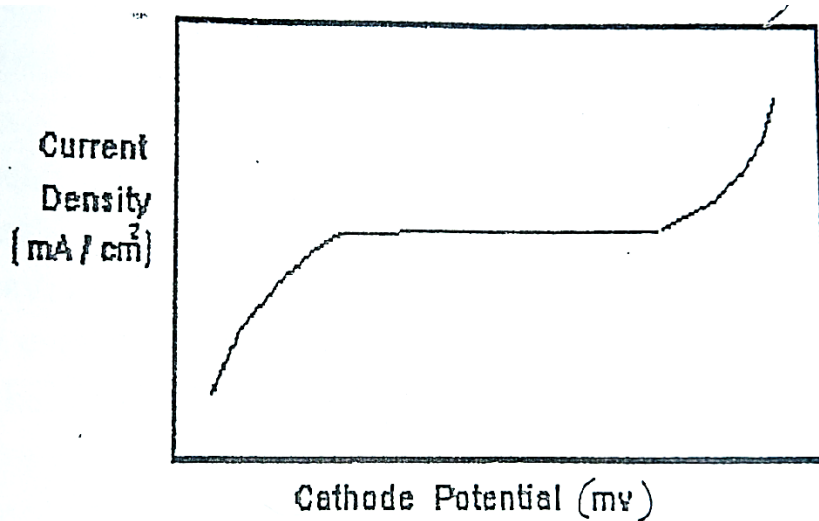
Figure 2-4 Typical limiting current curve [26].

From fig. 2-4, as the applied potential is increased, the current is increased exponentially and approaches a constant value, i.e., limiting current asymptotically. Under the condition of a limiting current, the ions transferred to the electrode surface react very soon and increasing potential does not result in an increase in the rate of the desired reaction. Also a further increase of the potential over the limiting current region causes a steep increase in current density due to the discharge by a secondary reaction such as hydrogen evolution on the cathode.

As the diffusion rate of ions is made to increase by increasing the flow rate, under the same conditions of electrolysis, the value of the limiting current is raised and the flat portion of the polarization curves disappears above a certain upper limit of the flow rate as shown fig. 2-5 [26].
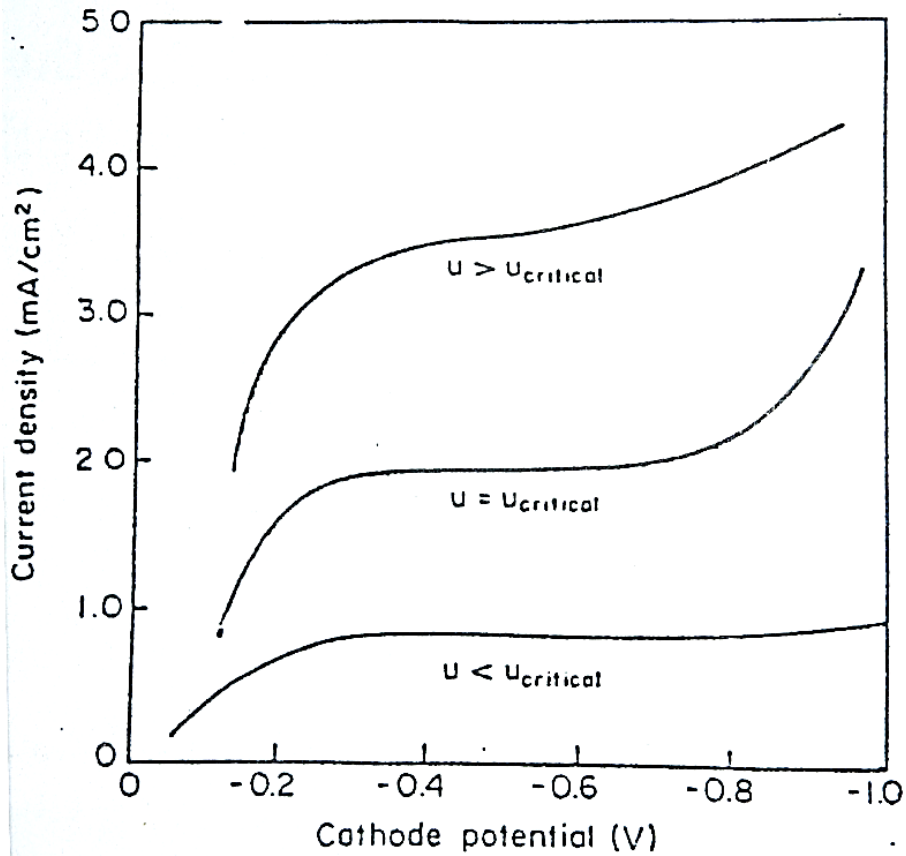
Figure 2-5 Critical Flow Rate [26].

In such situations the limiting is no longer indicated since the reaction is too slow to remove all ions reaching the electrode surface.

This upper limit of flow rate is called the critical flow rate , the higher reaction rate is the higher critical flow rate. The data above the critical flow rate should not be used in correlations since the concentration at the electrode surface is not zero [26].

2.5 Factors affecting the limiting current density

The limiting current density can be affected by factors such as

2.5.1 Temperature

A general rule, as temperature increases, limiting current increases. This is due to reaction kinetics themselves and the higher diffusion rate of many corrosive agents and reaction products at increased temperatures. This latter action delivers these by-products to the surface more efficiently. Occasionally, the limiting current in a system will decrease with increasing temperature. This can occur because of certain solubility considerations. Many gases have lower solubility in open systems at higher temperatures. As temperatures increase, the resulting decrease in solubility of the gas causes corrosion rates to go down [35].

2.5.2 Fluid velocity

Primarily the velocity affects electrochemical corrosion rate through its influence on diffusion phenomena. It has no effect on activation controlled processes. The manner in which velocity affects the limiting diffusion current is a marked function of the physical geometry of the system. In addition the diffusion process is affected differently by velocity when the flow conditions are laminar as compared to a situation where turbulence exists. For most conditions the limiting diffusion current can be expressed by the equation [36]:

$$i_L = kU^n \qquad\qquad (2.11)$$

Where k is a constant, U is the velocity of the environment relative to the surface and n is a constant for a particular system. Values of n vary from 0.2 to 1[36]. The effect of velocity on the limiting current density is shown in Fig. (2-6).
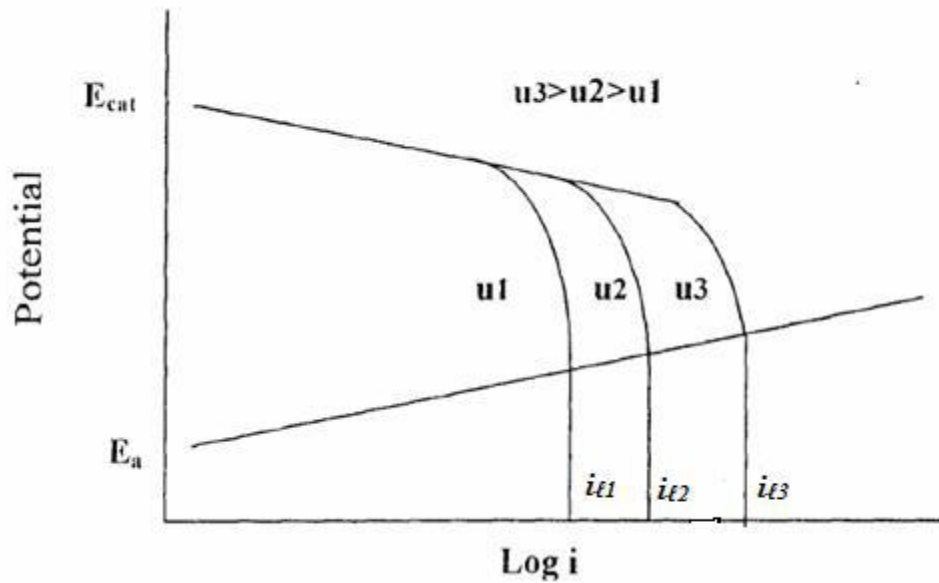
Figure 2-6 Effect of velocity on i_L [37].

The effect of velocity on corrosion rate, like the effect of oxidizer addition, complex and depends on the characteristics of the metal and the environment to which it is exposed. Fig. 2-7 shows typical observations when agitation or solution velocity is increased [38].

For corrosion processes which are controlled by activation polarization, agitation and velocity have no effect on the corrosion rate as illustrated by curve B in fig. 2-7. If corrosion process is under cathodic control, then agitation or velocity increases the corrosion rate as shown in curve A, section 1. Generally this effect occurs when an oxidizer present in very small amounts as in the case of dissolved oxygen in acids or water. If the process is under diffusion control and the metal is readily passivated, then the behavior corresponding to curve A, section 1 and 2, will be observed, curve C shows that at high velocities the passive film is removed [39].
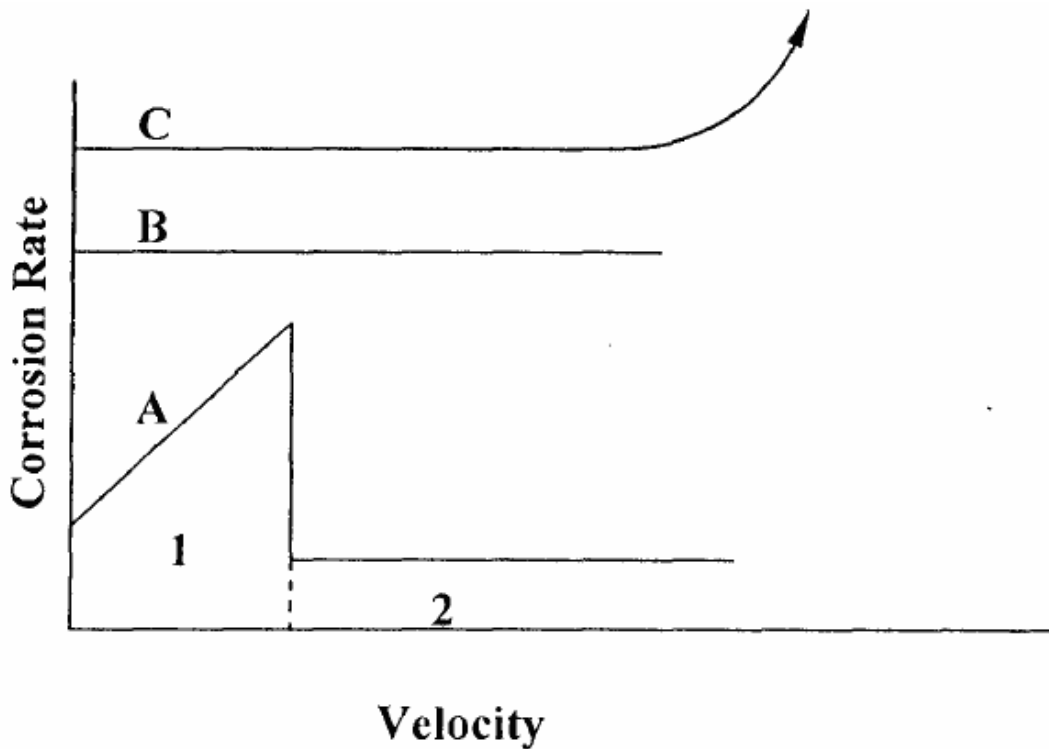
Figure 2-7 Effect of velocity on the Corrosion Rate [39].

2.5.3 Oxidizing agents

In some corrosion processes, such as the dissolution of zinc in hydrochloric acid, hydrogen may evolve as a gas. In others such as the relatively slow dissolution of copper in sodium chloride, the removal of hydrogen, which must occur so that corrosion may proceed, is effected by a reaction between hydrogen ion and some oxidizing chemical such as oxygen to form water. Because of the high rates of corrosion that usually accompany hydrogen evolution, metals are rarely used in solutions which evolve hydrogen at an appreciable rate.

Most of the corrosion observed in practice occurs under conditions in which the oxidation of hydrogen to form water is a necessary part of the corrosion process, Eq. 2.11,[40] For this reason, oxidizing agents are often powerful accelerators of corrosion, and in many cases the oxidizing power of a solution is most important property in so far as corrosion is concerned.

$$4H^+ + O_2 + 4e^- \rightarrow 2H_2O \qquad E^\circ = 1.229\ V \qquad (2.12)$$

Oxidizing agents that accelerate the corrosion of some materials may also retard corrosion of other through the formation on their surface of oxides or layers of adsorbed oxygen which make them more resistant to chemical attack. This property of chromium is responsible for the principal corrosion resisting characteristics of the stainless steels. It follows then, oxidizing substances, such as dissolved air, may accelerate the corrosion of one class of materials and retard the corrosion of another class. In the latter case, the behavior of the material usually represents a balance between the power of oxidizing compounds to preserve a protective film and their tendency to accelerate corrosion when the agencies responsible for protective-film breakdown are able to destroy the films [41].

2.5.4 Effect of Salt Content and Chloride Ion

Chlorides have probably received most consideration in relation to their effect on corrosion. The effect of sodium chloride concentration on the corrosion of iron in air saturated water at room temperature was found to increase the corrosion rate. The corrosion rate in air saturated water at room temperature was found to increase with the increase of sodium chloride solution concentration reaching maximum at about 3% NaCl (seawater concentration), and then decreases, the value falling below that of distilled water when saturation is reached (26 % NaCl). To understand this behavior, oxygen solubility in water decreases continuously with an increase in sodium chloride concentration, explaining the falling off of corrosion rate at higher sodium chloride concentration. The initial rise appears to be related to a change in the protective nature of the barrier rust film that forms on the corroding metal. On the other hand, chlorides increase the electrical conductivity of the water so that the flow of corrosion currents will be facilitated [40, 42].

An increase in suspended solids levels will accelerate corrosion rates. These solids include any inorganic or organic contaminants present in the fluid. Examples of these contaminants include clay, sand, silt or biomass [43].

2.6 Enhancement of mass transfer

Increase in mass transport for an electrochemical process can be achieved by modifying either the solution parameters (concentration, diffusion coefficient, viscosity, etc.) or the electrode physical and geometrical parameters (surface area, ratio of area to volume, etc.) [1].

Generally, the enhancement of mass transfer with rotating cylinder electrode can be achieved by:

- Roughening the electrode surface [1].
- Expanding its active area by using reticulated vitreous carbon rotating cylinder [8] and rotating cylinder of expanded metal and mesh [9,10].
- Using of alumina particles in the solution [44].
- Using turbulent promoters with rotating cylinder [45].
- All these factors will be illustrated as given in literature:

Eisenberg *et al.* [46] (1956) were the first to study the mass transfer to the rotating cylinder electrode under turbulent flow conditions. From measurement of limiting current densities at a smooth RCE made of Ni using $Fe(CN)_6^{-3}/Fe(CN)_6^{-4}$ redox couple in alkaline medium and in the range of Re from (1000 to 100,000) and Sc from (835 to 11,490). They found that

$$sh = 0.0791 \ Re^{0.7} \ Sc^{0.356} \qquad (2.13)$$

Sed Ahmed[47](1977) measured the limiting currents and mass transfer coefficients for the electro-deposition of copper from an acidified solution of copper sulphate using a cell design involving an array of closely packed screens as a working electrode stirred by the counter-electrode gases. The reactor is composed of a vertical column in which the working electrodes are arranged alternately with the counter electrodes, i.e. each working electrode is placed between two counter electrodes, which ensures a uniform current distribution on the working electrodes. While the working electrode is composed of an array of closely packed screens, the counter electrode is composed of a single screen. For

a single-screen electrode, oxygen discharge was found to increase the mass transfer coefficient according to the equation:

$$log k = a + 0.377 log \bar{V} \qquad (2\text{-}14)$$

Where k is the mass transfer coefficient (cm s^{-1}), a is a constant, and $\bar{V}$ is oxygen discharge rate (cm^{3}cm^{-2}s^{-1}). Also, the increment in the mass transfer coefficient may be attributed to the ability of the screens to induce a high local solution velocity. But the increasing in the number of screens per array led to decrease mass transfer coefficient .This was explained by the fact that increasing the number of screens per array leads to an increase in the resistance of the array to the flow of the gas electrolyte system with a corresponding decrease in the mass transfer coefficient. The apparent advantage of this reactor is the appreciable enhancement of the rate of mass transfer without any consumption of external stirring energy. This should lead to a decrease in the operating costs of electrochemical processes.

  Gabe and Makanjuol [1] (1986) studied mass transfer at cylindrical electrodes, which were roughened by machining groove patterns, pyramidal knurling, and superimposing wires and meshes. The degree of roughness was estimated by rotating the electrodes in a turbulent regime, mass transfer for cathodic copper electro-deposition was determined and the degree of consequent enhancement relative to an equivalent smooth cylinder was calculated. Typically, the surface area has been increased by 10-40% and the mass transfer rate by 100-300% for turbulent flow defined by 7000 < *Re* < 80000. Gabe and Makanjuola concluded that:

1. Artificial roughness elements located at an electrode surface can be expected to generate high levels of mass transfer enhancement in a turbulent flow regime. However, it is essential that the size of a roughness element be several order of magnitudes greater than the diffusion sub-layer thickness.

2. Mass transfer enhancement was found to be independent of roughness height for geometrically similar roughness elements, i.e. those with similar roughness

pitch to roughness height ratios, but its magnitude was a function of roughness type.

3. Roughness elements with three-dimensional character were superior to two-dimensional types, but only at the lower Reynolds number ranges. A maximum enhancement of 275% was recorded with a weave-covered RCE at Re = 12 700.

4. With the exception of wire-wound electrodes, for which Reynolds number exponent was consistently higher than 0.7 (as for a smooth RCE), the marginal increment in mass transfer coefficient for all other rough RCEs invariably declined at higher Reynolds number.

Eklund and Simonsson [6] (1988) measured the enhanced mass transfer rate, for the rotating concentric cylindrical electrode with axial flow recirculated by a centrifugal pump, and compare with the smooth cylinder. The flow obstacles, turbulence promoters, used to enhance mass transfer were made of polypropene, which is resistant to potassium hydroxide for long periods. Three types of polypropepene, PP, were used, i.e., a grid which had a 1 cm spacing between the threads in a squared appearance. It was 1mm thick, so that when it was placed in the annulus it needed three consecutive layers, formed to a cylinder, to fill the annulus. The net had 1.0mm spacing between the threads, also in a squared appearance. It was 1.0 mm thick and three consecutive layers, formed to a cylinder, were used to fill the annulus. The cloth was a specially made carpet woven from Engtex (Y 840925 B) with a thickness of 3.5 mm and a weight of 404 g m $^{-2}$. It was fastened on the outer electrode and it filled the whole annulus and brushed on the inner rotating electrode.

 The effect of turbulence promoters can be estimated as an enhancement factor, which is defined as the ratio between the Sherwood numbers in the presence and in the absence of the promoter.

- In axial flow with no rotation this enhancement factor is 1.8-2.6 for the PP grid, 2.3-4.1 for the PP net and 2.9-4.4 for the PP cloth.

- In fully turbulent flow (Ta < 1000) the enhancement factor is 1.0 for the PP grid, 1.4 for the PP net and 3.5-4.6 for the PP cloth.

Eklund and Simonsson[6] concluded that when the turbulence promoters were applied in the annulus a significant increase in *Sh* was detected, up to five times the value for the smooth cylinder when the PP cloth was used. The reason for the great effect of the PP cloth on the mass transfer rate in rotational flow is that the PP cloth is in direct contact with the inner rotating cylinder electrode surface and gives a very efficient wiping effect, thereby decreasing the diffusion layer thickness.

Nahle et al. [8] (1995) reported mass-transfer data for rotating cylinder electrodes of reticulated vitreous carbon. Using copper deposition as test reaction they found that

- The RVCRCEs exhibit large limiting current enhancements when compared to their two dimensional analogues.
- The limiting current was dependent upon velocity to the power 0.55 to 0.71 depending upon the porosity of the carbon foam.
- The mass transport coefficients at RVCRCEs are comparable to those at a smooth RDE of the same diameter.
- The limiting current enhancements are due, in the main, to the large electro- active area of the three dimensional matrix.
- The mass transport coefficients of the foams are sufficiently similar to allow the use of a single, approximate correlation based upon macroscopic electrode parameters.

Stojak *et. al.* [44] (2001) investigated the effect of particle loading on the polarization behavior during co-electrodeposition of nanometric diameter alumina with copper on a rotating cylinder electrode from the kinetically-controlled to mass-transfer limitation conditions was studied using an optimal electrolytic bath composition of 0.1 M $CuSO_4$ + 1.2 M H_2SO_4 [32]. In the kinetically-controlled region, the particles in suspension led to a decrease in the current for a given potential value compared without particles in suspension for all particle loadings. For mass transfer limiting conditions, alumina particle

loadings at or below 120 g/l had no effect. However, a particle loading of 158 g/l was found to increase the limiting conditions by as much as 32%.

Grau and Bisang [9] (2005) studied the performance of electrochemical reactors with rotating cylinder electrodes of expanded metal. Using the ferricyanide reduction as test reaction they reported that

The Sherwood number was dependent on Reynolds number, both defined in terms of the hydraulic diameter as characteristic length, to the power of 0.63. To take into account the geometry of the expanded metal two additional dimensionless parameters were included in the empirical expression as shown in equation below :

$$Sh = 1.356 \left(Re * \frac{r_2}{\bar{r}} \right)^{0.63} SC^{1/3} \left(\frac{A}{\bar{r}} \right)^{0.94} \tag{2-15}$$

Where A short mesh aperture (m), r_1, r_2 internal and external radius respectively, $and\ \bar{r}$ is mean radius.

Mass transfer coefficients are about three times higher than those obtained with smooth rotating cylinder electrodes under the same conditions.

The enhancement in mass transfer conditions were attributed to the turbulence promoting action of the expanded structure.

The mass-transfer at rotating electrodes of expanded metal is influenced by the geometric parameters of the expanded metal. Nevertheless, the experimental results are well correlated by a single equation when two parameters characterizing the geometry of the expanded metal ($A/\bar{r}$ and $r_2/\bar{r}$) were included.

Grau and Bisang [10] (2006) studied mass transfer at rotating cylinder electrodes of woven-wire meshes using the reduction of ferricyanide as test reaction. They reported that:

- Mesh electrodes present a higher specific surface area and promote turbulence in the electrolyte flowing over them.

- Mass-transfer at rotating cylinder electrodes of woven wire meshes are well correlated by a dimensionless equation involving the Sherwood and Reynolds number, in terms of the hydraulic diameter as characteristic length, the Schmidt number and two additional parameters, characterizing the geometry of the three-dimensional structure as shown in the following equation:

$$Sh = 0.967 \left(Re * \frac{r_2}{\bar{r}}\right)^{0.58} Sc^{1/3} \left(\frac{H}{\bar{r}}\right)^{0.47} \tag{2-16}$$

Where H is distance between wires (m)

- The mass-transfer coefficients for rotating cylinder electrodes of woven-wire meshes are about three times higher than those obtained with smooth electrodes, because of the turbulence promoting action of the meshes.

Fernando, et al. [48](2007) studied the effect of using four-plate, six-plate and concentric cylinder as counter electrodes on the RCE mass transport characterization. The Cu(II)/Cu(0) process in sulfuric acid is employed as the model reaction. They conclude that

- Based on the analysis of the $Sh = aRe^b Sc^{0.356}$ correlation, the values of the constant a, associated with shape and cell dimensions, were 0.012, 0.014, and 0.022 for four-plate, six-plate and concentric cylinder, respectively. This behavior suggests that both the shape and area of the counter electrode, influence the values of a.

- The values of b, associated with the hydrodynamic regime, were similar for the six-plate and the concentric counter electrodes, b = 0.91; whereas for the four-plate counter electrode, b = 0.95. The fact that the four-plate device gives greater values of b suggests that this device has a higher turbulence-promoting action than the others.

- The mass transport at RCE with four plates is similar to that observed with the concentric counter electrode, which is important from the technical and economic standpoints.

Riveraa and Navab [49] (2010) studied the effect of using two different inter-electrode gaps on the RCE mass transport characterization. The average mass transport coefficient was calculated based on limiting current technique, using the soluble reduction of triiodide (smooth RCE interface) and the copper deposition (roughness RCE interface) in KNO3 and H2SO4, respectively. They concluded that:

- Based on the analysis of the $Sh = aRe^b Sc^{0.356}$ correlation, the values of the constant a, associated with shape and cell dimensions, were 0.89 and 3.8, in the soluble system (I_3^-/I^-), for the gaps of 2.4 and 3.2 cm, respectively, indicating that this coefficient increases with inter-electrode space. While for copper deposition, these values were 0.00081 and 0.014, for the gaps of 2.4 and 3.2 cm. The values of this constant, a, were higher for the (I_3^-/I^-) system (with diffusion coefficient of $1.12 \times 10^{-5} cm^2 s^{-1}$) than for the Cu(II)/Cu process (with diffusion coefficient of 5.94×10^{-6} cm^2 s^{-1}), suggesting that a is also favored with diffusion coefficient of electro-active specie.

- The constant b, associated with hydrodynamic regime, exhibits values of 0.43 and 0.33 for the gaps of 2.4 and 3.2 cm, respectively, in the system I_3^-/I^-, indicating that hydrodynamics on the smooth RCE diminishes according to the inter-electrode space. While for the system (Cu(II)/Cu), the values of b were 0.91 and 0.88, for the gaps of 2.4 and 3.2. These values were higher for the copper deposition than for the soluble system, due to micro turbulence at the roughened (and often powdery deposits) RCE interface.

- For the design purposes of RCE, it is recommendable that the electrochemical engineer should obtain experimentally the corresponding mass transport correlation, because it depends on the inter-electrode gap, hydrodynamics of smooth and rough RCE interface (given by the electrochemical reaction), transport properties of electrolyte, cell geometry, and anode and cathode arrangements.

Grau, and Bisang [45] (2011) studied mass transfer at a rotating cylinder electrode with different turbulence promoters using the reduction of ferricyanide

as a test reaction. Four types of turbulence promoters were examined: expanded plastic meshes, Teflon structures, a plastic woven mesh and a plastic perforated net, which were rotated together with the electrode. They concluded that:

- Mass-transfer coefficients for rotating cylinder electrodes with turbulence promoters are, in general, twice as large as those obtained with smooth electrodes.

- The influence of the geometrical parameters as well as the type of promoter was of little importance in mass-transfer behavior for the examined promoters.

- Woven meshes as turbulence promoters showed the best performance at higher rotation speeds, at 115 s^{-1} a mass transfer enhancement factor of 2.12 was obtained. At rotation speeds lower than 60 s^{-1} Teflon structures, with geometric dimensions more pronounced than expanded plastic meshes, presented an appropriate behavior.

- The increase in the number of sheets of a turbulence promoter, the use of static promoters and the employment of a rotating cylinder partially covered with a promoter diminished the mass-transfer performance.

Chapter three

Experimental work

3.1 Introduction

Throughout this investigation; the experimental work was carried out to determine the limiting current density of dissolved oxygen on brass under turbulent flow conditions for rotating speeds of 200, 400, 600, 800, and 1000 rpm in an aqueous 0.1N NaCl at applied temperatures of 35, 45, and 55°C.

The experimental work was divided into two main parts:

1. Determination of the limiting current density of dissolved oxygen on smooth rotating cylinder electrode with variable solution pH values of 5, 6, and 7.
2. Determination of the limiting current density of dissolved O_2 on enhanced rotating cylinder electrode one and two in order to compare with smooth normal rotating cylinder electrode at pH equals to six.

3.2. The electrolyte

Electrolyte solution used in this work was aqueous NaCl of concentration 0.6%. The concentration of NaCl ,which has a molecular weight of 58.44 g/gmol, was diluted by distilled water to obtain the required normality of 0.1 N NaCl. The required pH was adjusted by using analar hydrochloric acid HCl and analar sodium hydroxide NaOH. The concentrated acid, which has a molecular weight of 36.64 g/gmol, concentration 36%, and density of 1.17 gm/cm^3, was diluted by distilled water to obtain 1N of HCl. Likewise, sodium hydroxide which has a molecular weight of 40.0 g/gmol, was diluted by distilled water to obtain 1N of NaOH.

3.3 The Working Electrode (Specimen).

The working electrode (cathode) was a rotating cylinder 25 mm in diameter, 27 mm long with four rectangular extensions1 and 3 cm long, 1 cm wide , and 1 mm thick, made of brass to generate additional turbulence. The lower part of the electrode was open in order to allow the electrolyte flow between the longitudinal extensions. The configuration details are shown in fig. 3-1 below.

(a) Enhanced cylinder one**.**

(b) Enhanced cylinder two.
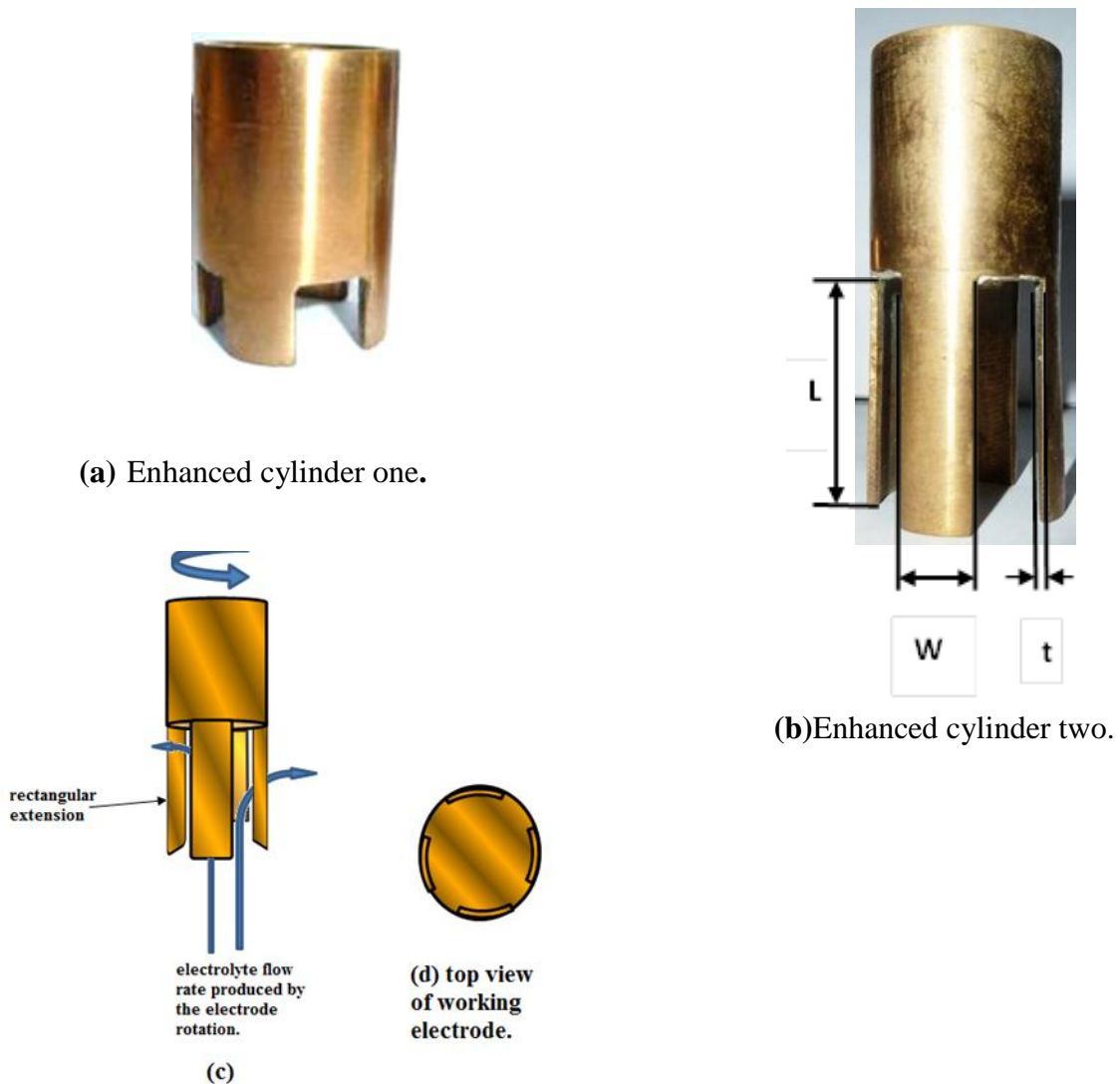
Figure 3-1. Schematic view of the working electrode**.**

However, the smooth cylinder, which provides a baseline for performance comparison, was used as a working electrode in a cylindrical shape for limiting current density measurement with a length of 2.7cm and 2.5 cm diameter, made of brass.

The material specifications of electrode used are given blow in table 3-1, analyzed by the State Company for Inspection and Engineering Rehabilitation of Engineering Industries &Minerals.

Table 3-1: Analysis of Specimen**.**

Elements	Zn	Pb	Sn	P	Mn	Fe	Ni	Si	Mg	Cr	As	Sb	S	C	Cu
Weight%	2.49	5.09	5.91	0.008	0.0005	0.041	0.638	0.001	0.0001	0.0009	0.040	0.132	0.131	0.0016	Rest.

3.4 Specimen clean-up

The following solvents were used to decrease and clean the specimens:

- Acetone: CH_3CH_6O of concentration = 99 % supplied by FLUKA.
- Emery paper grades 120, 220, 320, 400, and 2000.

3.5 Apparatus

- **Thermometers**: They are made of glass to measure temperature up to100^oC.
- **Water bath**: Water bath with temperature controller was used, type Memmert, Model WNB 10, Power Rating   230 V (+/- 10%), 50/60 Hz calories 1.200 W (during heating).Temperature Range from +10 °C (however, at least 5 °C above ambient) up to +95 °C with additional boiling mode +100 °C).

- **pH-meter**: A digital pH-meter, manufactured by Hanna ,type pH 211, was used to measure and monitor the pH of the working solution during the test, range from -2.00 to 16 pH, accuracy at 20°C / 68°F ± 0.01 pH, Power supply 12 VDC adapter (included).   pH Calibration 1 or 2 point calibration, 5 buffers available (4.01, 6.86, 7.01, 9.18, 10.01).
- **DC Adjustable power supply**, type BLT, Voltage Output 0-30V, Current Output 0-5A.
- **Direct driven digital stirrer**, type HAP-DO GLOBAL LAB, to obtain different rotational velocities.
- **Electronic Balance:** High accuracy digital balance with 4 decimal points of type (Sartorius BL210 S). The balance has 0.1 mg accuracy and 210 g maximum load.
- **Resistance box**, type POPULAR- PE06RN, with maximum range of 10 MΩ, to control the current flow.
- **Digital Ammeter**, type Pros Kit MT-1210, to measure the current.
- **Digital Voltmeter**, type Pros Kit MT-1210, to measure the potential.
- **Saturated Calomel Electrode (SCE)**, as a reference electrode employed to measure the potentials.
- **Graphite electrode,** as auxiliary electrode (anode).
- **Carbon brush,** to attain electrical connection with cathode (specimen)**.**
- **Desiccator**.
- **Luggin capillary probe.**
- **Brass shaft.**

3.6 Accessories

- Beakers (2 and 3 liters).
- Electrical connection wires**.**
- Hooks.
- Stand.

- Pipette.
- Graduated cylinder (1000 milliliters).
- Teflon tape.
- Conical flask.

3.7 Experimental apparatus

Figure 3-2 shows the experimental apparatus (as illustrated in Figs. 3-3, 3-4, 3-5) that was used for performing the experimental test runs.
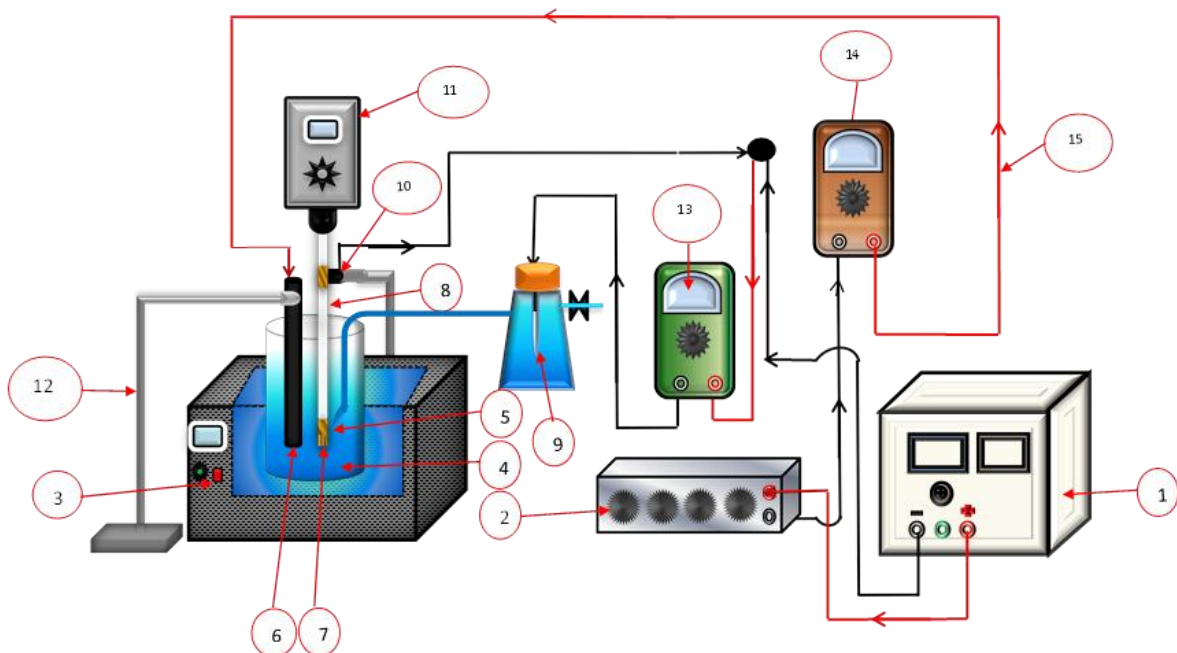
No.	Name	No.	Name
1	Power supply	9	Reference Saturated Calomel Electrode (SCE).
2	Resistance box	10	Carbon brush
3	water bath	11	Stirrer
4	0.1M NaCl	12	Stand
5	Luggin capillary tip	13	Voltmeter
6	Graphite electrode (anode)	14	Ammeter
7	Working electrode	15	Electrical wires
8	Rotating shaft		

Figure 3-2. Experimental System

Figure 3-3. Rotating Cylinder Electrode RCE system.

Figure 3-4. Smooth Rotating Cylinder Electrode.
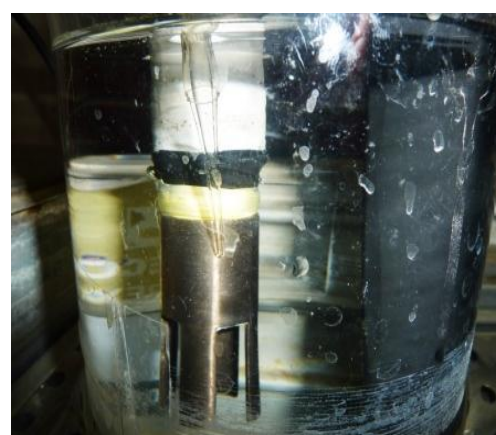
Figure 3-5. Enhancement Rotating Cylinder Electrode.

3.8 Experimental program:

3.8.1 Specimen Preparation:

Before each experiment the specimen was abraded in a sequence of emery papers grades: (120, 220, 320, 400, and 2000.), washed with tap water followed by distilled water, dried with clean tissue, immersed in annular acetone for 1 minute, dried with clean tissue. The specimen then was stored for 24 h in vacuum desiccator over high activity silica gel until use.

3.8.2 Experimental Procedure:

1) The specimen was connected to -ve terminal of power supply to serve as cathode and graphite to +ve terminal to serve as anode.
2) When the bath reached the required temperature, the specimen was immersed and the electrical circuit was switched on.
3) The power supply was set at 5 V (applied voltage).
4) Anode (graphite) and cathode (working electrode) are both immersed in cell beaker to start the run.
5) The area of anode (graphite), which immersed in water, was 3 times the area of cathode (working electrode) to ensure the limiting current density occurs on cathode.
6) Read steady state current (i = mA) and potential (V = volt) of rotating cylinder after each one minute of test run.
7) The capillary tip was always placed at a fixed distance 1-2 mm from cathode (specimen) [55] ,while connected to calomel electrode to measure the specimen potential for each run.
8) Change resistance of resistance box (0 to 10^6 Ohm) to nullify the current, i.e., i =0 mA.
9) Then the polarization curve can be drawn and the limiting current can be obtained.

10) The experimental runs were repeated three times or more for checking reproducibility and accuracy.

11) The total number of runs were 90, 45 runs for smooth rotating cylinder electrode with variable solution pH values of 5, 6, and 7, and 45 runs for smooth, enhancement one, and two rotating cylinder electrode .

Chapter four

Experimental Result

4.1 Introduction

 The experimental results for determining the limiting currents of dissolved oxygen from cathodic polarizations curves on brass rotating cylinder are presented in this chapter. All experiments were carried out in 0.1N NaCl solution of various pH values, different rotational velocities at the temperatures 35, 45 and 55° C.

The experimental work was performed in two parts leading to the results presently introduced as follows:

1. ***Part one***: Cathodic polarization curves using smooth rotating cylinder electrode in solutions of pH values 5, 6, and 7 to assess to the influence of hydrogen evolution.

2. ***Part two***: Cathodic polarization curves on two types of rotating cylinder electrode to evaluate the level or degree of enhancement at the above temperatures in solutions of pH equal to six.

The physical properties, i.e., viscosity, density, oxygen diffusion coefficient and solubility are presented in Appendix A.

4.2 Part one

Figures 4-1 to 4-9 show the cathodic polarization curves on brass in 0.1 N NaCl at 35 45, and 55°C respectively at different flow rotational velocities. From these figures it is clear that the limiting current is increased with increasing rotational velocity and temperature in NaCl solutions.

0.1 N NaCl of pH 5 at 35ºC
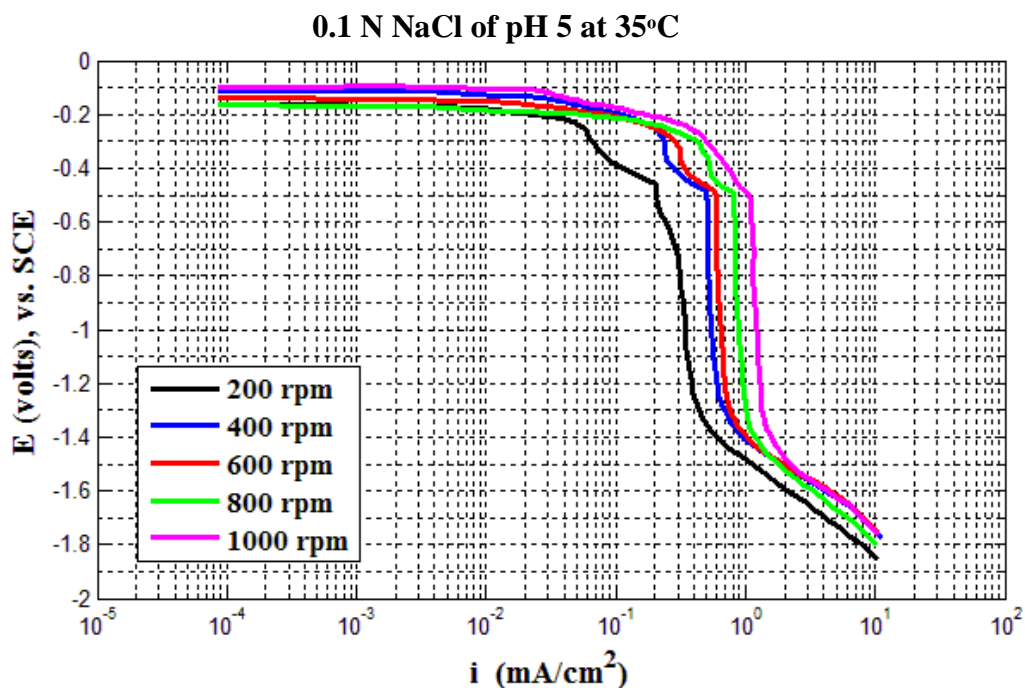
Figure 4-1 Cathodic polarization curves on brass rotating cylinder in 0.1 N NaCl of pH 5 at 35ºC.

0.1 N NaCl of pH 5 at 45ºC
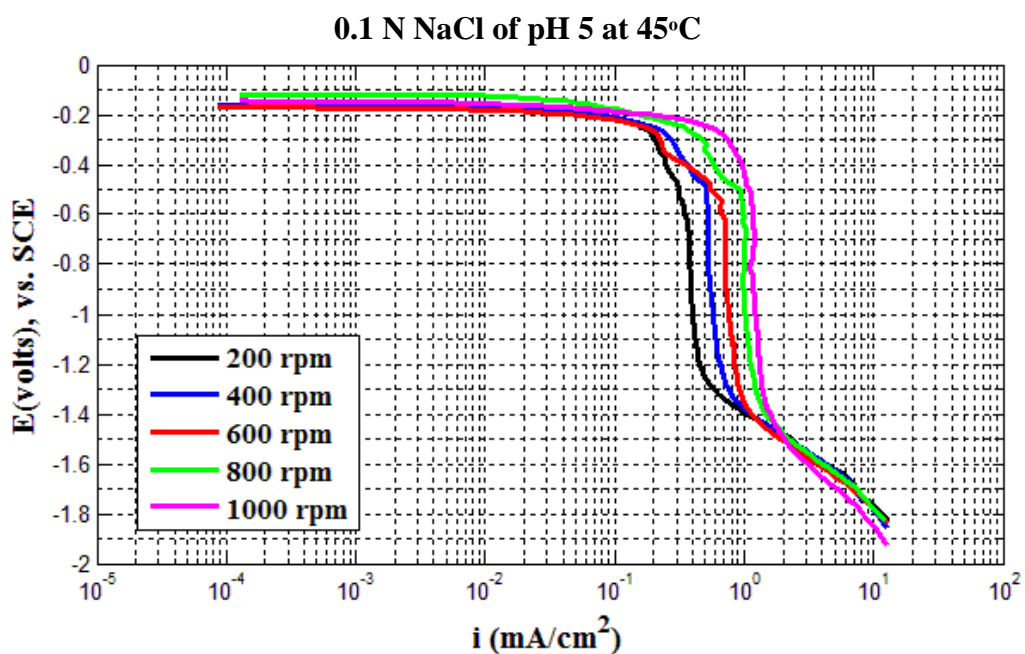
Figure 4-2 Cathodic polarization curves on brass rotating cylinder in 0.1 N NaCl of pH 5 at 45ºC.

0.1 N NaCl of pH 5 at 55°C

Figure 4-3 Cathodic polarization curves on brass rotating cylinder in 0.1 N NaCl of pH 5 at 55°C.

0.1 N NaCl of pH 6 at 35°C

Figure 4-4 Cathodic polarization curves on brass rotating cylinder in 0.1 N NaCl of pH 6 at 35°C.

0.1 N NaCl of pH 6 at 45°C

Figure 4-5 Cathodic polarization curves on brass rotating cylinder in 0.1 N NaCl of pH 6 at 45°C.

0.1 N NaCl of pH 6 at 55°C

Figure 4-6 Cathodic polarization curves on brass rotating cylinder in 0.1 N NaCl of pH 6 at 55°C.

0.1 N NaCl of pH 7at 35°C
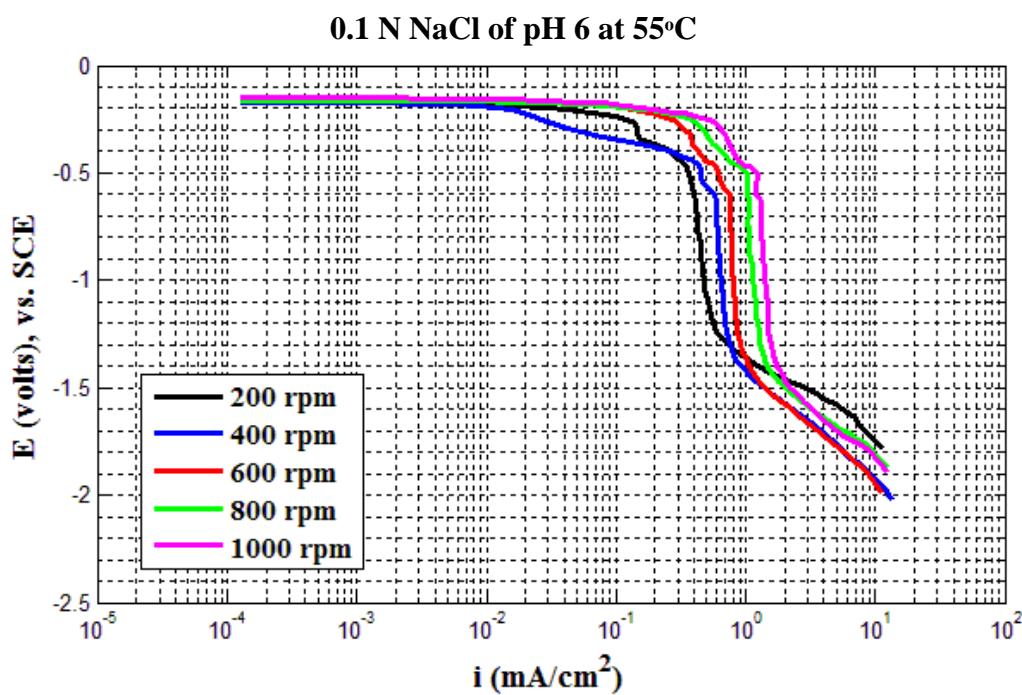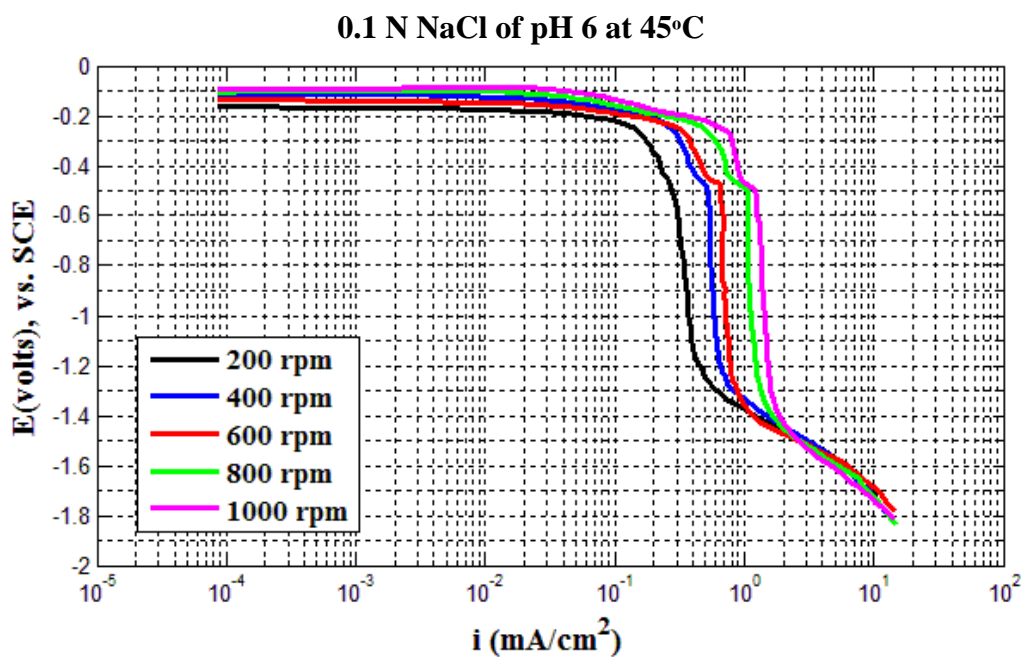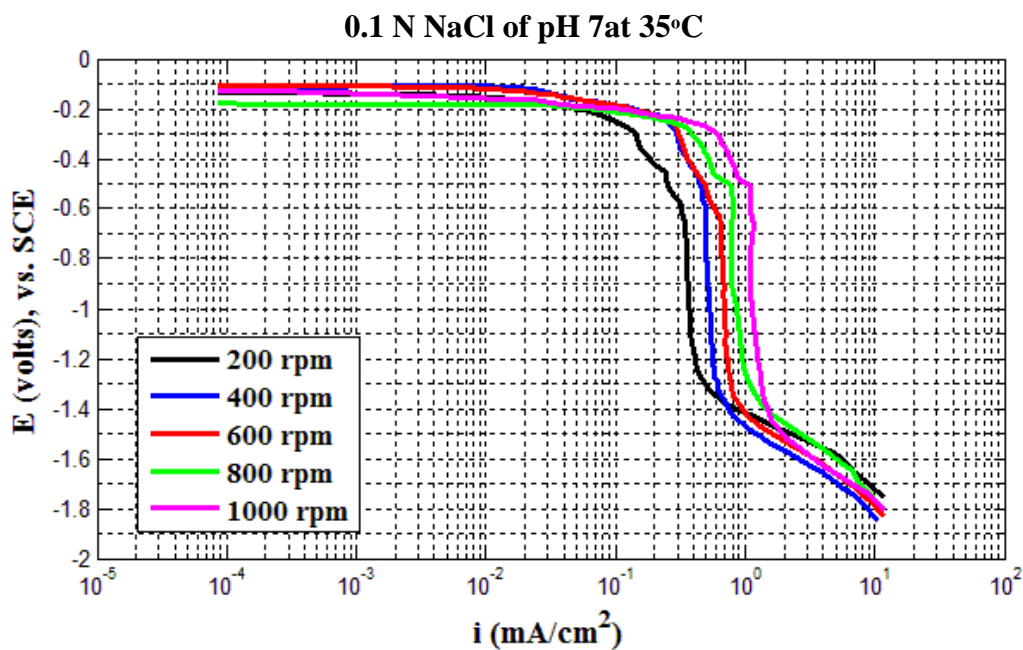
Figure 4-7 Cathodic polarization curves on brass rotating cylinder in 0.1 N NaCl of pH 7 at 35°C.

0.1 N NaCl of pH 7 at 45°C
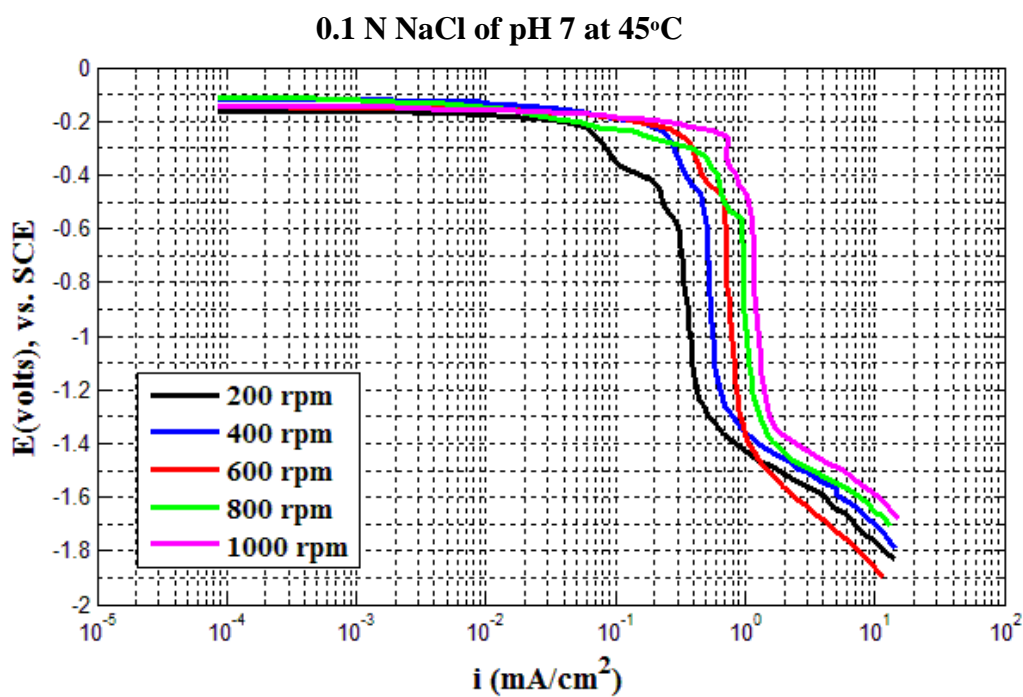
Figure 4-8 Cathodic polarization curves on brass rotating cylinder in 0.1 N NaCl of pH 7 at 45°C.

0.1 N NaCl of pH 7 at 55°C
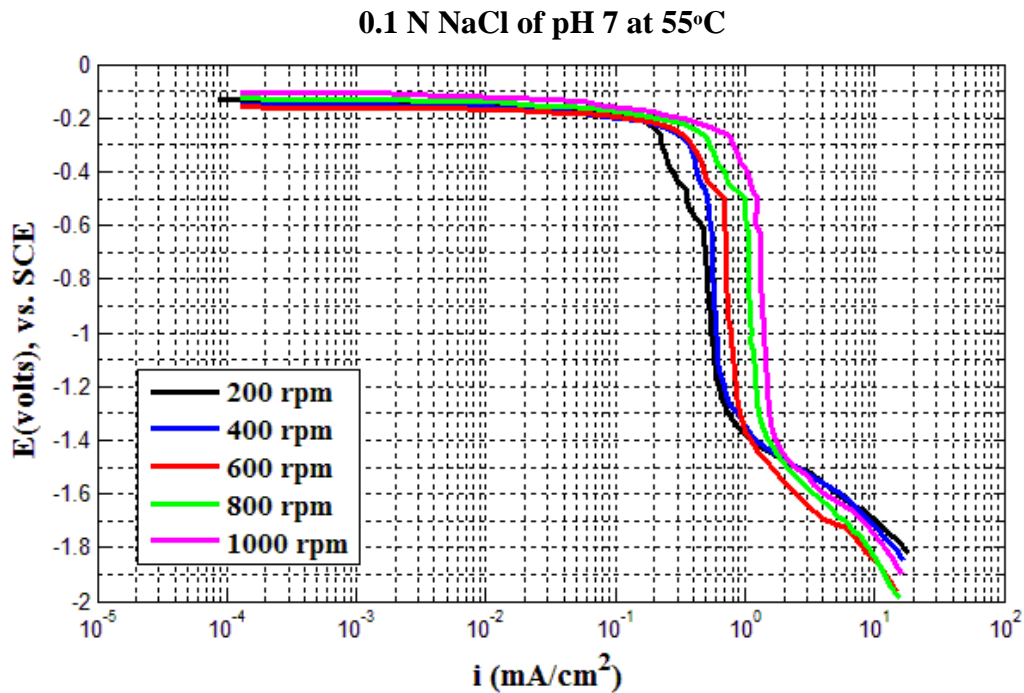
Figure 4-9 Cathodic polarization curves on brass rotating cylinder in 0.1 N NaCl of pH 7 at 55°C.

Table 4-1 shows the experimental results of dissolved oxygen limiting current (i_{O2}) on brass in solutions of pH 5, 6, and 7 at 35, 45 and 55°C respectively. From these results it is evident that that increasing of rotational velocity leads to increase the limiting current density of oxygen which is dependent on the variations of physical properties due to temperature. Also the pH effects on limiting current density is slight and negligible at the given temperature and rotational velocity. The limiting current density i_L is obtained from polarization curves by using Gabe and Makanjoula method[34] which was referred to in chapter one. The values of u in m/s were calculated using the following simple conversion equation:

$$u\left(\frac{cm}{s}\right) = \frac{\pi * d(cm) * \omega(rpm)}{60} \tag{4. 1}$$

Table 4-1: Experimental limiting current densities on brass rotating cylinder in 0.1 N NaCl solutions of pH 5, 6, and 7 as a function of velocity at different temperatures.

Temperature	Rotation velocity ω(RPM)	limiting current density, i_l (mA/cm^2) at pH=5	limiting current density, i_l (mA/cm^2) at pH=6	limiting current density, i_l (mA/cm^2) at pH=7
35°C	200	0.31275	0.3134	0.3277
	400	0.5017	0.5041	0.5139
	600	0.6165	0.61715	0.6212
	800	0.88697	0.8956	0.91085
	1000	1.1269	1.137	1.1565
45°C	200	0.34145	0.3543	0.3614
	400	0.53575	0.5443	0.5518
	600	0.7079	0.7194	0.73005
	800	0.9874	1.0012	1.00905
	1000	1.2235	1.236	1.240
55°C	200	0.36845	0.371	0.3852
	400	0.65765	0.66855	0.67025
	600	0.8016	0.80865	0.8106
	800	1.13325	1.146	1.1565
	1000	1.3880	1.3965	1.405

4.3 Part two :

Figures 4-10 to 4-24 show cathodic polarization curves of dissolved oxygen on brass in 0.1N NaCl of pH 6 at 35 45, and 55°C respectively. These were at different rotational flow velocities as stated above for enhanced one, and enhanced two rotating cylinder electrodes. The experimental cathodic polarization curves for a similar smooth rotating cylinder electrode are also reported in these figures, which

provide a baseline for performance comparison. It can be seen that the limiting current density values for enhanced one and two cylinders are higher than smooth cylinder devoid of longitudinal extensions. These longitudinal extensions present a higher specific area and promote additional turbulence in the electrolyte flowing over the cylinder surface.
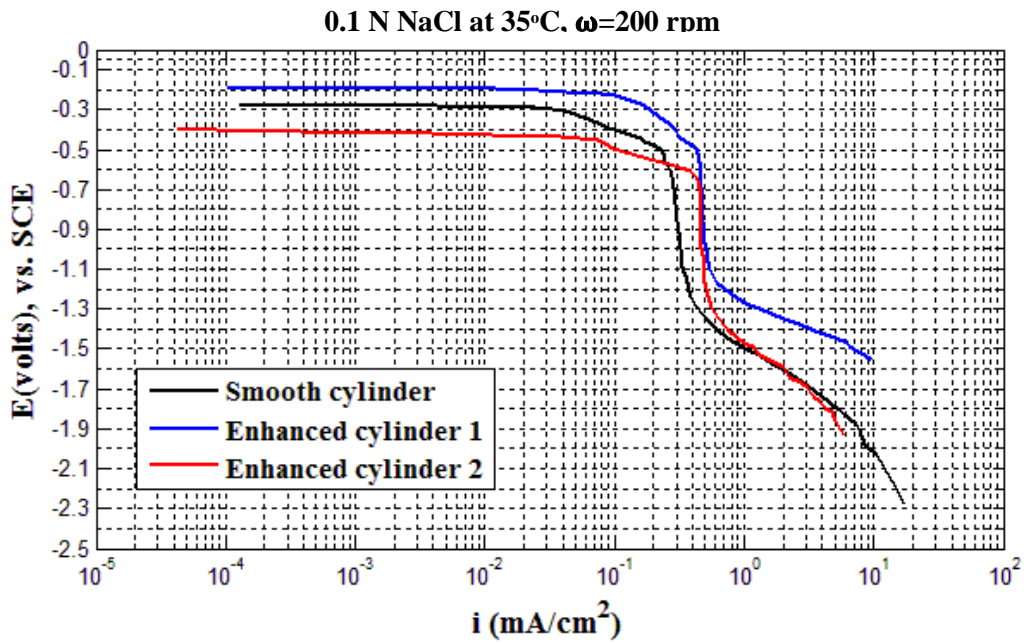
Figure 4-10 Cathodic polarization curves on brass rotating cylinder in 0.1 N NaCl for smooth, enhanced one, and two rotating cylinder at 200 rpm and 35°C.

0.1 N NaCl at 35°C. ω=400 rpm
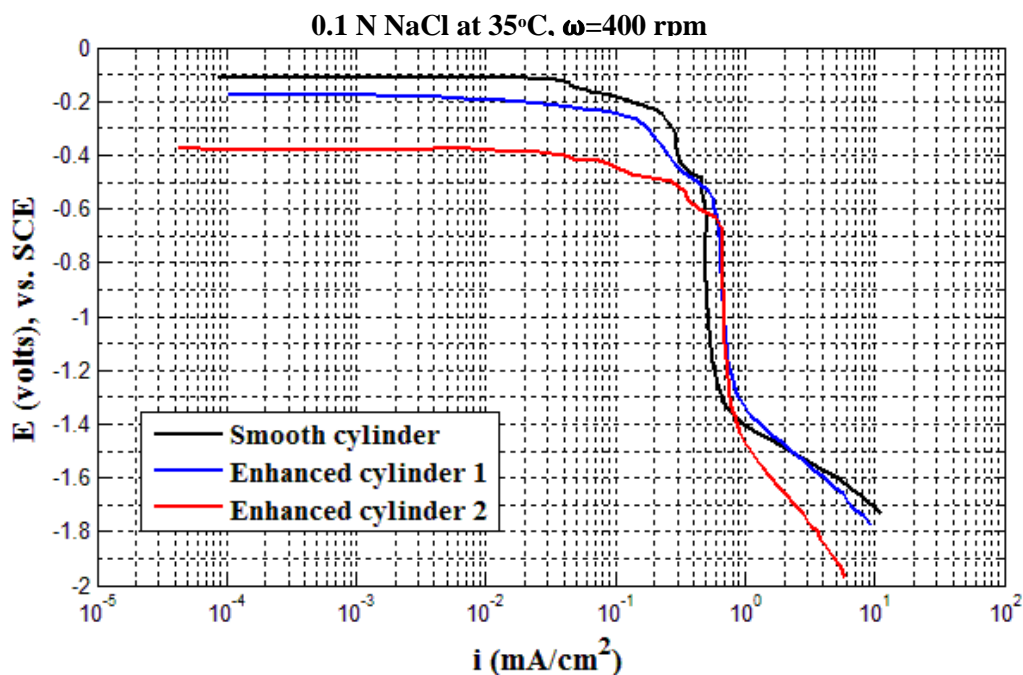
Figure 4-11 Cathodic polarization curves on brass rotating cylinder in 0.1 N NaCl NaCl for smooth, enhanced one and two rotating cylinder at 400 rpm and 35°C

0.1 N NaCl at 35°C. ω=600 rpm
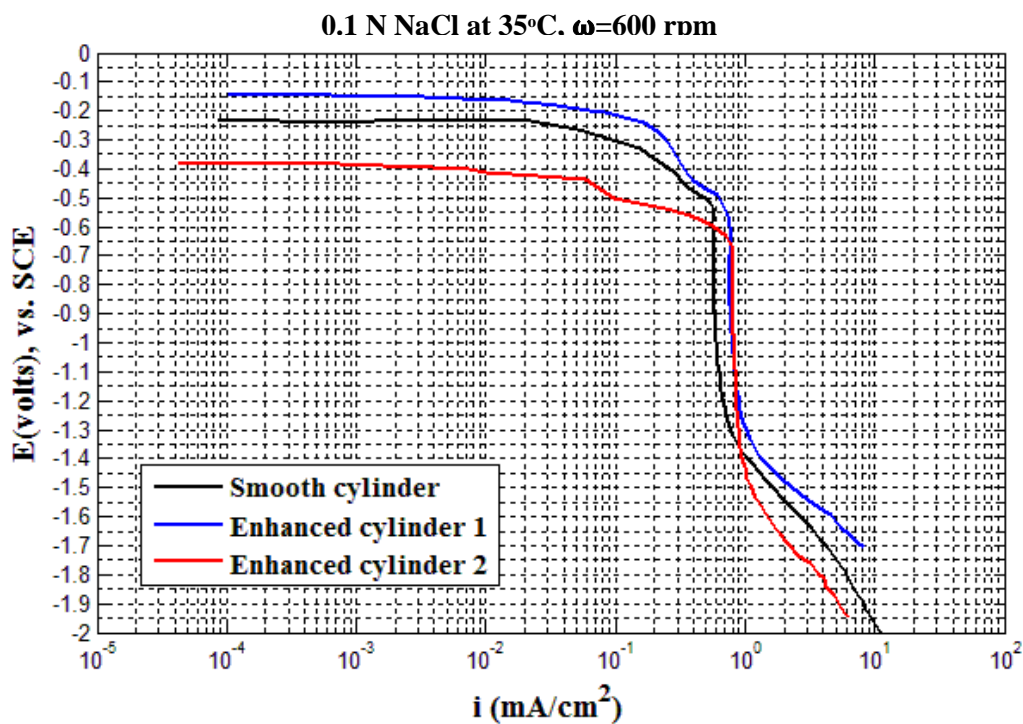
Figure 4-12 Cathodic polarization curves on brass rotating cylinder in 0.1 N NaCl for smooth, enhanced one and two rotating cylinder at 600 rpm and 35°C
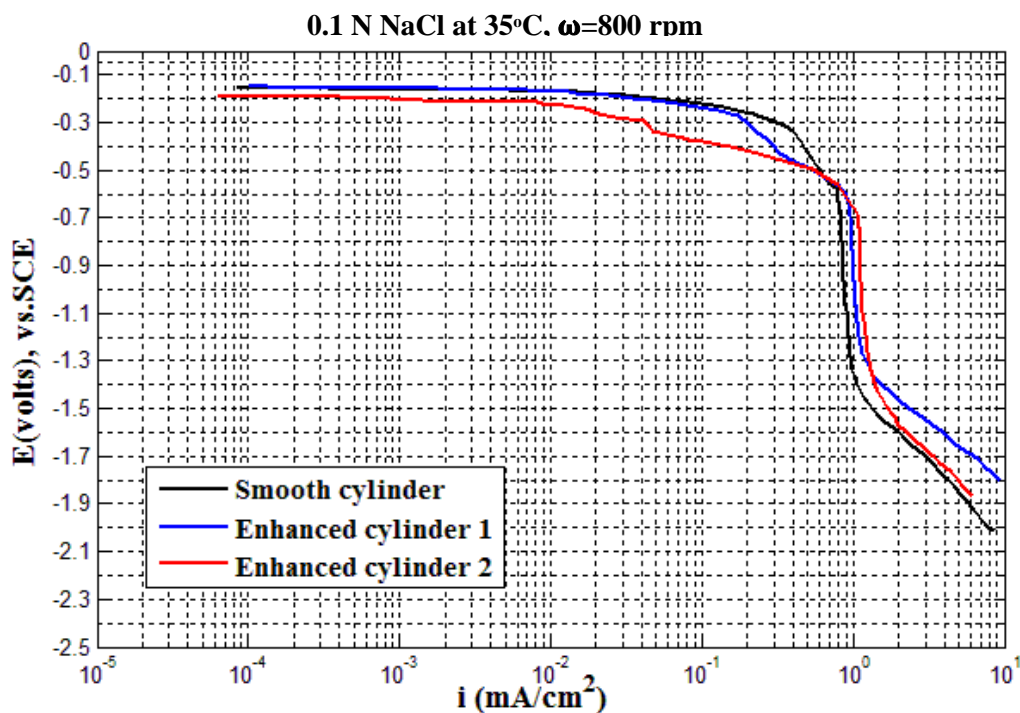
Figure 4-13 Cathodic polarization curves on brass rotating cylinder in 0.1 N NaCl for smooth, enhanced one and two rotating cylinder at 800 rpm and 35°C.
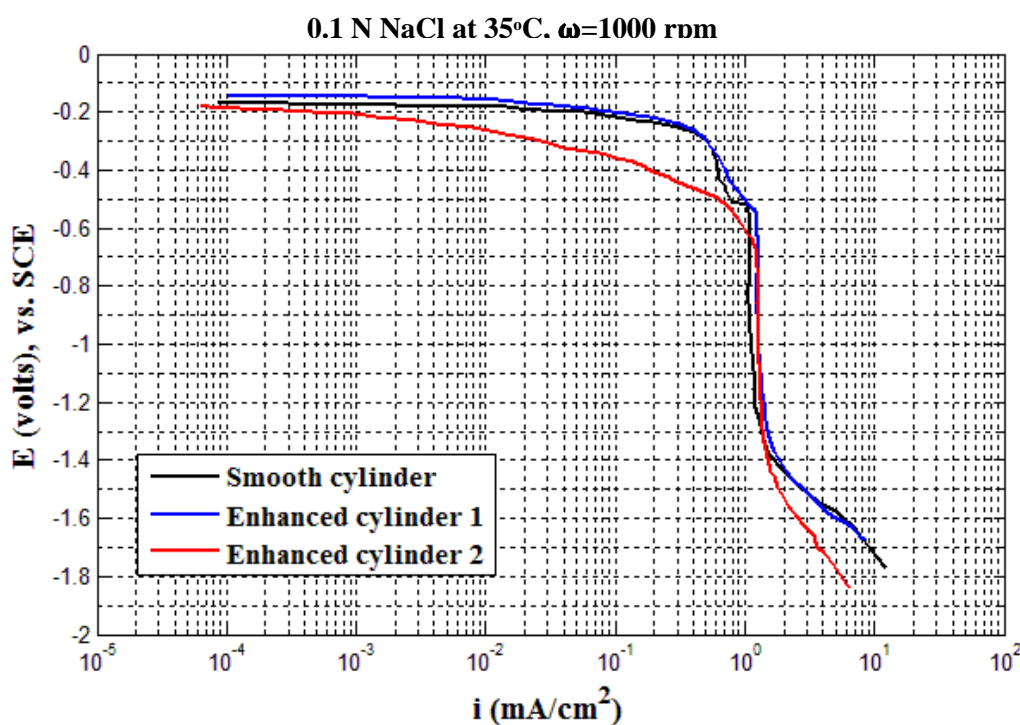
Figure 4-14 Cathodic polarization curves on brass rotating cylinder in 0.1 N NaCl for smooth, enhanced one and two rotating cylinder at 1000 rpm and 35°C
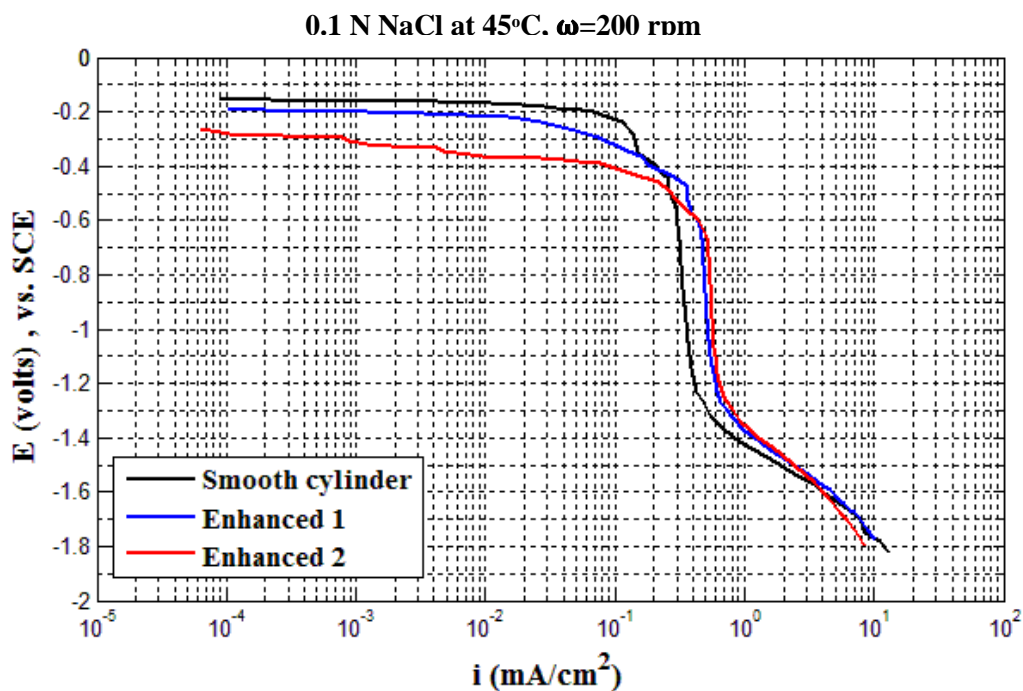
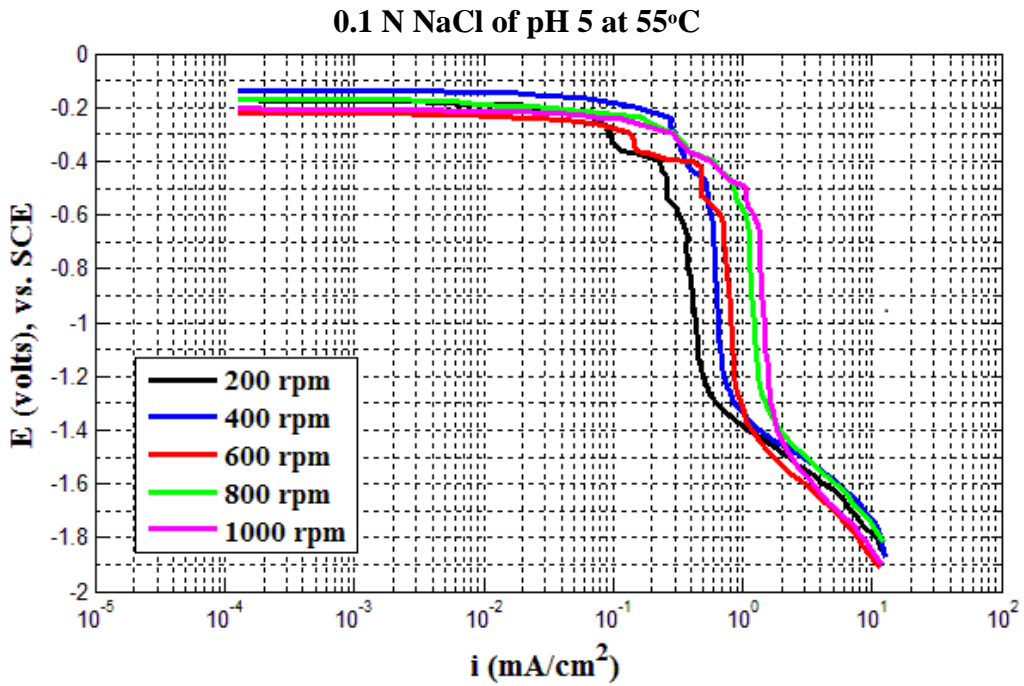**Figure 4-15** Cathodic polarization curves on brass rotating cylinder in 0.1 N NaCl for smooth, enhanced one and two rotating cylinder at 200 rpm and 45°C.
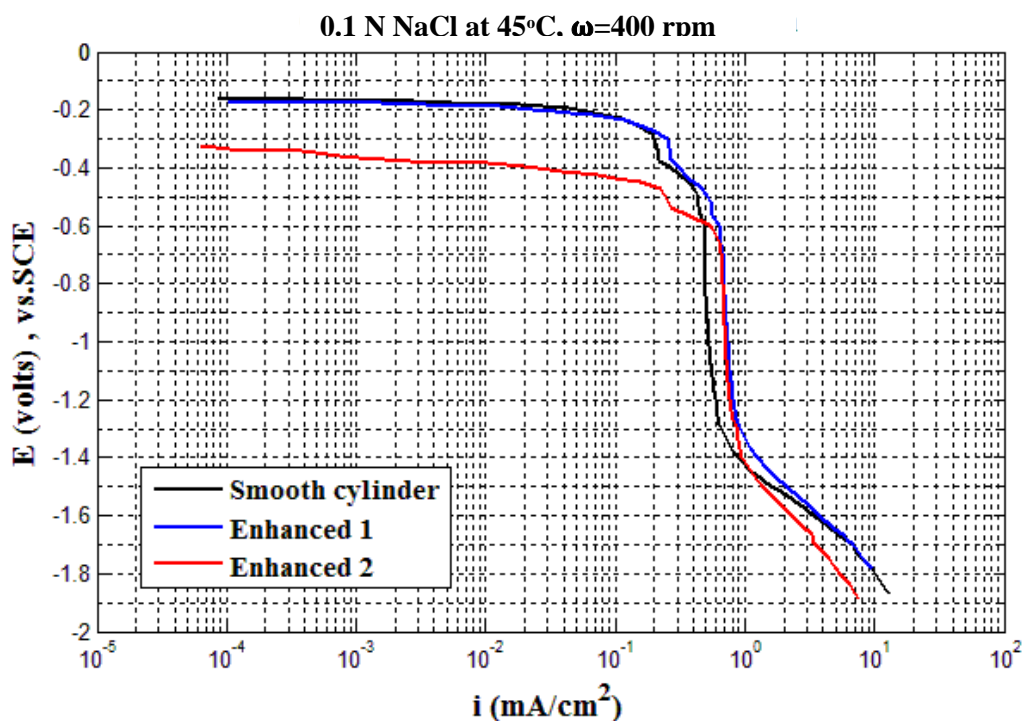
Figure 4-16 Cathodic polarization curves on brass rotating cylinder in 0.1 N M NaCl for smooth, enhanced one and two rotating cylinder at 400 rpm and 45°C.

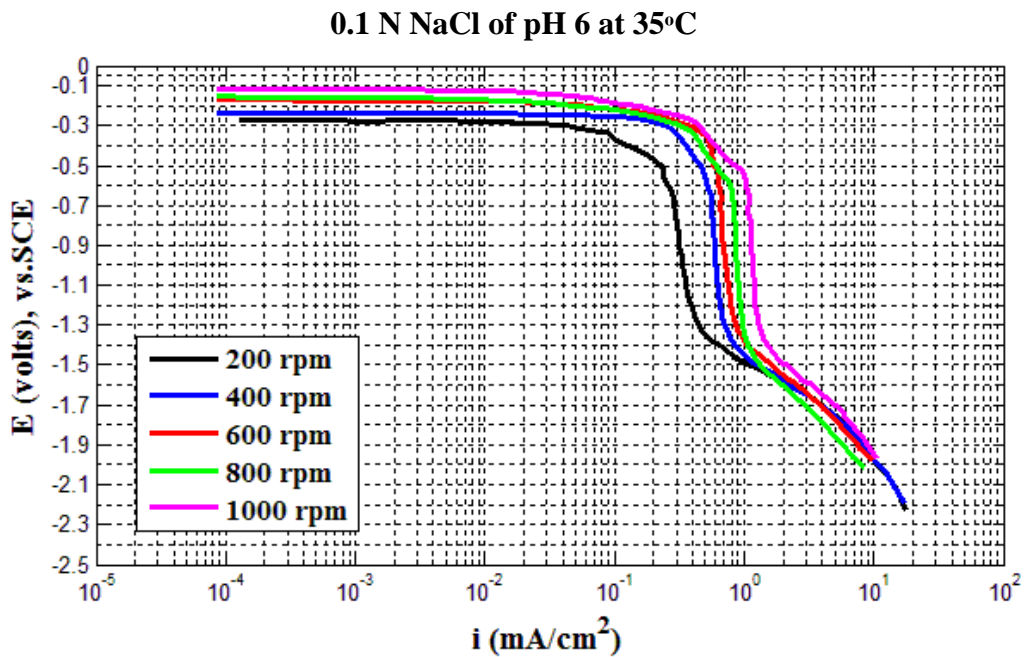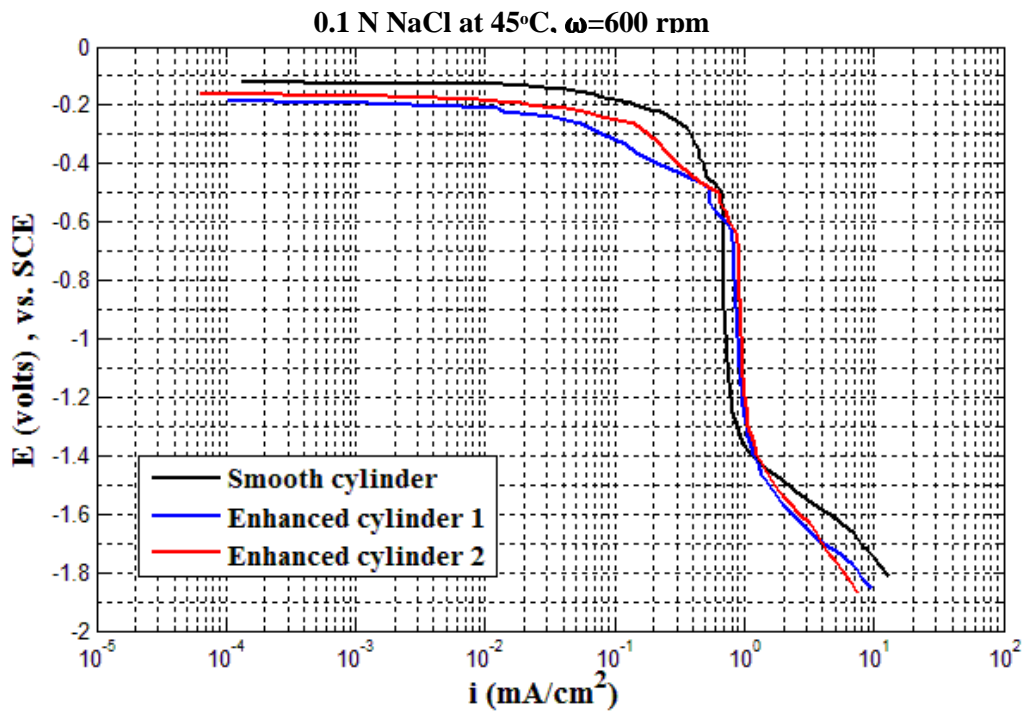**Figure 4-17** Cathodic polarization curves on brass rotating cylinder in 0.1 N NaCl for smooth, enhanced one and two rotating cylinder at 600 rpm and 45°C.
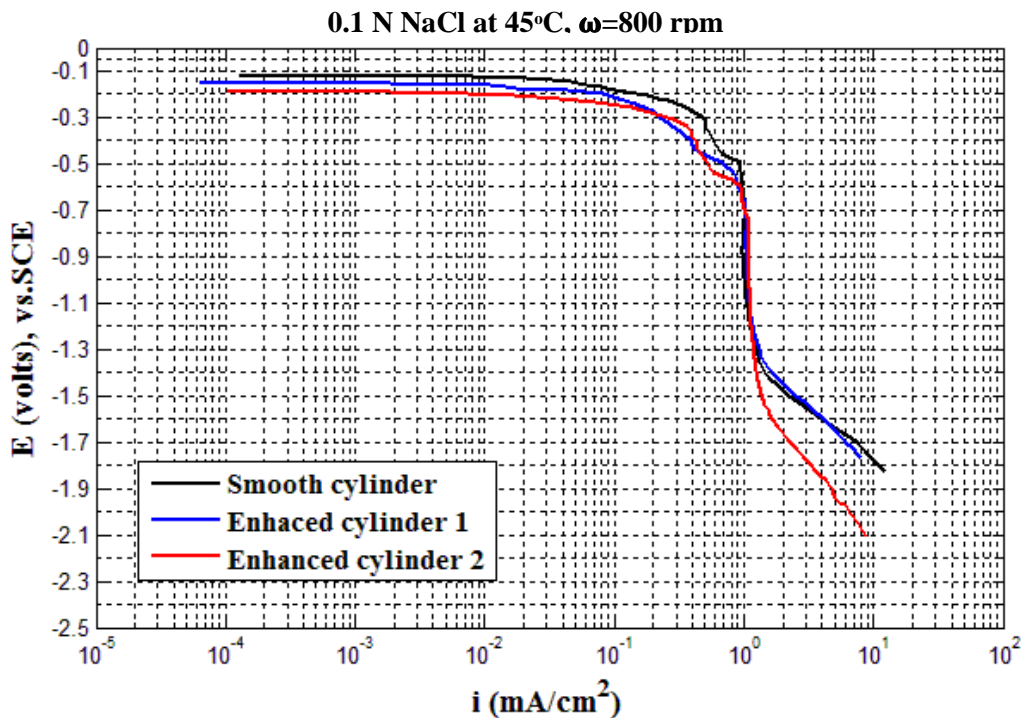
Figure 4-18 Cathodic polarization curves on brass rotating cylinder in 0.1 N NaCl for smooth, enhanced one and two rotating cylinder at 800 rpm and 45°C.

0.1 N NaCl at 45°C, ω=1000 rpm
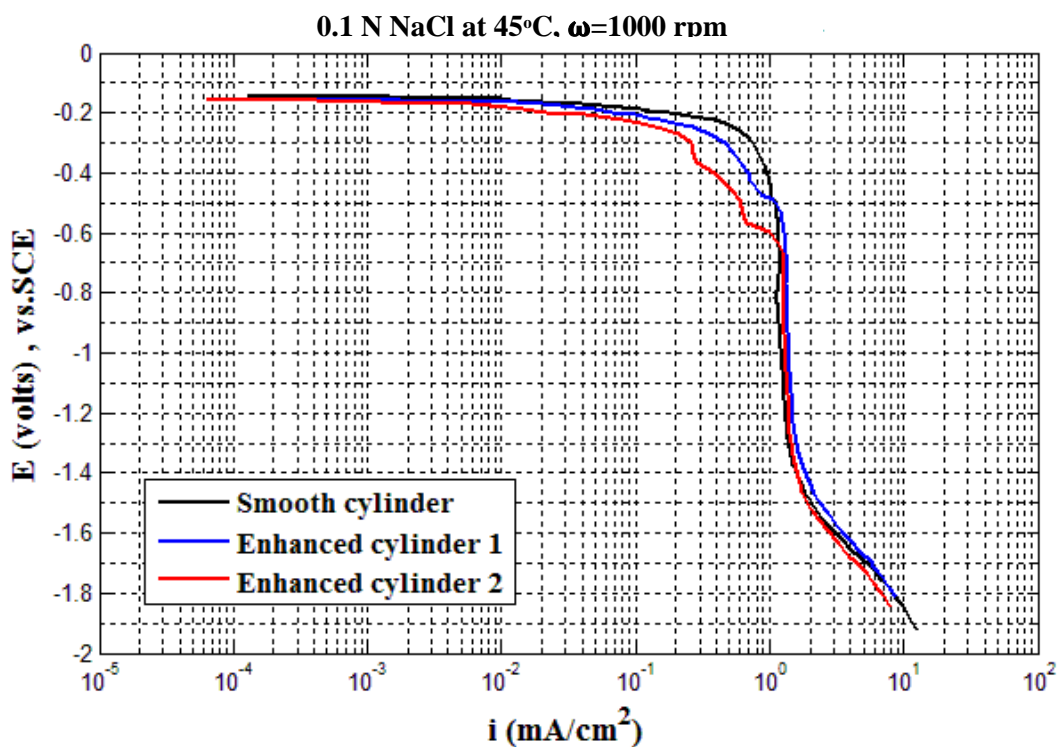
Figure 4-19 Cathodic polarization curves on brass rotating cylinder in 0.1 N NaCl for smooth, enhanced one and two rotating cylinder at 1000 rpm and 45°C.

0.1 N NaCl at 55°C, ω=200 rpm
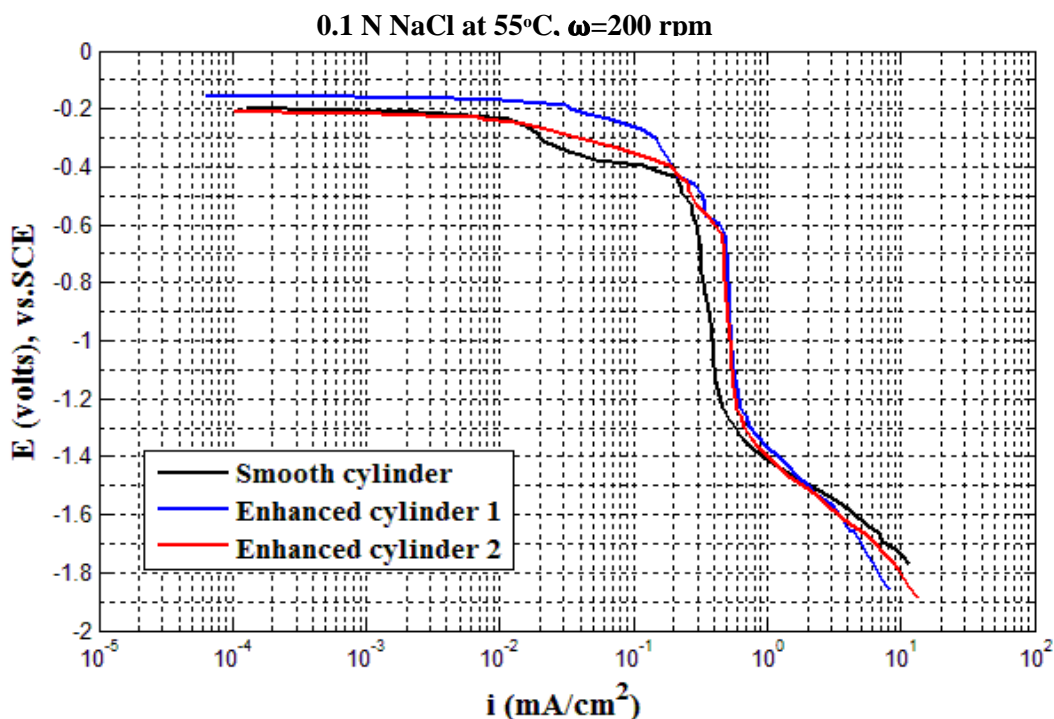
Figure 4-20 Cathodic polarization curves on brass rotating cylinder in 0.1 N NaCl for smooth, enhanced one and two rotating cylinder at 200 rpm and 55°C.

46
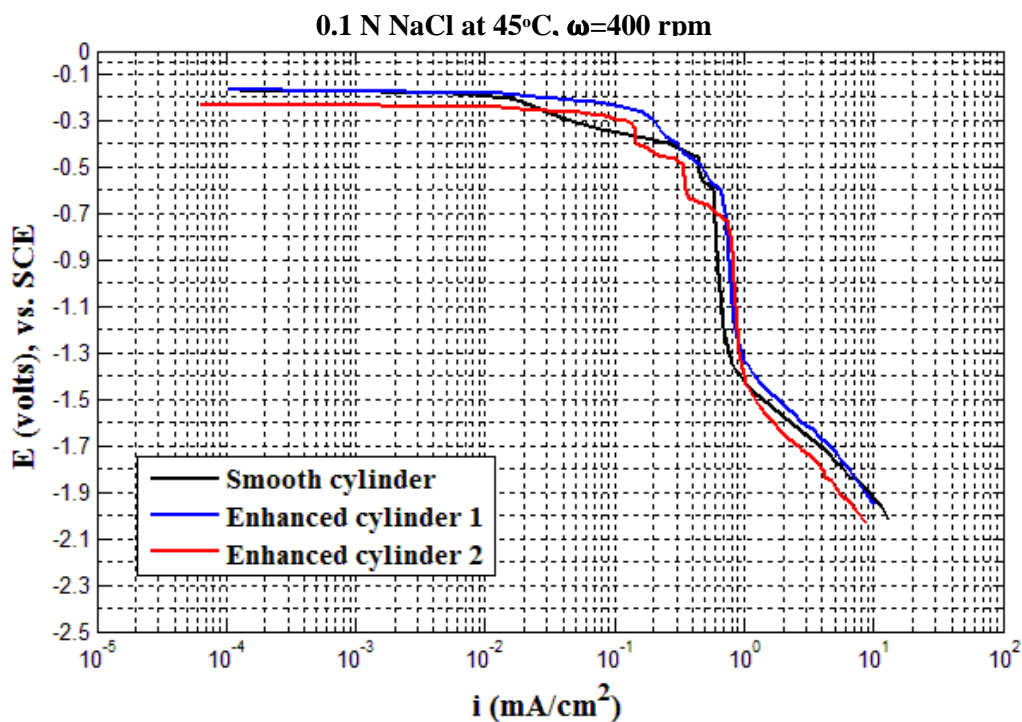
Figure 4-21 Cathodic polarization curves on brass rotating cylinder in 0.1 N NaCl for smooth, enhanced one and two rotating cylinder at 400 rpm and 55°C.
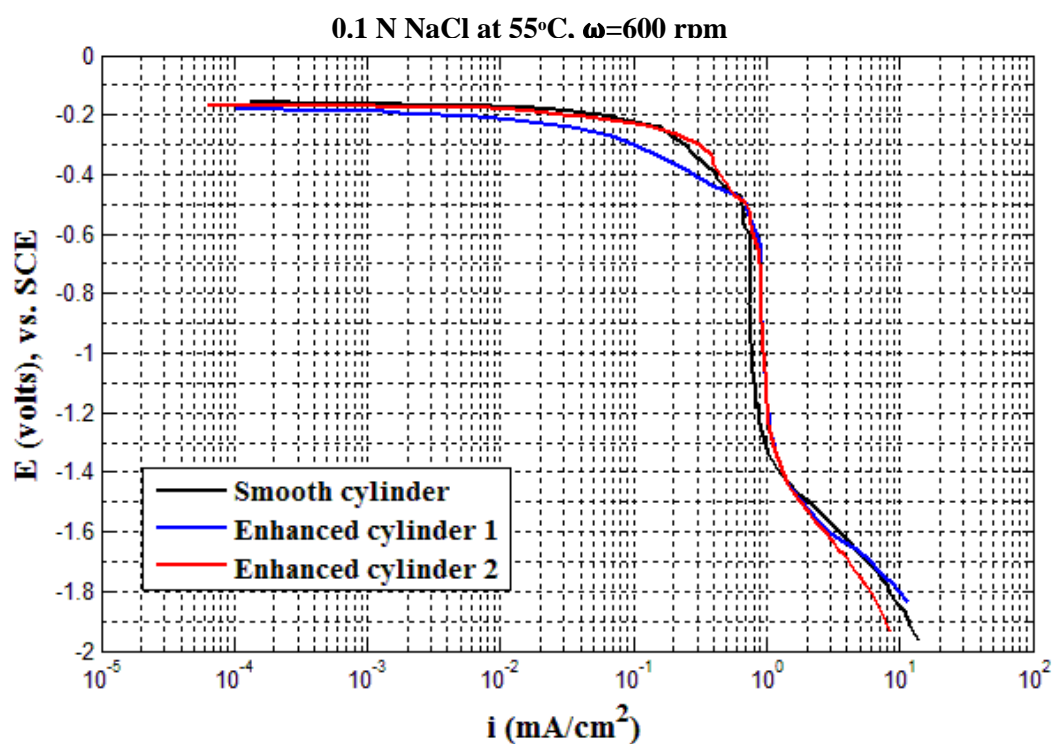
Figure 4-22 Cathodic polarization curves on brass rotating cylinder in 0.1 N NaCl for smooth, enhanced one and two rotating cylinder at 600 rpm and 55°C.

0.1 N NaCl at 55ºC, ω=800 rpm
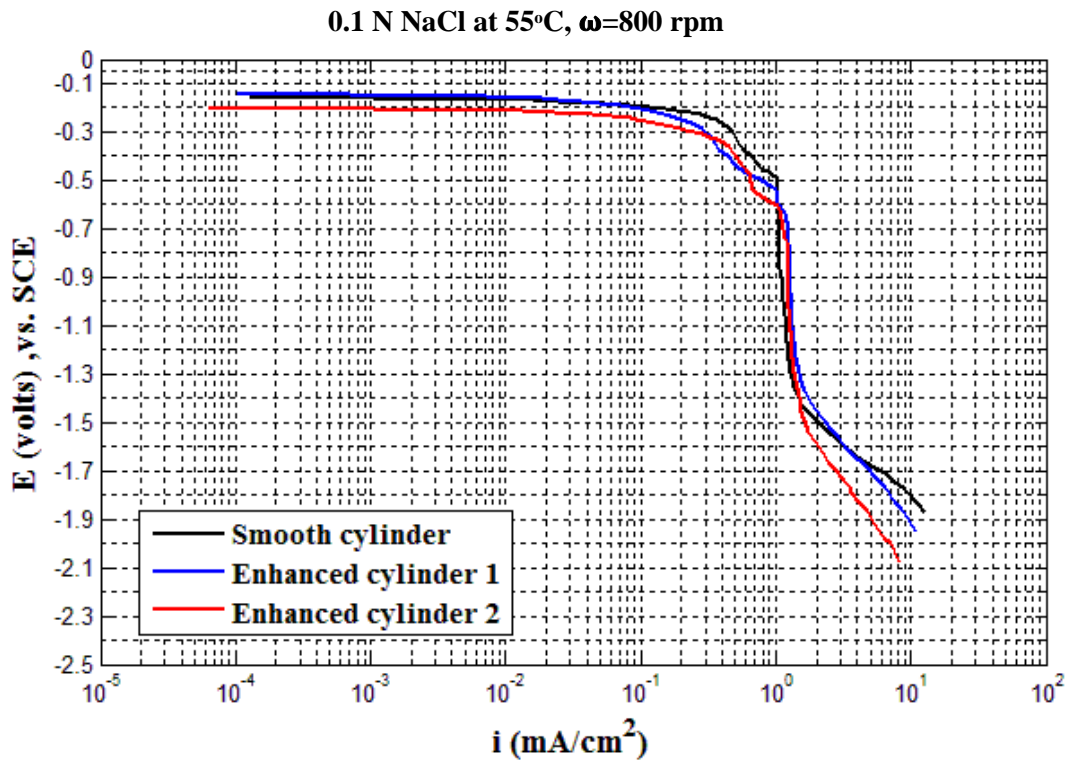
Figure 4-23 Cathodic polarization curves on brass rotating cylinder in 0.1 N NaCl for smooth, enhanced one and two rotating cylinder at 800 rpm and 55ºC.

0.1 N NaCl at 55ºC. ω=1000 rpm
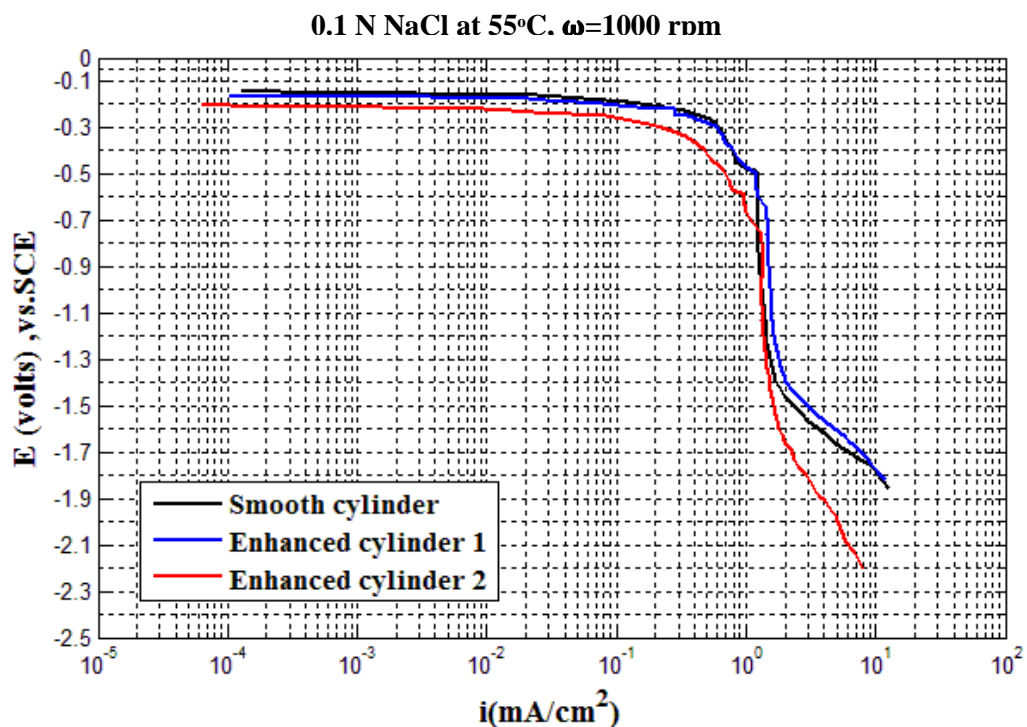
Figure 4-24 Cathodic polarization curves on brass rotating cylinder in 0.1 N M NaCl for smooth, enhanced one and two rotating cylinder at 1000 rpm and 55ºC.

The limiting current density was calculated for smooth rotating cylinder of geometrical characteristics (25mm diameter, 27mm long), enhanced cylinder one, and two including the areas of the extensions as listed in Table 4-2.

Table 4-2 Experimental limiting current density as a function of Reynolds number at different temperatures.

Temperature	ω(RPM)	u(cm/s)= $\frac{\pi*d*\omega}{60}$	Re= $\frac{\rho u d}{\mu}$	limiting current density, i_L (mA/cm^2) on smooth cylinder	limiting current density,i_L (mA/cm^2) on enhanced cylinder one	limiting current density,i_L (mA/cm^2) on enhanced cylinder two
35°C	200	26.1798	8991.5382	0.3134	0.4815	0.49523
	400	52.3598	17983.0764	0.5041	0.70845	0.7243
	600	78.5397	26974.694	0.61715	0.8068	0.8367
	800	104.71975	35966.1872	0.8956	1.0855	1.138
	1000	130.9896	44957.75635	1.137	1.271	1.286
45°C	200	26.1798	10803.8137	0.3543	0.53175	0.56535
	400	52.3598	21607.627	0.5443	0.7454	0.7543
	600	78.5397	32411.48248	0.7194	0.894	0.9223
	800	104.71975	43215.29622	1.0012	1.14715	1.1455
	1000	130.9896	54019.1471	1.236	1.3645	1.3515
55°C	200	26.1798	12677.2621	0.371	0.54765	0.566
	400	52.3598	25354.5242	0.66855	0.8509	0.8656
	600	78.5397	38031.8348	0.80865	0.9586	0.96835
	800	104.71975	50709.09692	1.146	1.308	1.302
	1000	130.9896	63386.4026	1.3965	1.5325	1.469

Also, Table 4-3 lists the values of mass transfer coefficient k (calculated using Eq.(2-10)) , and enhancement percentage for enhanced one, and two rotating cylinder.The efficiency of Enhancement Percentage(EP) due to extensions can be defined as:

$$EP\% = \frac{k_{for\ Enhanced\ cylinder} - k_{for\ Smooth\ cylinder}}{k_{for\ smooth\ cylinder}} * 100 \qquad (4\text{-}2)$$

Table 4-3 mass transfer coefficient k ,Enhancement Percentage EP% as a function of rotational velocity at different temperatures.

Temperature	ω(RPM)	k*10^5 (m/s) on smooth cylinder	k*10^5 (m/s) on Enhanced cylinder one	k*10^5 (m/s) on Enhanced cylinder two	Enhancemnt percentage (EP) %, enhanced cylinder one	Enhancemnt percentage (EP)%, enhanced cylinder two
35° C	200	3.738827	5.74424	5.90803	53.6375	58.018
	400	6.493438	8.451729	8.640812	40.53	43.6818
	600	7.36253	9.625034	9.98173	30.7299	35.5748
	800	10.6847	12.9498	13.5762	21.201	27.062
	1000	13.564	15.1628	15.3418	11.785	13.104
45° C	200	4.904169	7.360407	7.730677	50.084	57.6347
	400	7.136861	9.914645	10.085869	36.996	38.581
	600	9.957831	12.37462	12.7663	24.2702	28.204
	800	13.8584	15.8786	15.8558	14.577	14.412
	1000	17.10853	18.8872	18.4996	10.396	9.344
55° C	200	6.22118	9.183367	9.491072	47.614	52.5606
	400	11.2107	14.26846	14.514	27.275	29.472
	600	13.56	16.0744	16.2379	18.543	19.748
	800	19.2169	21.933	21.8328	14.136	13.613
	1000	23.417	25.698	24.633	9.738	5.191

Chapter Five

Discussion

This chapter presents the discussion of experimental results for the whole investigated ranges of pH values, rotational velocities, temperature, and enhancement due to longitudinal leg extensions. These variables influence the experimental findings which need to be interpreted, discussed, and understood.

5.1 limiting current density

5.1.1 Effect of velocity and temperature on the Limiting current,

Table 4-1 in chapter four is shown plotted in Figs. 5-1, 5-2 and 5-3 to illustrate the effect of velocity on limiting current density using normal cylinder (without extensions) as function of Reynolds number (Re) and temperature in solutions of pH 5, 6, and 7. All figures in this chapter are obtained by least square method.
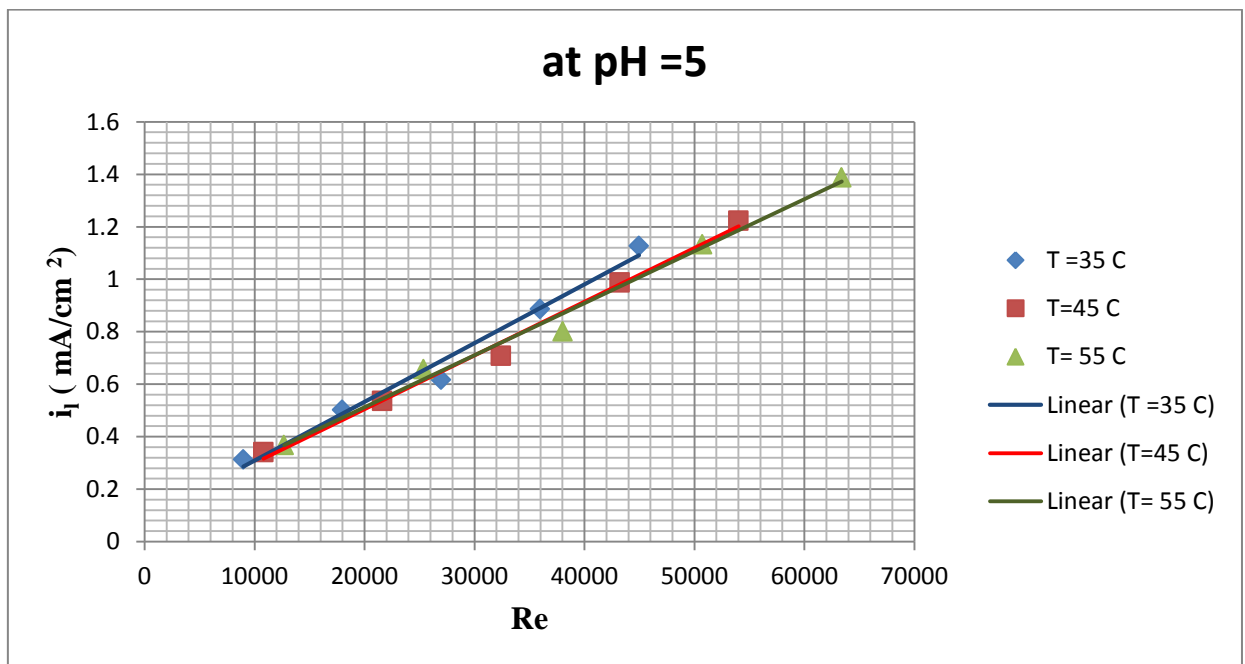
Figure 5-1 Effect of Re on i_l at three temperatures in 0.1N NaCl solution of pH = 5 using normal cylinder.
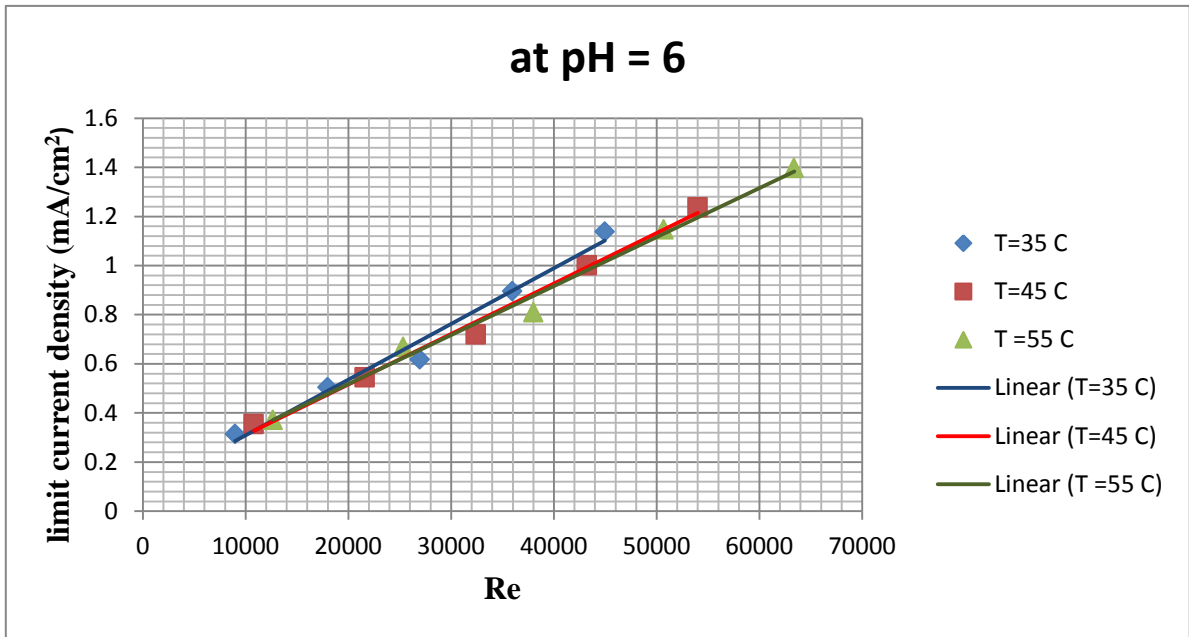
Figure 5-2 Effect of Re on i_l at three temperatures in 0.1N NaCl solution of pH = 6 using normal cylinder
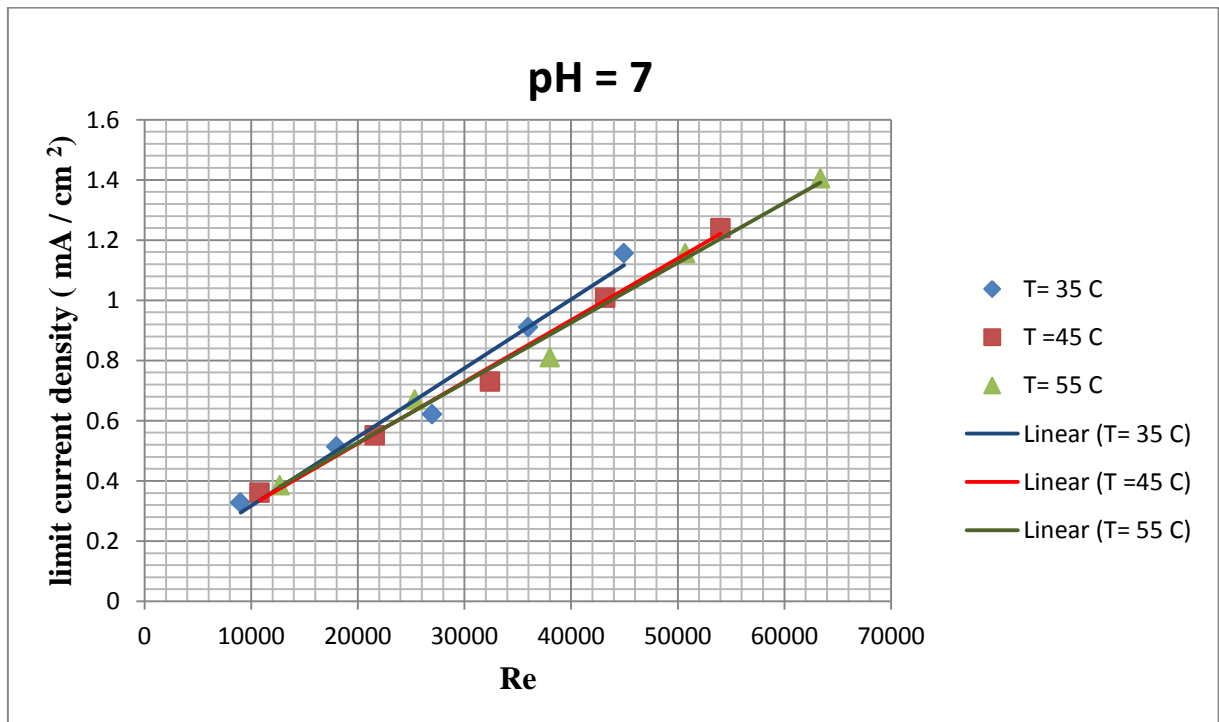
Figure 5-3 Effect of Re on i_l at three temperatures in 0.1 N NaCl solution of pH = 7 using normal cylinder

Form these figures it can be seen that as Reynolds number increases limiting current density (i_l) is increased. This can be attributed to the increase in oxygen supply from the bulk of the solution to the metal surface leading to higher i_l [43]. Also increasing in temperature increases i_l which is due to the fact that increasing temperature accelerates reaction rate as dictated by Arrhenius equation [26]. Likewise, increasing temperature will increase the rate of oxygen diffusion to the metal surface and decrease the viscosity of water which will aid oxygen diffusion [43]. Moreover, as temperature increases, the oxygen solubility decreases [44]. This would show that the influence of temperature surpasses the decrease in oxygen solubility in controlling the limiting current.

5.1.2 Effect of pH on the limiting current density on normal cylinder.

Figures. 5-4, 5-5 and 5-6 show the effect of pH 5, 6, and 7 on limiting current density as a function of rotational velocity on normal cylinder without longitudinal leg extensions for given temperature. It can be seen that the relation between i_l and pH is all most horizontal showing that the effect of pH is indeed negligible when compared with the influence of rotational velocity and temperature. Thus as stated above that cathodic hydrogen evolution has not affected the limiting current of dissolved oxygen at all. For this reason pH 6 is chosen as a base for the present work to evaluate enhancement of mass transfer due to leg extensions.
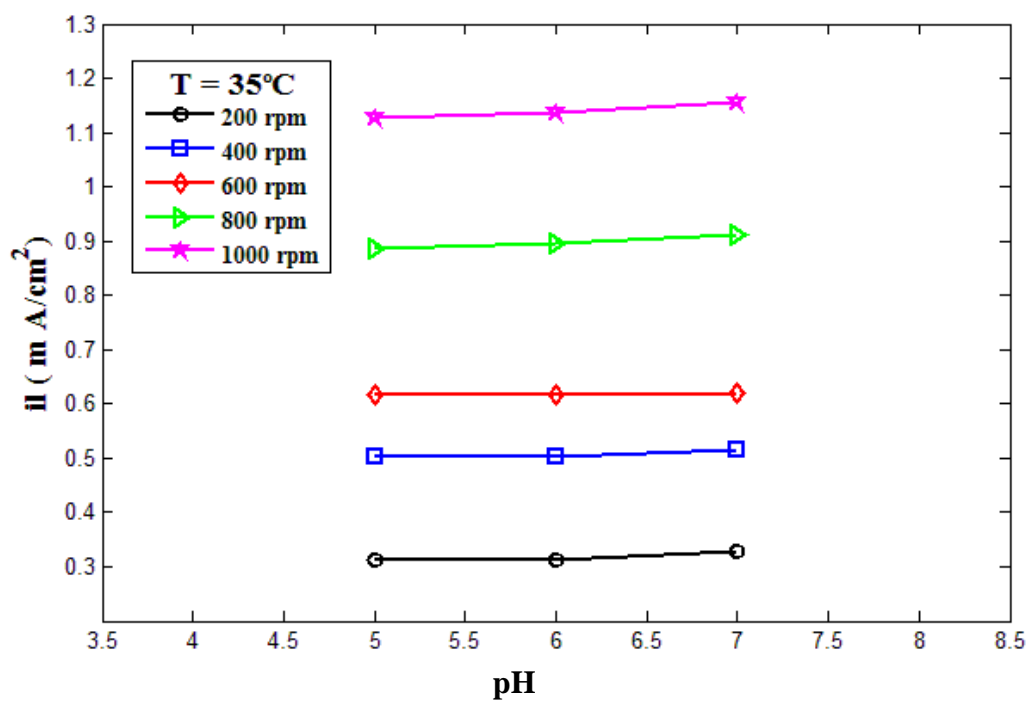
Figure 5-4 limiting current density vs. pH for various rpm values at 35°C .
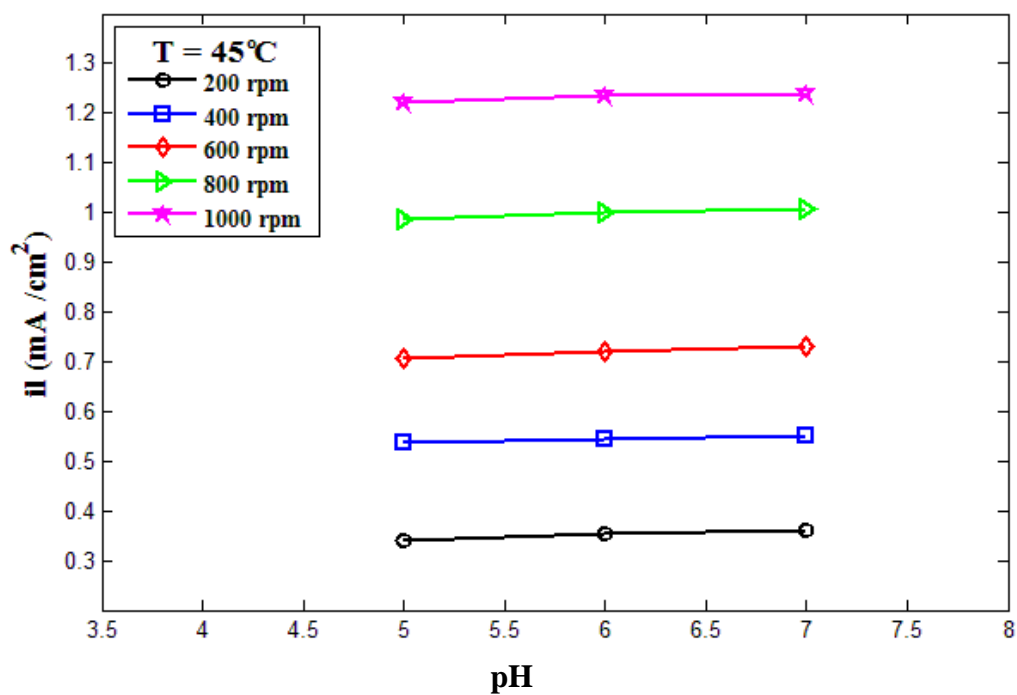
Figure 5-5 limiting current density vs. pH for various rpm values at 45^{0}C
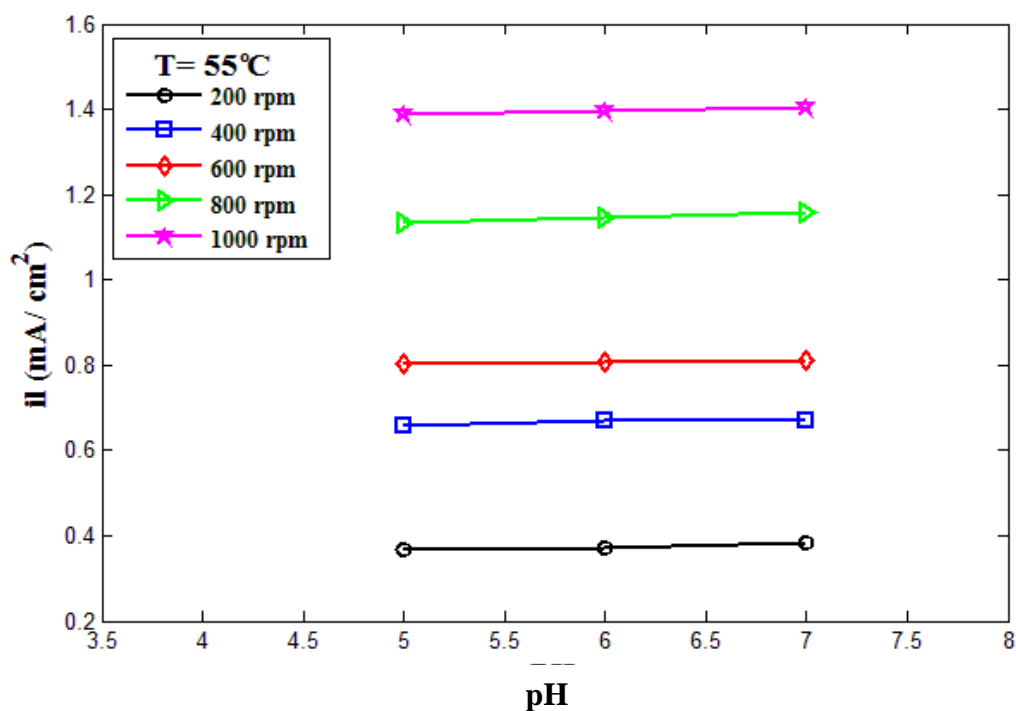
Figure 5-6 limiting current density vs. pH for various rpm values at 55^0C.

5.1.3   Effect of longitudinal leg extensions on the limiting current density

Figures 5-7, 5-8, and 5-9 show the limiting current density, i_l, as a function of Reynolds number for enhanced one, two and normal rotating cylinder electrodes at pH equal to six and different temperatures.

It can be seen that i_l values for enhanced one and two cylinders are higher than normal cylinder. This is due to the additional supply of dissolved oxygen from the bulk of the solution to the metal surface leading to higher i_l values as compared with ordinary cylinder. Thus the longitudinal extensions have promoted additional turbulence in the electrolyte flowing over the cylinder surface, i.e., higher mass transport to enhance the limiting current density.
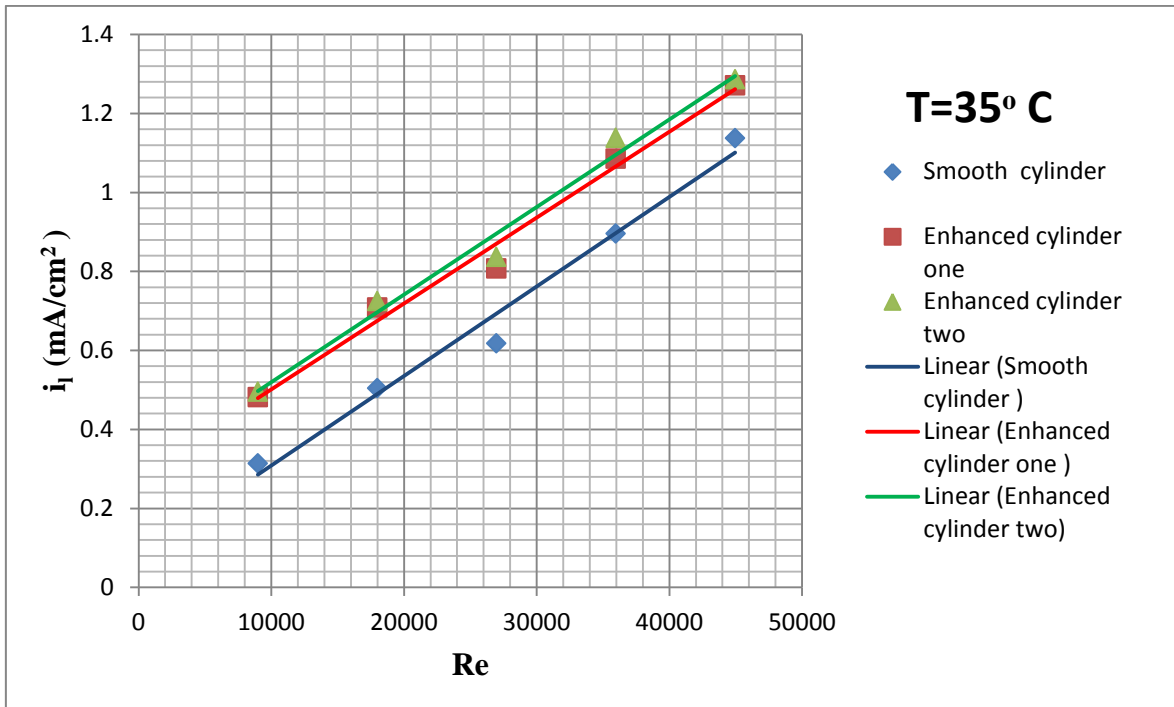
Figure 5-7 **Limiting current density** i_l vs. Re in 0.1N NaCl solution of pH = 6 at 35^0C for the three types of RCE.
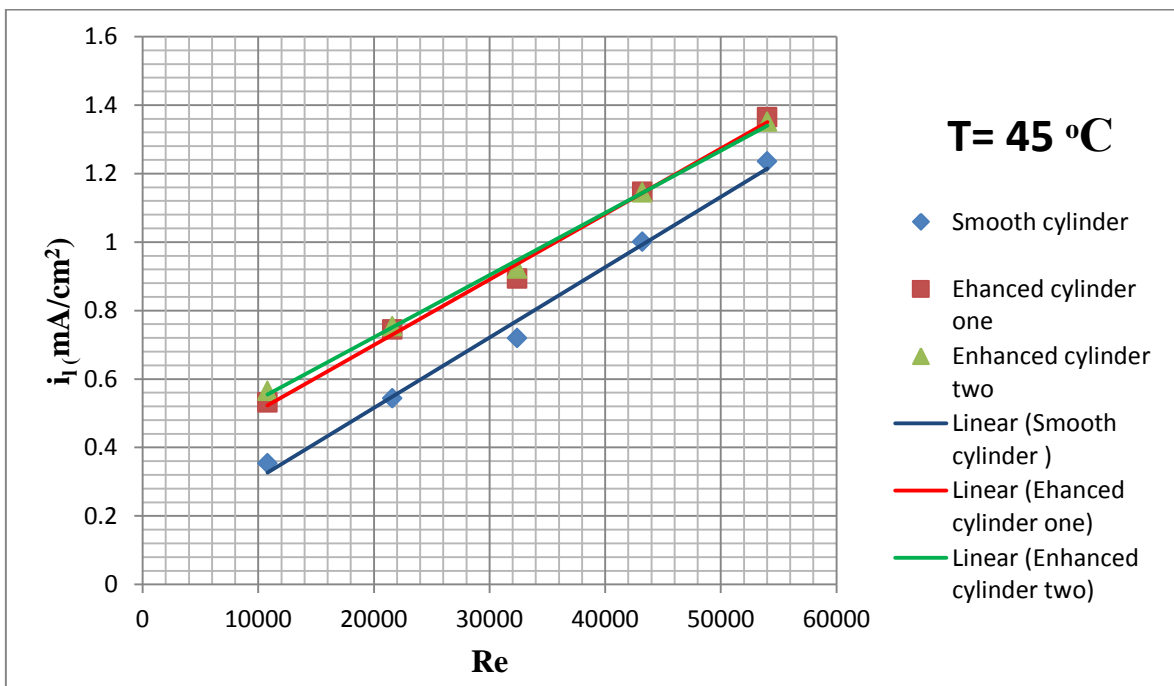
Figure 5-8 **Limiting current density** i_l vs. Re in 0.1N NaCl solution of pH = 6 at 45^0C for the three types of RCE.
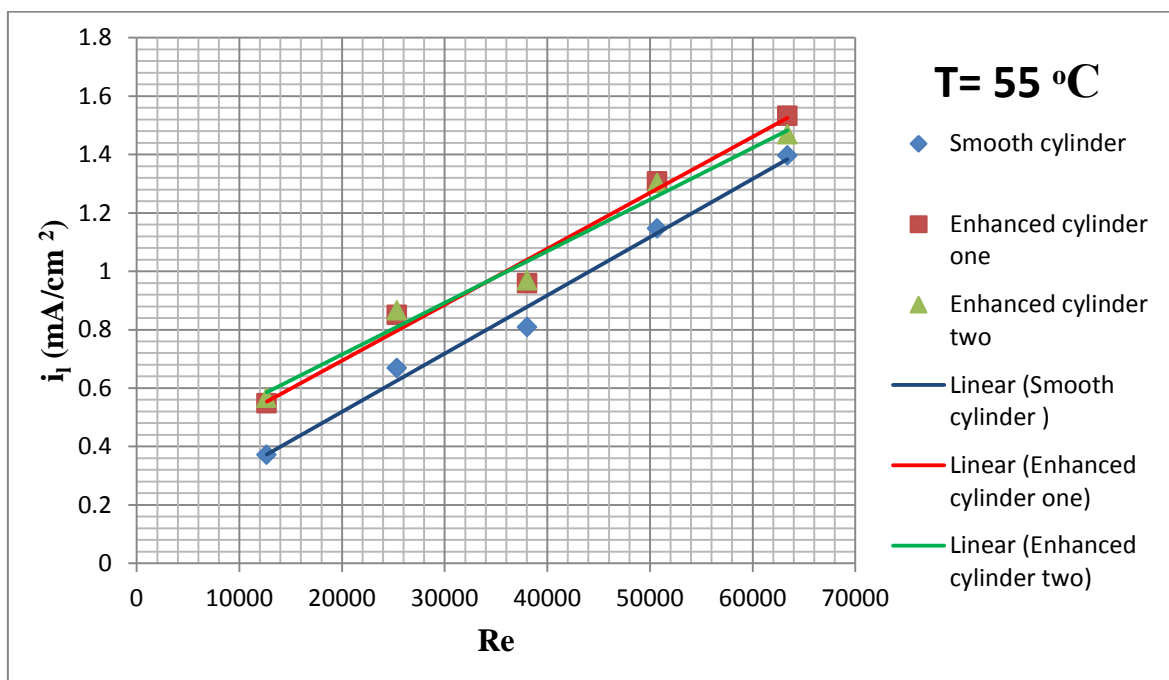
Figure 5-9 Limiting current density i_l vs. Re in 0.1N NaCl solution of pH = 6 at 55^0C for the three types of RCE.

5.2 *Mass transfer coefficient*

5.2.1 Effect of velocity on mass transfer coefficient

Figures 5-10, 5-11, and 5-12 show the mass transfer coefficient, k, as a function of Reynolds number for enhanced one, and enhanced two rotating cylinder electrodes at different temperatures and pH equal to six. The experimental mass-transfer coefficients for a similar normal rotating cylinder electrode are also reported in these figures, which provide a baseline for performance comparison.

It can be seen that as Reynolds number increases k is increased. This can be attributed to the increase in oxygen supply from the bulk of the solution to the metal surface leading to higher i_L [43] according to equation (2-10), thus k will be increased. This is because of leg extensions, which present a higher specific area and promote additional turbulence in the electrolyte flowing over the cylinder

surface. The k values for enhanced one and two cylinders are higher than dictated by the additional cylinder area only as displayed in figures.
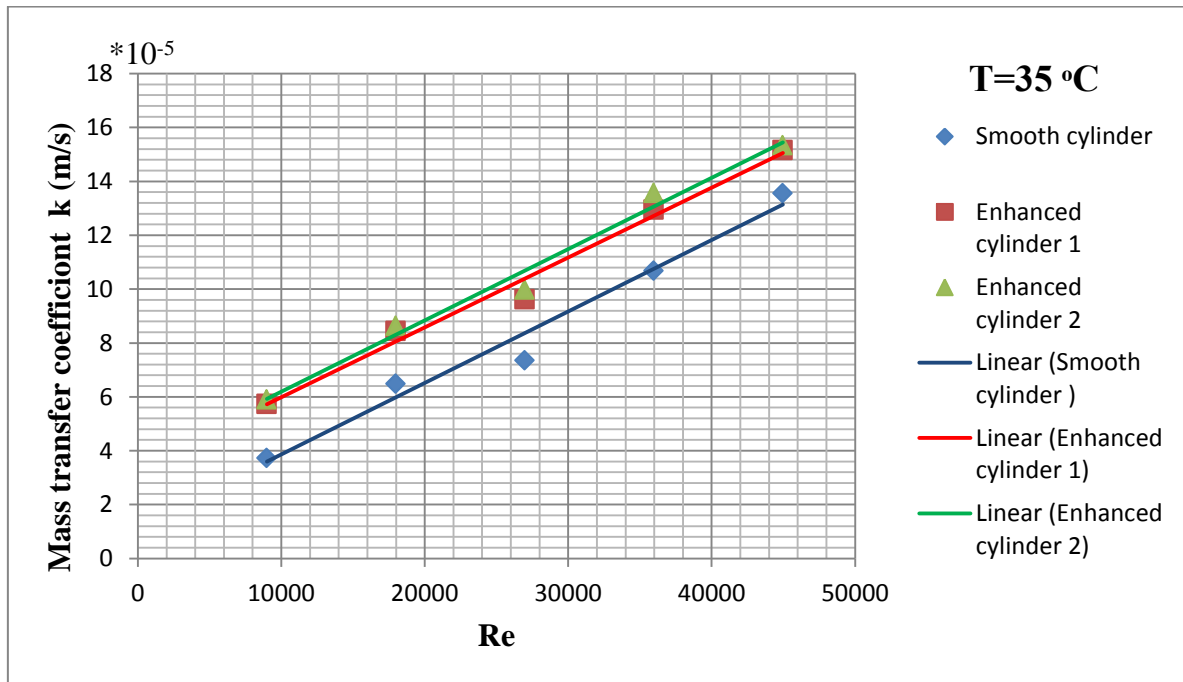
Figure 5-10 Mass transfer coefficient of dissolved oxygen k vs. Re at 35^0C in 0.1N NaCl solution of pH = 6.
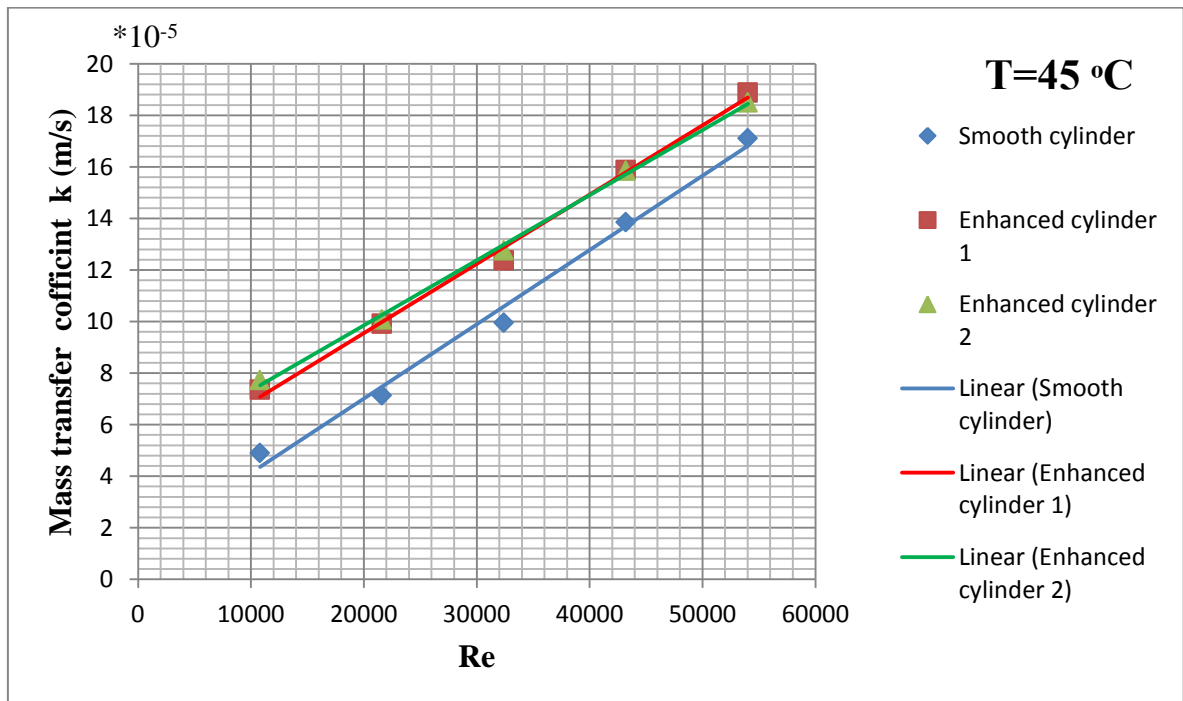
Figure 5-11 Mass transfer coefficient of dissolved oxygen k vs. Re at 45^0C in o.1N NaCl solution of pH = 6.
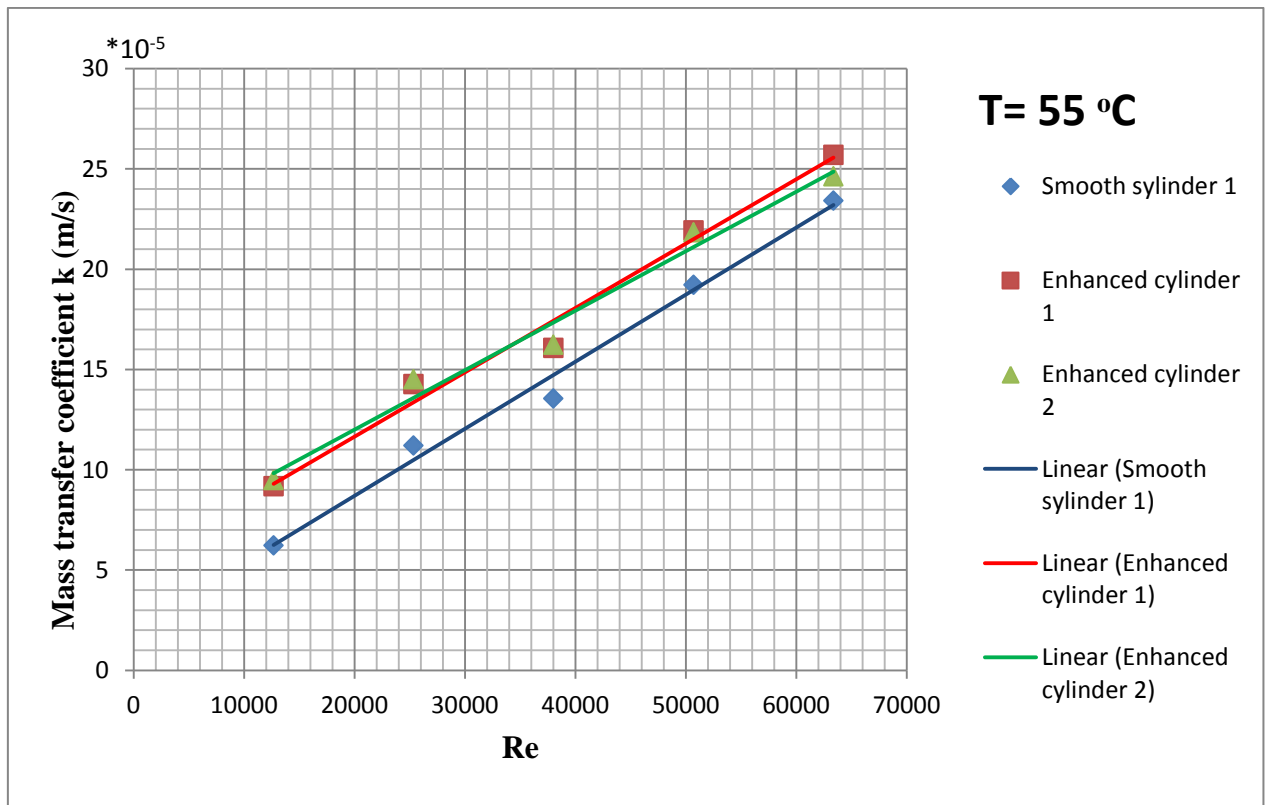
Figure 5-12 Mass transfer coefficient of dissolved oxygen k vs. Re at 55^0C in 0.1N NaCl solution of pH = 6.

5.2.2 Effect of temperature on mass transfer coefficient

Figures 5.13 ,5.14, and 5.15 show mass transfer coefficient, k, as a function of temperature for normal, enhanced one, and two rotating cylinder electrodes at different Re numbers. It is clear that as temperature increases k increases. This is due to the fact that increasing temperature accelerates reaction rate as dictated by Arrhenius equation. Likewise, increasing temperature will increase the rate of oxygen diffusion to the metal surface and decrease the viscosity of water which will aid dissolved oxygen diffusion. Moreover, as temperature increases, oxygen solubility decreases. The k values are still higher showing that the diffusion has a higher degree of effect than O_2 solubility due to temperature increase [26].

59
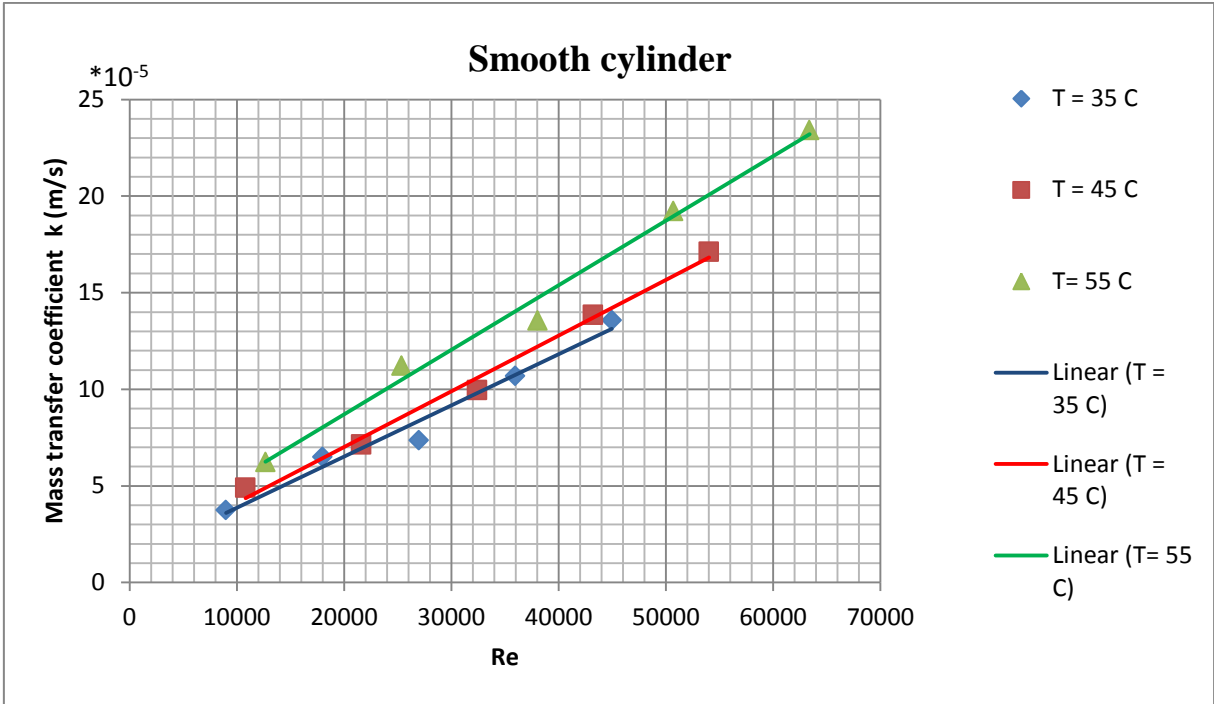
Figure 5-13 Effect of temprature on mass transfer coefficient of dissolved oxygen k on normal cylinder in 0.1N NaCl solution of pH = 6.
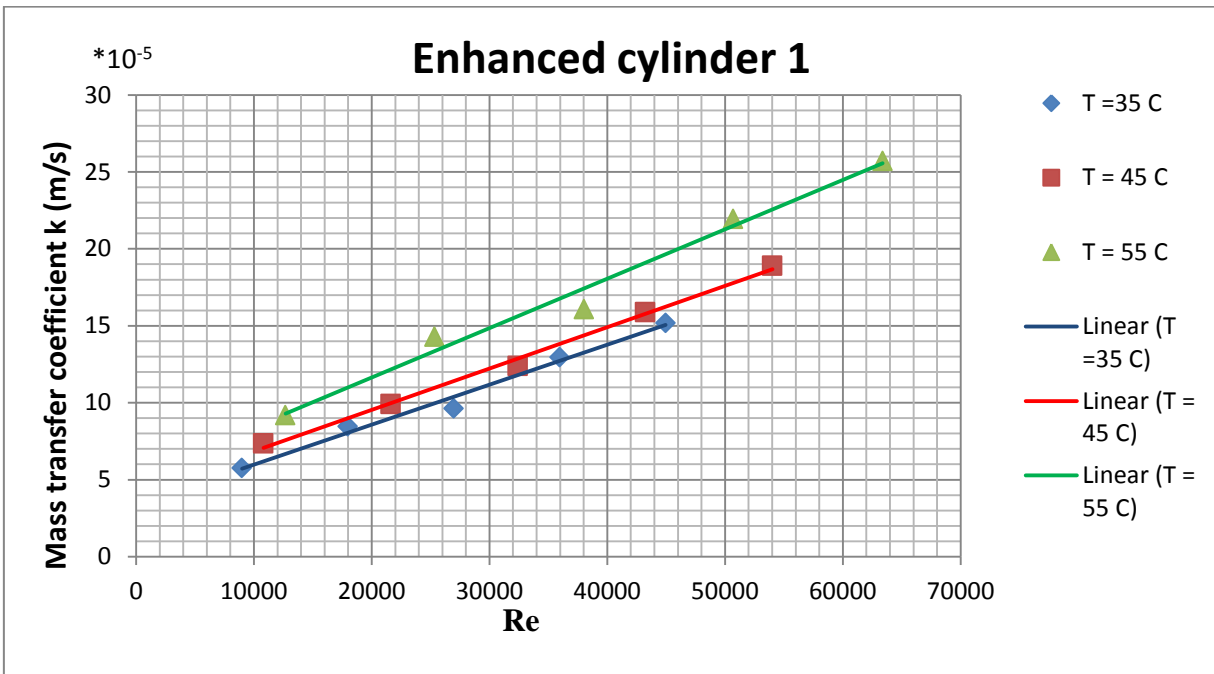
Figure 5-14 Effect of temprature on mass transfer coefficient of dissolved oxygen k on enhanced cylinder one in 0.1N NaCl solution of pH = 6.
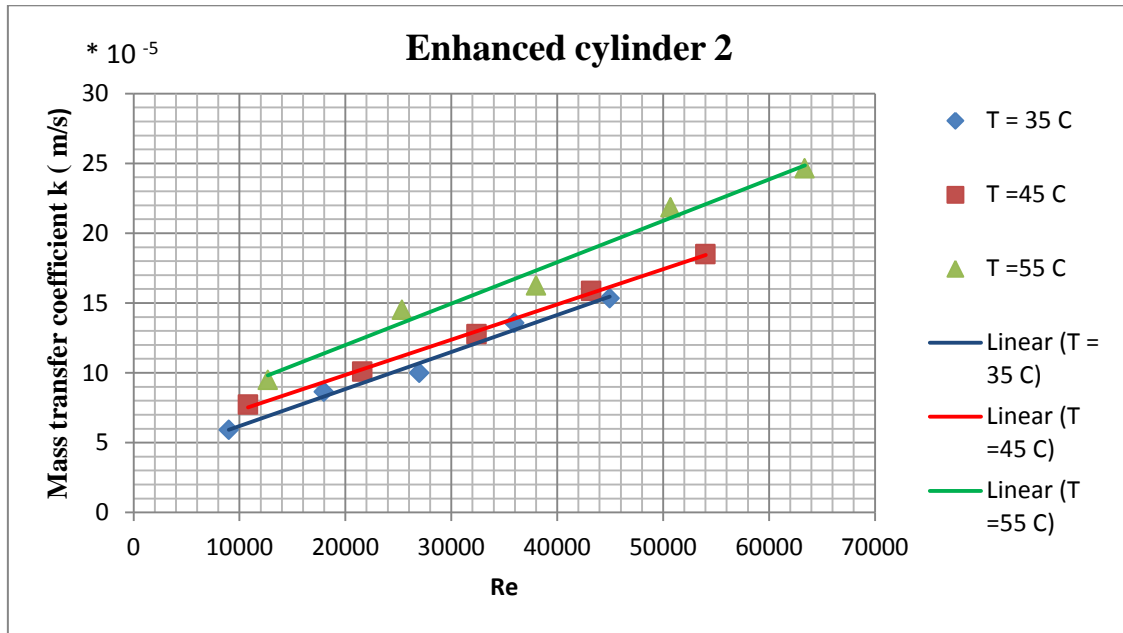
Figure 5-15 Effect of temprature on mass transfer coefficient of dissolved oxygen k on enhanced cylinder two in 0.1N NaCl solution of pH = 6.

5.3 *Mass transfer enhancement*

5.3.1 Effect of velocity on enhancement percentage of mass transfer

Figure 5-16 shows the enhancement percentage as function of Re number for enhanced cylinder one, and two at different temperatures. The enhancement percentage ranges from 58% to 5% depending mainly on rotational velocity; the greater Re the smaller is the enhancement percentage for a given temperature. This may be attributed to the fact that the effect of longitudinal extensions which act as turbulence promoters is rather of limited extent, since full turbulence has already been achieved by means of rotation in presence of these extensions, i.e, Re [28, 29, and 30].
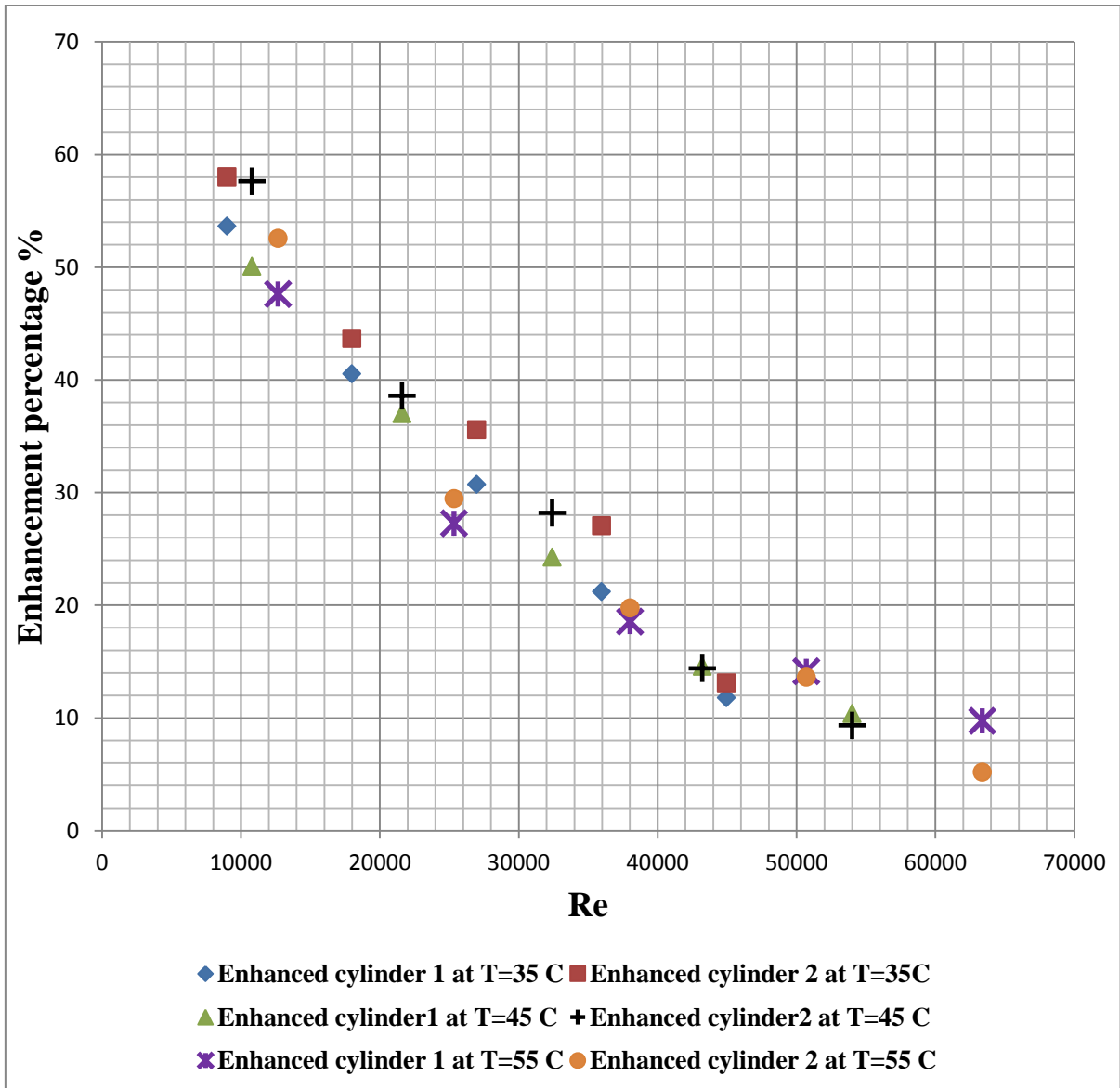
Figure 5-16   Enhancement percentage as a function of Re for enhanced cylinder one and two at different temperatures.

5.3.2   Effect of temperature on Enhancement Percentage of mass transfer

Figures 5-17and 5-18 show the enhancement percentage as function of Re number for enhanced cylinder one and two at different temperatures.

It is to be noticed that at present test temperatures the enhancement percentages are close to each other, i.e., approximately similar within the accuracy of experimental reproducibility of the results. The decrease of dissolved oxygen solubility is compensated by temperature rise in effecting higher mass transport. This can also be explained that as temperature increases mass transfer coefficient increases on smooth and enhanced cylinder electrodes to different extents. The effect of leg extensions acting as turbulent promoters will be diminished due to less dissolved oxygen in solution, therefore less mass transport leading to the values of k approximately close to each other and enhancement percentage to be reduced.
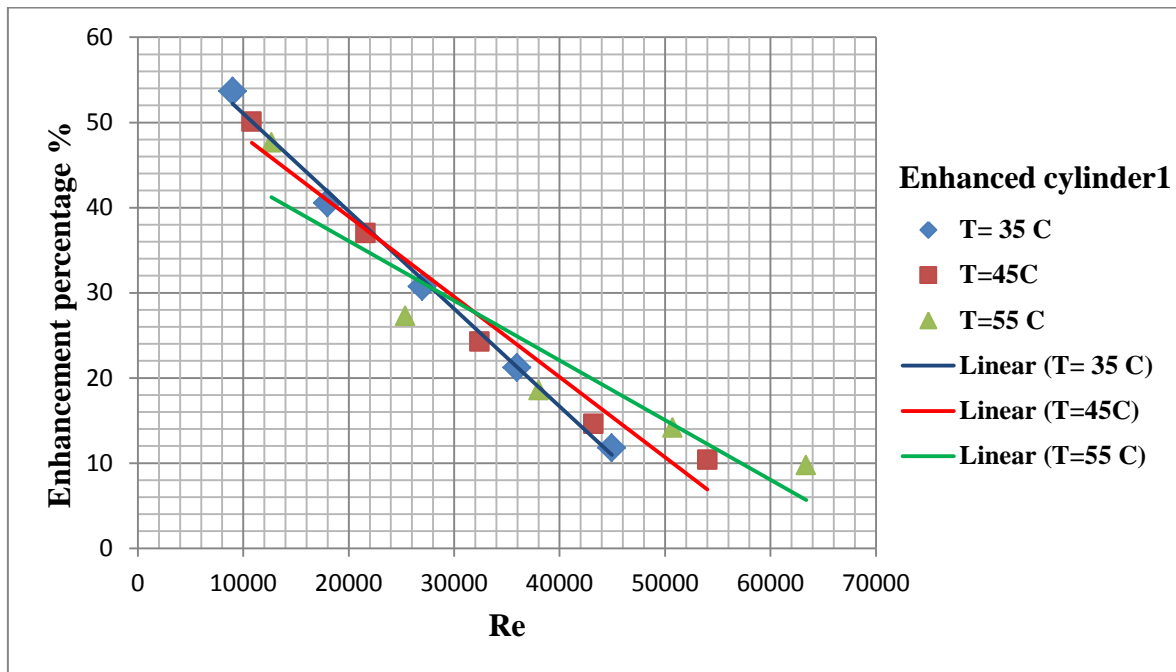
Figure 5-17 Enhancement percentage as a function of Re at different temperatures on enhanced cylinder 1.
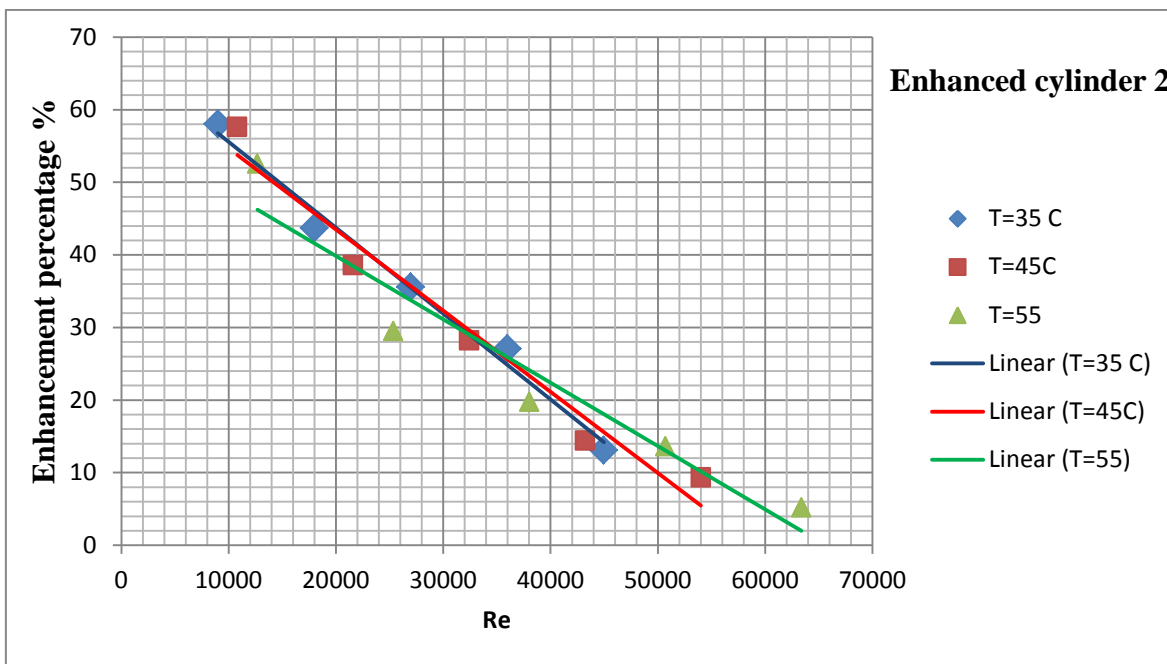
Figure 5-18 Enhancement percentage as a function of Re at different temperatures on enhanced cylinder 2.

5.4 Comparison of mass transfer enhancement of enhanced rotating cylinder electrodes.

Figures 5-19, 5-20, and 5-21 compare enhancement percentages for enhanced cylinder one and two. As shown in these figures that enhanced cylinder two is slightly more efficient than one. This indicates that turbulence occurs slightly earlier on cylinder 2 due to promoters but it is still within the experimental reproducibility of the results. However the geometry of promoters is important to be always sought for improvement.
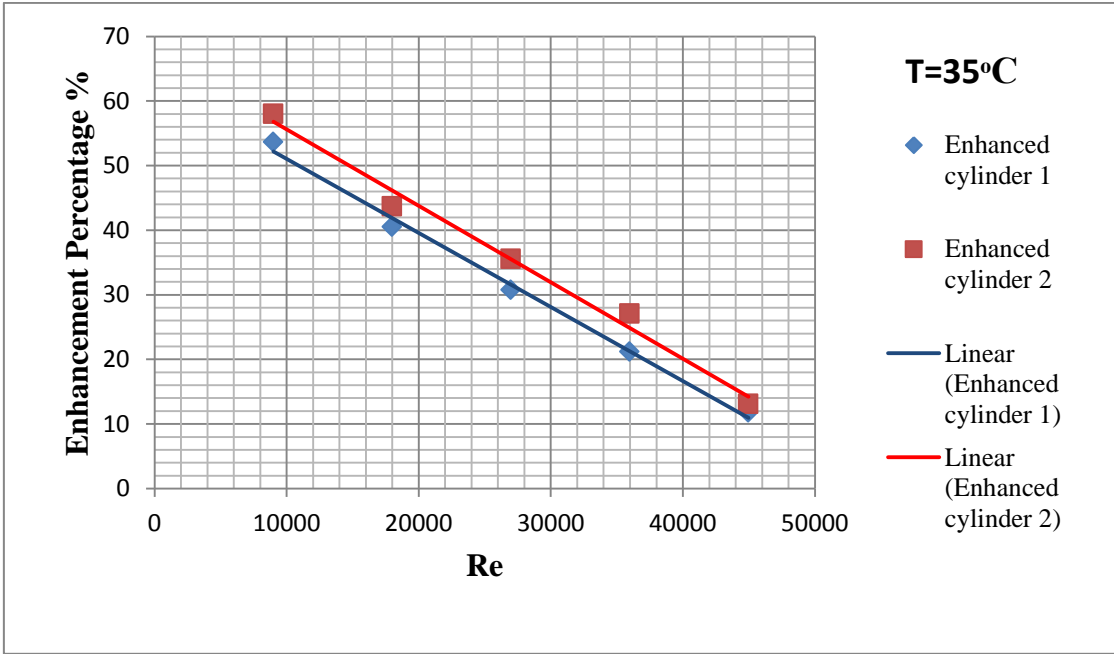
Figure 5-19 Enhancement percentage as a function of Re at T=35 ℃.
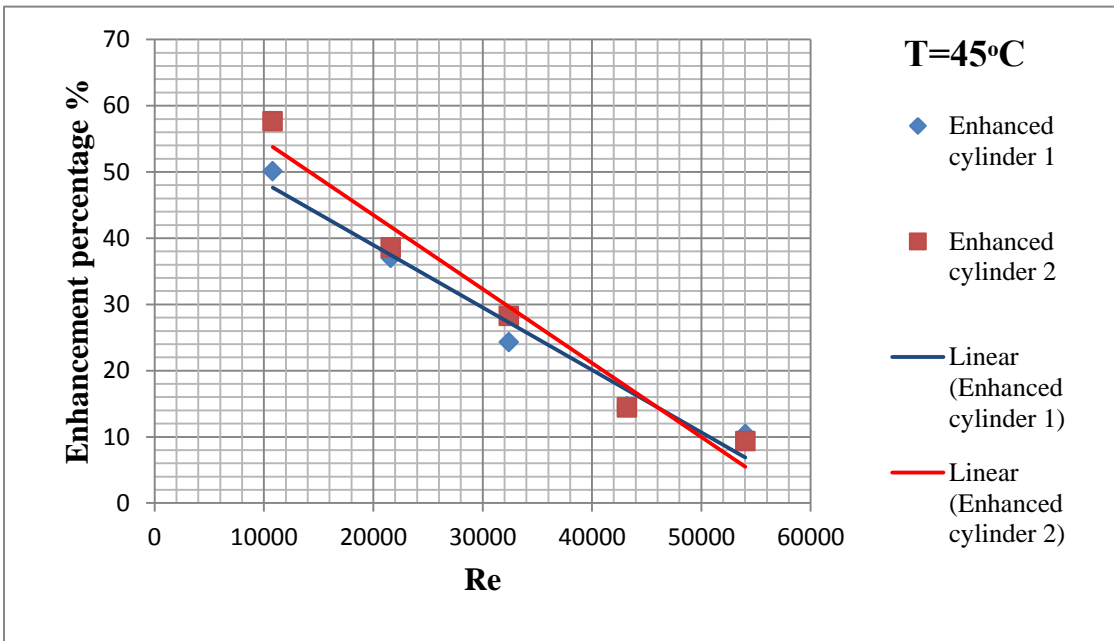
Figure 5-20 Enhancement percentage as a function of Re at T=45℃.

65
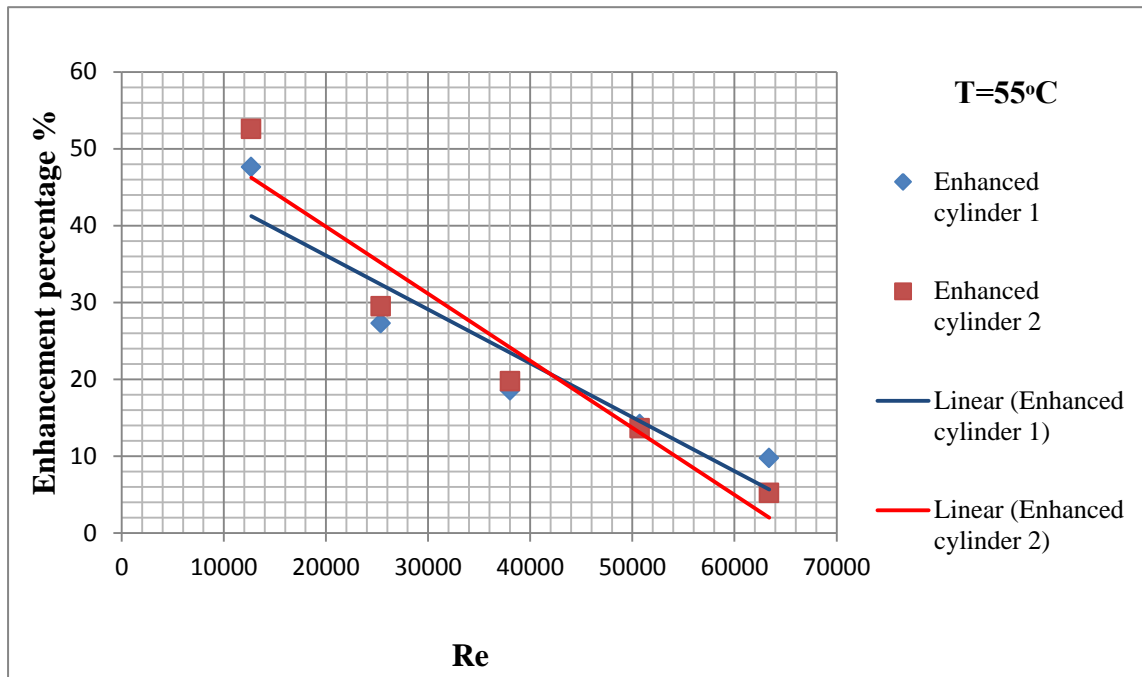
Figure 5-21 Enhancement percentage as a function of Re at T=55°C.

Chapter six

Conclusions and Suggestions for Future Work

6.1 Conclusions

The following conclusions can be drawn from present work:

1. Mass transfer coefficients on the surface of enhanced rotating cylinder electrode are, in general, about 53% or 58% higher those obtained with normal rotating electrode without extensions.
2. Mass transfer enhancement is mainly due to longitudinal leg extensions, which present a higher specific area and promote additional turbulence in the electrolyte flowing over the cylinder surface.
3. The enhancement percentage decreases as Re increases.
4. The enhancement percentage decreases as the temperature increases.
5. The effect of extensions length on the enhancement is found little, i.e., limited.

6.2 Suggestions for Future Work

1. Using leg extensions made of plastic or Teflon.
2. Increase or decrease number of leg extensions and study the effect on mass transfer enhancement.
3. Use longitudinal leg extensions of different angles with vertical level.
4. Repeat the experimental work with axial flow.
5. Use leg extensions of roughened surface.
6. Use different geometrically shaped leg extensions.

References

1. GABE D. R., MAKANJUOLA P. A. "Enhanced mass transfer using roughened rotating cylinder electrodes in turbulent flow", Journal of Applied Electrochemistry March 1987, Volume 17, Issue 2, pp 370-384

2. Gabe DR, Walsh FC. "Enhanced mass transfer at the rotating cylinder electrode: characterization of a smooth cylinder and roughness development in solutions of constant concentration",. J Appl Electrochem 1984, Vol.14,PP. 555–64.

3. Nadebaum PR, Fahidy TZ. "A Novel electrochemical cell employing a rotating bipolar electrode",. J Electrochem Soc 1975 ,Vol.122, PP. 1035–42.

4. Nadebaum PR, Fahidy TZ. ,"The rate of mass transfer at a rotating cylindrical electrode with wiper blades." Can J Chem Eng ,1975, Vol. 53,PP.259–66.

5. Radwan A, El Kyar A, Farag HA, Sedahmed GH.," The role of mass transfer in the electrolytic reduction of hexavalent chromium at gas evolving rotating cylinders", J Appl Electrochem ,1992 Vol. 22,PP.1161–6.

6 EKLUND.A., and SIMONSSON. D. , "Enhanced mass transfer to a rotating cylinder electrode with axial flow ",Journal of Applied Electrochemistry September 1988, Volume 18, Issue 5, pp 710-714

7. Coeuret F, Legrand J." Mass transfer at the electrodes of concentric cylinder reactors combining axial flow and rotation of the inner cylinder", Electrochim Acta, 1981,Vol.26 ,PP.865–72.

8. NAHLI H., G. W. READE, F. C. WALSH ," Mass transport to reticulated vitreous carbon rotating cylinder electrodes" ,Journal of Applied Electrochemistry May 1995, Volume 25, Issue 5, pp 450-455

9.GRAU .J.M. and J.M. BISANG. ,"Mass transfer studies at rotating cylinder electrodes of expanded metal", Journal of Applied Electrochemistry March 2005, Volume 35, Issue 3, pp 285-291

10. GRAU J. M. and BISANG .J. M.,"Mass transfer studies at packed bed rotating cylinder electrodes of woven-wire meshes" , Journal of Applied Electrochemistry July 2006, Volume 36, Issue 7, pp 759-763

11.Landaw,U.,"Tutorail Lectures in Electrochemical Eng . and Tech.",AICHE Symposium Series ,vol.77,1981 ,P-75 .

12. Walsh FC , "A First Course in Electrochemical Engineering. The Electrochemical Consultancy", Romsey, 1993,p 104

13. Gabe D.R. and P.A. Makanjoula,, EFCF Publication Series No. 15, Electrochemical Eng., AICHE Symposium Series 1986, No. 98, P.309.

14.Vilar, E. O., Cavalcanti, E. B., Albuquerque, I. L. T." A Mass Transfer Study withElectrolytic Gas Production, Advanced Topics in Mass Transfer," Mohamed El-Amin (Ed.) , 2011,InTech

15. GABE D. R., WILCOX G. D., "The rotating cylinder electrode: its continued development and application", JOURNAL OF APPLIED ELECTROCHEMISTRY , Vol.28 ,No.49 ,1998, PP.759-780.

16. Recendiz, A., Leon, S., Nava, J. L., Rivera, F. F. "Mass transport studies at rotating cylinder electrode during zinc removal from dilute solutions". *Electrochimica Acta*,2011 Vol. 56, pp. 1455-1459

17. Poulson B.Corrosion Sci., Vol. 23, 1983, pp. 23.

18.Sliverman ,D.C, corrosion ,vol.40,1984,p-220.

19.Newman,J.S.Ind.Eng.chem.,Vol.60,1968,P-12.

20.Gartland ,per O .,B.Einar ,R.E.andersen ,and R.Johnsen ,Corrosion, Vol.40,1984,P-127.

21. Newman ,j.s.electrochmecal system ,prentice-hall,N.J.,1973.

22. Walsh .F.C., in Genders D. and N. Weinberg (Eds), 'Electrochemistry for a Cleaner Environment', (The Electrosynthesis Company, New York, 1992, pp. 101–159.

23. EISENBERG M., C. W. TOBIAS, AND C. R. WILKE ,"Ionic Mass Transfer and Concentration Polarization at Rotating Electrode", J. Electrochem. Soc. **1954** volume 101, issue 6, pp. 306-320.

24.Tobias W., Eisenberg M., and C. R. Wilke ,"diffusion and convection in electrolysis - a theoretical reviewc",electrochemistry of ionic crystals ,Vol. 99, No. 12 ,PP 359-365

25. Bagotsky V.S., "Fundamental of Electrochemist", 2nd , Wiley Interscience Publication, (2006). pp. 410

26. Mizushina, T.,"Advances in Heat transfer ",Irvine ,T.F .and J.P.Hartnett (Ed),vol.7,Acadimic press,N.Y.,1971

27 .Lin,C.S,E.B.Denton ,H.S.Gaskill, and G.L.Putnam,Ind.Eng.chem,Vol,45,1951,P-2136.

28. Hubbard, D.W. and E.N. Lightfoot, Ind.Eng.chem.Fundamentals,Vol.5,1966,P-370.

29-Dawson, D.A, and O. Trass ,Int.J.Heat Mass Transfer,vol.15,1972,P-1317.

30.Mitchell,J.E.and T.J.Hanratty,J.fluid Mech.,Vol.26,1966,P-199.

31.Landau,U.,PH.D.Thesis,University of California,Berkeley,1976. vol.77,1981 ,P-75 .

32.Rantz,W.E.,AICHE J.,Vol.4,1958 , P-338.

33.Shaw,D.A. and T.J.Hanratty,AICHE.J,Vol23,1977,P-28.

34. Ponce-de-Leo´n C. Low .C. T. J. G. Kear .F. C. Walsh.,"Strategies for the determination of the convective-diffusion limiting current from steady state linear sweep voltammetry", Journal of Applied Electrochemistry November 2007, Volume 37, Issue 11, pp. 1261-1270

35. Coway B. E ., Beatty E.M., and De Maine P.A.D.,Electrochemical Acta., 1990 Vol .7, p.p.No.39

36. Ross T. K. and Johnes D. H., J. App. Chem., Vol. 12,(1962) pp.314.

 37.Stern M., Corrosion-NACE, Vol. 13, (1957). pp.97,

38. Poulson B.Corrosion Sci., Vol. 23, 1983, pp. 23.

39. Fontana M.G., and Green N.D., "Corrosion Engineering", 2nd. Edition, Londan (1984). pp. 30

40. Uhlig H. H.,"Corrosion and Corrosion Control", 3rd Edition, Wiley- Interscience publication, New Yourk, (1985). pp. 100

41. Perry R.H, and Green D.W, Perry Chemical Engineers Handbook, 7thed, M.C. Graw-Hill, United States, 1997. pp. 625

42.Shereir L.L.,"Corrosion Handbook", Newnes – Butter, London, 2nd Edition, Vol. 1,(2000). pp. 685

43. Perry R.H, and Green D.W, Perry Chemical Engineers Handbook, 7thed, M.C. Graw-Hill, United States, 1997. pp. 625

44. Jean L. Stojak, Jan B. Tablot," advance in electrochemical science and engineering J.Appl. electrochem" ,.2001., Vol.7, No.31pp. 563

45.   Grau, J.M. Bisang,"Mass-transfer studies at rotating cylinder electrodes with turbulence   promoters",J.M. Chemical   Engineering   &   Processing: Process Intensification vol. 50 issue 9 September, 2011. p. 940-943

46. Eisenberg, M., Tobias, C. W., Wilke, C. R. Ionic mass transfer and concentration polarization at rotating electrodes. Journal of the Electrochemical Society, (1954). Vol. 101, pp. 306-320

47. SEDAHMED G. H., " Mass transfer enhancement by the counter-electrode gases in a new cell design involving a three-dimensional gauze electrode" Journal of Applied Electrochemistry September 1978, Volume 8, Issue 5, pp 399-404

48. Fernando F. Rivera, and Jos´e L. ," Mass transport studies at rotating cylinder electrode (RCE)", Electrochimica Acta vol. 52 issue 19 May 25, 2007 pp. 5868–5872

49. Fernando F. Riveraa, and José L. Navab. Electrochimica Acta No. 55 .(2010).pp. 3275–3278

50. Robert G. Kelly and John R. Scully, Electrochemical Techniques in Corrosion Science and Engineering, 10$_{th}$ ed, Marcel Dekker ,New York ,2003.p.161.

51. Mahato B. K., C. Y. Cha and W. Shemlit, "Unsteady State Mass Transfer Coefficients Controlling Steel Pipe Corrosion under Isothermal Flow Conditions", Corrosion Science, vol.20, pp.,42,421–441, 1980.

52. Fage A. and Townend H.C., Proc, Soc., London, Vol.354, (1932). pp.646 .

53 .Joseph Kestin ,H.Ezzat Khalifa , and Robert J.correia ,"Table of the dynamic and Kinematic viscosity of Aqueous NaCl solution",J.Phys.Chem.Ref.Data, 1981.Vol.10,No.1,

54. Audin A., and L.John, J. Chem. Eng. Data.1972,, No.3, Vol. 17, p.789.

55. Sense F., "Oxygen Solubility", North California State,2001.

56. Copper *3T*Specifications Datasheet, aalco Ltd.

57. Bird R.B., W.E. Stewart, and E.N. Lightfoot, "Transport Phenomena", second edition, John Wiley & Sons, New York, 2002.

Appendix -A

Table A-1 Values of density and viscosity for 0.1 N NaCl at different temperatures [43,53].

T (ºC)	Density (Kg/m^3)	Viscosity $*10^4$ (kg/m.s)
35	993.95	7.235
45	990.059	5.9978
55	985.458	5.08769

Table A-2 Values of oxygen Diffusivity and solubility for 0.1 N NaCl at different temperatures [54,55].

T (ºC)	D$_o$ * 10^9(m2/s)	Solubility (mg/l)	C$_b$ (mole/m^3)
35	2.4954	5.9445	0.21718
45	3.286	4.894	0.18718
55	3.186	4.9445	0.154515

Table A-3 Analysis of Specimen.

Elements	Zn	Pb	Sn	P	Mn	Fe	Ni	Si	Mg	Cr	As	Sb	S	C	Cu
Weight%	2.49	5.09	5.91	0.008	0.0005	0.041	0.638	0.001	0.0001	0.0009	0.040	0.132	0.131	0.0016	Bal.

Table A-4 Copper properties [56].

Copper properties	
Atomic mass	63.546 g.molP -1
Density	8.9 g.cm-3at 20°C
Melting point	1083 °C
Boiling point	2595 °C
Standard potential	+ 0.522 V (Cu+/ Cu) ; + 0.345 V (Cu2+/ Cu)

Appendix –B-

Table B-1 Data for polarization experiments in 0.1 N NaCl for normal cylinder at pH 6 and 35 °C

200 rpm		400 rpm		600 rpm		800 rpm		1000 rpm	
i (mA/cm²)	E*-1 (V)	i (mA/cm²)	E*-1(v)	i (mA/cm²)	E*-1(v)	i (mA/cm²)	E*-1(v)	i (mA/cm²)	E*-1 (v)
400	2.28	390	2.23	260	2.21	270	2.01	290	2.15
330	2.18	320	2.12	290	1.966	230	1.996	250	2.01
280	2.09	270	2.04	270	1.917	200	1.98	220	1.996
250	2.03	240	1.996	230	1.892	180	1.957	200	1.979
200	1.98	210	1.96	200	1.866	173.8	1.929	180	1.968
180	1.913	180.3	1.930	185.3	1.839	159.6	1.884	161.1	1.933
170.6	1.875	166.3	1.891	170.9	1.788	128.8	1.864	132.7	1.894
147.4	1.84	144	1.862	158.1	1.744	108.8	1.828	118.8	1.861
138	1.828	127.2	1.837	115.8	1.709	98.6	1.797	87.4	1.838
129.6	1.81	114.7	1.791	95.8	1.694	87.1	1.79	72	1.797
116.5	1.786	99.4	1.763	88.2	1.676	68.3	1.764	59.7	1.77
105.5	1.764	76.7	1.728	76.3	1.642	56.6	1.73	51.3	1.736
92.3	1.733	67.7	1.692	65.7	1.61	49.6	1.696	43.7	1.709
82.5	1.707	52.8	1.658	52.4	1.587	36.6	1.673	38.7	1.681
72.4	1.683	48.6	1.624	45.5	1.565	28.9	1.649	36	1.659
64.6	1.656	35.1	1.597	33.4	1.538	27.7	1.618	34.1	1.627
54.1	1.628	24.1	1.564	29.6	1.507	24.9	1.595	31.7	1.599
45.2	1.595	21.5	1.532	26.1	1.474	24	1.578	30.6	1.577
40.6	1.579	19.9	1.491	20.6	1.447	23.2	1.548	29.8	1.546
34.9	1.555	18.13	1.468	18.8	1.418	22.8	1.52	28.4	1.514
30.6	1.533	17.56	1.437	17.81	1.389	22.5	1.495	28.3	1.485
24.9	1.502	16.99	1.388	17.28	1.355	22.4	1.473	27.6	1.458
22.5	1.485	15.9	1.356	16.58	1.321	22.1	1.458	28	1.424
19	1.461	15.66	1.328	15.99	1.29	21.8	1.425	27.3	1.391
16.87	1.433	15.43	1.29	15.74	1.275	21.5	1.398	27	1.379
14.23	1.397	15.14	1.265	15.31	1.246	21.5	1.368	26.4	1.349
12.93	1.378	14.38	1.23	15.02	1.219	21.1	1.337	26.2	1.31
11.41	1.34	14.83	1.187	14.69	1.198	20.9	1.301	25.5	1.281
10.58	1.31	14.78	1.158	14.45	1.166	20.7	1.284	25.7	1.257
9.64	1.27	14.76	1.126	14.09	1.138	20.5	1.26	25.3	1.221
9.1	1.24	14.73	1.098	13.91	1.097	20.3	1.231	25.2	1.19
8.92	1.215	14.64	1.067	13.7	1.075	20.1	1.191	25.1	1.155

200 rpm		400 rpm		600 rpm		800 rpm		1000 rpm	
i (mA/cm²)	E *-1(V)	i (mA/cm²)	E*-1(v)	i (mA/cm²)	E*-1(v)	i (mA/cm²)	E*-1 (v)	i (mA/cm²)	E*-1 (v)
8.72	1.194	14.63	1.032	13.65	1.035	20	1.163	24.8	1.132
8.56	1.166	14.36	0.992	13.58	0.994	19.9	1.137	25.5	1.088
8.19	1.135	14.39	0.972	13.5	0.965	19.9	1.09	25.5	1.067
7.88	1.088	14.11	0.953	13.4	0.931	19.9	1.065	25.6	1.031
7.8	1.045	13.81	0.89	13.49	0.898	19.8	1.035	25.6	0.987
7.69	1.013	13.55	0.851	13.39	0.867	19.7	0.987	25.5	0.956
7.59	0.998	12.87	0.812	13.37	0.834	19.7	0.961	25.4	0.921
7.47	0.953	12.61	0.79	13.37	0.797	19.6	0.932	25.6	0.893
7.39	0.921	12.26	0.756	13.35	0.76	18.86	0.897	25.1	0.86
7.28	0.899	11.9	0.723	13.16	0.738	18.7	0.873	24.3	0.837
7.2	0.859	11.23	0.698	13.03	0.688	18.42	0.846	18.1	0.791
7.12	0.823	10.96	0.653	13.5	0.648	18.02	0.82	16.76	0.766
7.04	0.795	10.37	0.633	13.41	0.615	16.09	0.795	16.1	0.73
6.93	0.784	9.87	0.598	13.25	0.597	14.82	0.765	14.98	0.676
6.9	0.741	8.82	0.562	12.8	0.584	13.74	0.732	14.47	0.649
6.82	0.730	7.86	0.532	11.59	0.553	12.43	0.694	13.92	0.623
6.7	0.698	6.58	0.493	10.89	0.542	11.38	0.661	13.17	0.591
6.68	0.676	6.07	0.481	8.42	0.534	10.8	0.635	11.99	0.573
6.6	0.655	5.26	0.452	6.41	0.521	9.99	0.598	9.62	0.545
6.52	0.64	4.64	0.42	5.06	0.502	8.24	0.577	6.31	0.518
6.44	0.617	3.75	0.398	3.61	0.497	6.94	0.554	4.59	0.505
6.16	0.594	3.42	0.372	1.2	0.466	5.09	0.523	3.39	0.472
5.9	0.574	1.24	0.355	0.61	0.445	4.49	0.505	1.65	0.456
5.75	0.556	0.925	0.342	0.526	0.425	3.32	0.489	1.376	0.429
5.64	0.523	0.628	0.334	0.372	0.398	1.96	0.451	0.924	0.387
5.58	0.512	0.476	0.312	0.121	0.375	0.908	0.425	0.631	0.359
.395.3	0.497	0.349	0.298	0.074	0.355	0.619	0.402	0.421	0.329
4.75	0.478	0.125	0.292	0.046	0.326	0.468	0.397	0.344	0.309
4.03	0.458	0.063	0.284	0.037	0.312	0.377	0.372	0.184	0.297
3.68	0.445	0.047	0.281	0.033	0.298	0.181	0.343	0.076	0.292
3.37	0.435	0.034	0.28	0.021	0.292	0.123	0.325	0.048	0.287
2.37	0.403	0.012	0.279	0.015	0.291	0.075	0.314	0.034	0.284
2.12	0.389	0.011	0.278	0.009	0.287	0.042	0.309	0.007	0.279
1.84	0.374	0.006	0.278	0.006	0.286	0.034	0.297	0.002	0.279
1.5	0.351	0.004	0.278	0.004	0.284	0.021	0.292	0	0.278

200 rpm		400 rpm		600 rpm		800 rpm		1000 rpm	
i (mA/cm²)	E*-1 (V)	i (mA/cm²)	E *-1(v)	i (mA/cm²)		i (mA/cm²)	E (v)	i (mA/cm²)	
1.243	0.328	0.003	0.277	0.003	0.279	0.011	0.287		
1.18	0.319	0.002	0.277	0.002	0.277	0.004	0.282		
1.062	0.312	0	0.277	0	0.276	0.003	0.279		
0.966	0.306					0.002	0278		
0.789	0.295					0	0.278		
0.572	0.293								
0.368	0.290								
0.132	0.288								
0.1	0.281								
0.081	0.28								
0.072	0.278								
0.012	0.278								
0.009	0.278								
0.006	0.278								
0.004	0.278								
0.003	0.276								
0	0.276								

Table B-2 Data for polarization experiments in 0.1 N NaCl for Enhanced cylinder one at pH 6 and 35 °C .

200 rpm		400 rpm		600 rpm		800 rpm		1000 rpm	
i (mA/cm²)	E *-1(V)	i (mA/cm²)	E*-1(v)	i (mA/cm²)	E*-1(v)	i (mA/cm²)	E*-1(v)	i (mA/cm²)	E*-1 (v)
280	1.557	270	1.778	1.778	240	240	1.802	220	1.677
250	1.533	240	1.743	1.743	210	210	1.769	200	1.656
220	1.512	210	1.722	1.722	190	200	1.741	180	1.636
200	1.499	190	1.7	1.7	160	180	1.718	140.1	1.619
189	1.486	180	1.68	1.68	134.8	150	1.696	124.5	1.591
184.4	1.473	169.1	1.66	1.66	109.1	130	1.663	112.7	1.573
148.6	1.448	139.5	1.632	1.632	88.7	111.6	1.634	99.5	1.556
113.3	1.417	114.7	1.593	1.593	67.1	95.2	1.595	79.9	1.536
95.6	1.398	97.1	1.565	1.565	56.5	83.3	1.595	69.4	1.495
77.6	1.375	81.8	1.536	1.536	47.2	67.2	1.563	61.3	1.466
59.6	1.345	65.8	1.495	1.495	39.2	58.8	1.568	54.1	1.438
45.4	1.318	55.1	1.465	1.465	35.3	52.4	1.537	52.1	1.398
38.3	1.299	46	1.437	1.437	31.9	45.3	1.491	49.5	1.394
31.7	1.279	37.6	1.397	1.397	29.2	40	1.462	46.5	1.36
25.9	1.242	32.3	1.367	1.367	27.9	35.1	1.437	44.2	1.339
22.1	1.213	28.9	1.336	1.336	26.9	34	1.39	42.5	1.291
20.4	1.194	25.9	1.298	1.298	26.6	33	1.367	41.8	1.262
18	1.167	224.3	1.267	1.267	25.1	32.1	1.337	40.7	1.28
16.69	1.136	23.3	1.234	1.234	24.4	31.4	1.298	39.9	1.192
15.96	1.097	22.2	1.198	1.198	24.3	31	1.265	39.3	1.168
15.44	1.066	21.7	1.162	1.162	23.4	30.6	1.232	38.6	1.133
15.19	1.036	21.4	1.138	1.138	23.1	30.4	1.193	38.3	1.09
14.9	.999	21	1.09	1.09	22.8	30	1.165	37.7	1.067
14.63	.968	20.7	1.06	1.06	22.5	29.8	1.136	37.2	1.031
14.5	.933	20.4	1.031	1.031	22.5	29.4	1.093	36.9	1.19
14.32	.895	20.3	0.996	0.996	22.4	29.2	1.064	36.5	.992
14.2	.863	20	0.968	0.968	22.6	29.1	1.035	36.4	.961
14.1	.836	19.8	0.936	0.936	22.6	28.9	.99	36.5	.932
13.95	.79	19.5	0.889	0.889	22.6	28.8	.964	36.8	.892
13.95	.765	19.4	0.86	0.86	22.7	28.4	.933	36.7	.859
13.92	.73	19.2	0.834	0.834	22.7	28.3	.891	36.9	.833
13.81	.698	19.1	0.797	0.797	22.7	27	.838	37	.765

200 rpm		400 rpm		600 rpm		800 rpm		1000 rpm	
i (mA/cm²)	E*-1 (V)	i (mA/cm²)	E*-1(v)	i (mA/cm²)	E*-1(v)	i (mA/cm²)	E*-1(v)	i (mA/cm²)	E*-1 (v)
13.81	.667	18.94	0.732	22.2	0.664	27.8	.799	36.9	.73
13.66	.633	18.78	0.699	21.9	0.633	27	.758	36.7	.698
13.59	.599	18.43	0.668	20.6	0.596	25.6	.714	36.6	.667
13.33	.561	18.08	0.636	17.8	0.563	23.6	.697	36.3	.367
13.13	.536	17.08	0.598	15.75	0.538	19	.665	36	.598
12.26	.499	16.67	0.565	13.98	0.491	15.54	.635	35.5	.567
10.9	.473	15.43	0.535	11.53	0.477	11.93	.596	35.2	.527
10.29	.46	12.43	0.495	9.85	0.466	9.53	.566	33.4	.496
9.13	.435	12.46	0.464	8.82	0.437	8.62	.53	28.8	.468
8.6	.404	9.77	0.434	8.16	0.396	7.72	.495	25	.441
8.42	.395	8.42	0.395	7.19	0.364	6.68	.468	22.2	.435
7.63	.368	7.29	0.364	6.25	0.334	5.75	.427	20.1	.426
6.33	.332	6.55	0.334	4.79	0.297	5.1	.391	18.3	.404
5.5	.297	6.03	0.293	2.48	0.268	4.57	.366	16.9	.383
4.69	.273	5.02	0.268	2.21	0.238	3.78	.334	14.7	.373
4.2	.263	4.25	0.243	1.9	0.205	2.02	.298	12.11	.36
2.98	.231	2.78	0.235	1.558	0.202	1.38	.273	9.1	.322
2.3	.223	2.33	0.231	1.269	0.198	1.034	.262	6.26	.301
2.07	.221	2	0.219	1.049	0.193	0.703	.247	5.43	.288
1.65	.219	1.37	0.207	0.976	0.188	0.428	.217	4.28	.275
1.252	.212	0.828	0.2	0.796	0.183	0.39	.204	3.53	.264
1.008	.209	0.594	0.197	0.572	0.181	0.206	.199	2.81	.253
0.961	.208	0.423	0.194	0.453	0.176	0.085	.185	2.2	.238
0.779	.204	0.386	0.188	0.371	0.17	0.053	.176	1.89	.238
0.656	.204	0.203	0.184	0.195	0.165	0.039	.171	1.608	.226
0.44	.2	0.135	0.181	0.1	0.163	0.02	.165	1.343	.216
0.363	.197	0.06	0.179	0.045	0.156	0.008	.16	1.261	.206
0.211	.195	0.042	0.177	0.37	0.152	0.004	.158	.996	.204
0.191	.195	0.038	0.176	0.019	0.15	0.003	.155	.785	.194
0.13	.194	0.02	0.175	0.012	0.149	0	.154	.49	.188
0.079	.192	0.007	0.174	0.006	0.147			.366	.186
0.057	.191	0.003	.173	0.003	.146			.202	.178

200 rpm		400 rpm		600 rpm		800 rpm		1000 rpm	
i (mA/cm^2)	E *-1(V)	i (mA/cm^2)	E*-1(v)	i (mA/cm^2)	E*-1(v)	i (mA/cm^2)	E*-1(v)	i (mA/cm^2)	E*-1 (v)
0.036		0	.173	0	0.146			.193	.164
0.018								.1	.16
0.009								.057	.155
0.005								.036	.153
0.003								.019	.148
0								.006	.147
								.003	.147
								0	.146

Table B-3 Data for polarization experiments in 0.1 N NaCl for Enhanced cylinder two at pH 6 and 35 °C .

200 rpm		400 rpm		600 rpm		800 rpm		1000 rpm	
i (mA/cm²)	E*-1 (V)	i (mA/cm²)	E*-1(v)	i (mA/cm²)	E*-1(v)	i (mA/cm²)	E*-1(v)	i (mA/cm²)	E*-1 (v)
280	1.934	280	1.973	290	1.95	290	1.871	300	1.84
240	1.855	250	1.928	250	1.907	250	1.834	260	1.801
220	1.812	220	1.892	230	1.87	230	1.797	230	1.768
200	1.794	200	1.857	200	1.843	210	1.768	210	1.744
180	1.765	180	1.829	190	1.816	190	1.745	190	1.718
160	1.737	170	1.797	170	1.797	170	1.722	170	1.699
143.1	1.695	150	1.776	150	1.758	170	1.702	157.3	1.659
127.4	1.664	140	1.76	120.9	1.733	160	1.695	139.8	1.636
105.1	1.639	133.6	1.76	101.3	1.694	154.3	1.666	115.4	1.59
93.4	1.592	109.8	1.733	87.3	1.66	137.2	1.63	106.2	1.569
79.2	1.563	96.9	1.694	79.6	1.635	118.6	1.594	102.1	1.558
62.3	1.53	87	1.662	69.3	1.598	104.5	1.568	95	1.535
54.7	1.49	74.9	1.636	63	1.569	93.8	1.537	84.3	1.495
46.5	1.433	64.2	1.598	56.8	1.533	87.7	1.495	77.7	1.459
40	1.398	57.6	1.564	51.9	1.492	78.6	1.463	73.9	1.438
34.9	1.367	51.3	1.534	48.8	1.467	72.9	1.43	69.7	1.394
31.4	1.334	46.6	1.498	46.2	1.430	68.3	1.393	67.1	1.36
28.9	1.293	43.3	1.468	44.7	1.397	64.4	1.363	66.2	1.339
26.5	1.261	40	1.435	43.1	1.363	62.5	1.339	64.5	1.291
25.6	1.239	38.4	1.396	42.6	1.335	61.3	1.296	63.8	1.262
24.5	1.194	37	1.368	41.9	1.292	59.8	1.26	63.3	1.238
23.9	1.166	35.9	1.334	41.2	1.26	58.2	1.232	62.8	1.192
23.5	1.13	35.1	1.297	40.8	1.234	57.7	1.191	62.6	1.168
23.3	1.094	34.4	1.261	40.6	1.193	56.7	1.166	62.2	1.133
23.1	1.063	34.2	1.23	40.3	1.162	56.3	1.131	62.1	1.09
22.9	1.034	33.5	1.192	39.6	1.136	55	1.093	61.4	1.067
22.5	0.997	33.2	1.16	39	1.09	54.2	1.06	60.7	1.031
22.1	0.926	32.9	1.136	38.9	1.062	53.6	1.039	60.7	0.992
22.1	0.936	32.7	1.098	38.6	1.033	54	0.998	59.4	0.961
22	0.887	32.4	1.062	38.1	0.991	53.2	0.968	59.5	0.932
22	0.866	32.3	1.031	38.2	0.968	52.8	0.931	59.8	0.892
21.9	0.832	32.1	0.991	37.9	0.933	52.4	0.891	59.4	0.859

200 rpm		400 rpm		600 rpm		800 rpm		1000 rpm	
i (mA/cm²)	E *-1(V)	i (mA/cm²)	E*-1(v)	i (mA/cm²)	E*-1(v)	i (mA/cm²)	E*-1(v)	i (mA/cm²)	E*-1(v)
21.6	0.798	32	0.966	38.3	0.896	52.3	0.856	58.8	0.833
21.5	0.775	31.8	0.934	38	0.859	52.1	0.831	59	0.79
21.6	0.723	31.8	0.894	37.9	0.837	51.9	0.786	59.5	0.765
21.5	0.693	31.9	0.861	37.9	0.793	51.6	0.762	59.2	0.73
21.5	0.648	31.6	0.824	37.9	0.753	50.6	0.737	58.8	0.698
21.2	0.638	31.6	0.797	37.4	0.730.698	48.4	0.697	55.5	0.667
20.6	0.604	31.7	0.761	36.3	0.664	45.2	0.688	53.45	0.637
20.1	0.597	31.3	0.733	33.9	0.598	40.8	0.38	45.4	0.598
18.1	0.564	30.7	0.695	26.3	0.575	36.9	0.598	41.2	0.567
7.13	0.548	28.1	0.668	20.6	0.562	31.1	0.562	34.7	0.527
4.61	0.532	20.5	0.634	17.8	0.535	24.9	0.531	28.6	0.496
4.15	0.495	17	0.599	11.52	0.499	17.3	0.498	20	0.468
3.44	0.475	15.88	0.533	4.63	0.464	12	0.469	14.2	0.441
1.83	0.449	12.43	0.499	3.44	0.439	9.07	0.435	13.3	0.435
0.543	0.436	6.19	0.469	2.76	0.428	7.4	0.414	12.1	0.426
0.35	0.429	4.21	0.434	1.85	0.419	6.24	0.403	9.2	0.404
0.184	0.426	3.48	0.423	0.76	0.413	4.76	0.393	7.51	0.383
0.076	0.42	2.06	0.418	0.483	0.403	3.84	0.382	6.34	0.373
0.035	0.417	1.86	0.406	0.355	0.397	3.51	0.374	4.82	0.36
0.018	0.414	1.238	0.66	0.187	0.388	2.2	0.368	3.57	0.342
0.009	0.41	0.555	0.668	0.077	0.385	2.11	0.336	1.91	0.322
0.004	0.407	0.357	0.634	0.035	0.382	2.01	0324	1.272	0.301
0.003	0.403	0.187	0.599	0.018	0.381	1.92	0.306	0.976	0.288
0.002	0.401	0.078	0.566	0.007	0.381	1.28	0.296	0.665	0.275
0	0.401	0.039	0.533	0.004	0.38	0.983	0.276	0.504	0.264
4.61	0.532	20.5	0.634	17.8	0.535	24.9	0.531	28.6	0.496
4.15	0.495	17	0.599	11.52	0.499	17.3	0.498	20	0.468
3.44	0.475	15.88	0.533	4.63	0.464	12	0.469	14.2	0.441
1.83	0.449	12.43	0.499	3.44	0.439	9.07	0.435	13.3	0.435
0.543	0.436	6.19	0.469	2.76	0.428	7.4	0.414	12.1	0.426
0.35	0.429	4.21	0.434	1.85	0.419	6.24	0.403	9.2	0.404
0.184	0.426	3.48	0.423	0.76	0.413	4.76	0.393	7.51	0.383

200 rpm		400 rpm		600 rpm		800 rpm		1000 rpm	
i (mA/cm²)	E *-1(V)	i (mA/cm²)	E*-1(v)	i (mA/cm²)	E*-1(v)	i (mA/cm²)	E*-1(v)	i (mA/cm²)	E*-1 (v)
0.076	0.42	2.06	0.418	0.483	0.403	3.84	0.382	6.34	0.373
0.035	0.417	1.86	0.406	0.355	0.397	3.51	0.374	4.82	0.36
0.018	0.414	1.238	0.66	0.187	0.388	2.2	0.368	3.57	0.342
0.009	0.41	0.555	0.668	0.077	0.385	2.11	0.336	1.91	0.322
0.004	0.407	0.357	0.634	0.035	0.382	2.01	0324	1.272	0.301
0.003	0.403	0.187	0.599	0.018	0.381	1.92	0.306	0.976	0.288
0.002	0.401	0.078	0.566	0.007	0.381	1.28	0.296	0.665	0.275
0	0.401	0.039	0.533	0.004	0.38	0.983	0.276	0.504	0.264
		0.035	0.499	0.002	0.38	0.799	0.261	0.371	0.253
		0.018	0.469	0	0.38	0.673	0.244	0.195	0.238
		0.007	0.434			0.582	0.237	0.134	0.226
		0.003	0.423			0.411	0.225	0.068	0.216
		0.002	0.418			0.375	0.218	0.045	0.206
		0	0.418			0.375	0.216	0.037	0.204
						0.197	0.21	0.013	0.194
						0.068	0.205	0.006	0.188
						0.014	0.201	0.004	0.186
						0.037	0.199	0.003	0.178
						0.019	0.195	0	0.178
						.006	0.193		
						0.004	0.19		
						0.003	0.188		
						0	0.188		

الخلاصة

الهدف من الدراسة الحالية هو تعزيز انتقال كتلة الأوكسجين المذاب باستخدام محفزات الجريان المضطرب (turbulent promoters) من خلال تحليل النتائج التجريبية باستخدام قطب اسطواني دوار مصنع من النحاس الاصفر (RCE) لحساب كثافة التيار المحدد (LCD) Limiting Current Density في ظل ظروف الجريان المضطرب (turbulent flow) عند ثلاث درجات حرارة مختلفة ٣٥، ٤٥،و ٥٥ م . تم اجراء التجارب في ٠،١ عياري من محلول ملح كلوريد الصوديوم وبأس هيدروجيني ٦ ، ومعدل السرعة الدورانية يتراوح بين ٢٠٠-١٠٠٠ دورة في الدقيقة. كما تم بحث تأثير الاس الهيدروجيني بالرقم ٥,٦,٧ على كثافة التيار المحدد.

تم فحص نوعين من اسطوانة دوارة، المصنوعة من النحاس الاصفر: اسطوانة معززة رقم واحد(enhanced cylinder one)، مع أربعة ملحقات مستطيلة بابعاد ١٠*١٠*١ مليمتر ،وتعزيز اسطوانة رقم اثنين (enhanced cylinder two) مع أربعة ملحقات مستطيلة بابعاد ٣٠ *١٠*١ مليمتر.

أظهرت النتائج أن العلاقة بين LCD وpH علاقة خط أفقي تبين عدم تأثير ظهور غاز الهيدروجين على قيمة كثافة التيار المحدد وعليه فأن مدى الاس الهيدروجيني المذكور اعلاه معدوم التأثير عند مقارنته مع تأثير السرعة ودرجة الحرارة.

كان اداء الاسطوانة المعززة رقم ٢ ألافضل ولكن الفرق بينهما قليل ويقع لربما ضمن فروقات دقة توليد النتائج والتكرارية. مدى تعزيز انتقال الكتلة بالمقارنة مع القطب الاسطواني الدوار العادي الخالي من الملحقات كان بحدود ٥٣% و ٥٨% للقطب المعزز الاول والثاني على التوالي.

النسبة المئوية لتحسين انتقال الكتلة تقل كلما زادت السرعة الدورانية عند كل من الدرجات الحرارية المدونة اعلاه حيث يمكن تعليل ذلك بالوصول الى حالة الجريان الاضطرابي المناسب عمليا عن طريق الدوران (rotation) ومروجات أو معززات حركة الاضطراب.

النسبة المئوية لتحسين وتعزيز انتقال الكتلة يتناقص مع زيادة درجة الحرارة. ان زيادة درجة الحرارة يؤدي الى زيادة معامل انتقال الكتلةعلى الاسطوانة العادية والمعززة وفي نفس الوقت يقلل تركيز الاوكسجين الذائب في المحلول. وعليه فأن تأثير معززات الحركة الاضطرابية يقل وبالتالي فأن قيم معاملات انتقال المادة تتقارب مع بعضها مما يؤدي الى تقليص نسبة التعزيز وأن زيادة طول معززات الحركة الاضطرابية تبين لها تأثير قليل أو محدود حاليا. ايضا فأن عملية أنتقال المادة نتيجة لأرتفاع درجة الحرارة تجاوز تأثير نقص الاوكسجين المذاب في المحلول.

شكر وتقدير

اود ان اتقدم بخالص شكري وتقديري الى الاستاذ المشرف الدكتور قاسم جبار سليمان لجهوده القيمة في الاشراف و المشورة العلمية و الوقت الوفير الذي قدمه لي خلال فترة البحث لاخراج هذا العمل في افضل صورة ممكنة .

اتقدم بالشكر والامتنان الى من تعهداني بالتربية في الصغر ، وكانا لي نبراساً يضيء فكري بالنصح و التوجيه في الكبر و الى من علموني النجاح والصبر ،إلى من افتقدهم في مواجهة الصعاب ،الى لم تمهلهم الدنيا ليكونوا معي في مواصلة مسيرتي العلمية أبي ، وأمي و رفيق دربي اخي ابراهيم (رحمهم الله تعالى) ، والى جميع افراد عائلتي .

كما اتقدم بالشكر الجزيل الى رئيس قسم الهندسة الكيمياوية وكادره التدريسي والاداري لاسهامهم في اظهار هذه الرسالة بالشكل المناسب والى كافة زملائي لمساعتهم بطريقة او باخرى لانجاز هذا العمل.

بُراق شهاب احمد

الباحثة

تحسين أنتقال المادة بأستخدام أسطوانة دوارة معززة

رسالة

مقدمة إلى كلية الهندسة في جامعة النهرين

و هي جزء من متطلبات نيل درجة ماجستير علوم

في الهندسة الكيمياوية

من قبل

بُراق شهاب احمد

(بكالوريوس علوم في الهندسة الكيمياوية ٢٠٠٨)

ذو الحجة   ١٤٣٤

تشرين الأول   ٢٠١٣